Copyright Warning & Restrictions

The copyright law of the United States (Title 17, United States Code) governs the making of photocopies or other reproductions of copyrighted material.

Under certain conditions specified in the law, libraries and archives are authorized to furnish a photocopy or other reproduction. One of these specified conditions is that the photocopy or reproduction is not to be "used for any purpose other than private study, scholarship, or research." If a, user makes a request for, or later uses, a photocopy or reproduction for purposes in excess of "fair use" that user may be liable for copyright infringement,

This institution reserves the right to refuse to accept a copying order if, in its judgment, fulfillment of the order would involve violation of copyright law.

Please Note: The author retains the copyright while the New Jersey Institute of Technology reserves the right to distribute this thesis or dissertation

Printing note: If you do not wish to print this page, then select "Pages from: first page # to: last page #" on the print dialog screen

ABSTRACT

REMOVAL OF VOLATILE ORGANIC COMPOUND (VOC) VAPORS IN BIOTRICKLING FILTERS: PROCESS MODELING AND VALIDATION WITH CHLORINATED AROMATIC COMPOUNDS

by
Christos J. Mpanias

This study dealt with the removal of vapors of volatile organic compounds from airstreams in biotrickling filters (BTFs). A detailed general model was developed for describing the process under steady-state conditions. The model accounts for mass transfer between phases (air, liquid, biofilm) and biodegradation of pollutants in the biofilm. It also accounts for potential kinetic interactions among pollutants as well as potential process limitations by oxygen availability.

The general model was experimentally validated using mono-chlorobenzene (m-CB) and ortho-dichlorobenzene (o-DCB) as model compounds either alone or in mixture with each other. Before BTF experiments were undertaken, a systematic kinetic study was performed with suspended cultures. Two microbial consortia, called m-CB and o-DCB consortium, were used. The o-DCB consortium could use both m-CB and o-DCB as sole carbon and energy sources whereas the m-CB consortium could not utilize o-DCB. In all cases it was found that self-inhibition (Andrews kinetics) takes place. When the two compounds are present in a mixture they are simultaneously used but are

involved in a competitive cross-inhibition which is stronger from m-CB presence on o-DCB removal than vice versa. Studies on the effect of pH showed that a value of 6.8 is optimal. Some kinetic studies were repeated after the biomass had been used in a BTF for about 8 months and showed that the kinetics, i.e., the values of the kinetic constants remained unaltered.

Experiments in a BTF with the m-CB consortium and m-CB as model compound were performed with air residence times between 3.0 and 8.8 min, liquid flow rates between 0.7 and 5.7 Lh^{-1}, and inlet m-CB concentrations between 0.4 and 4.4 gm^{-3}. The percent m-CB removal observed ranged from 79 to 96% and the maximum removal rate was 60 gm^{-3}-packing h^{-1}. Removal of o-DCB vapor was found to be more difficult. In fact, using a BTF with the o-DCB consortium percent o-DCB removal ranged from 57 to 76% and the removal rate never exceed 30 gm^{-3}-packing h^{-1}. In these experiments, the air residence time, liquid flow rate, and inlet o-DCB concentration were in the range of 3.0-6.5 min, 1.2-5.2 Lh^{-1}, and 0.25-3.5 gm^{-3}, respectively. In all cases, a very good agreement between data and model predictions was found. Regarding removal rates, the proposed model predicted the data with less than 10% error in most cases. Most experiments were performed in counter-current flow of liquid and air, but some were performed in co-current mode. Co-current operation was found to be slightly superior to the counter-current mode; this is also predicted by the model. The great majority of BTF experiments was performed at pH 6.8. Some experiments at lower pH values showed considerable VOC removal somewhat unexpected based on the suspended culture studies.

Experiments in a BTF with the o-DCB consortium and airstreams laden by both m-CB and o-DCB validated the proposed model for the case of mixtures. These experiments were performed in counter-current flow of air and liquid. The liquid flow rate was 6 Lh^{-1} whereas air residence time, and m-CB and o-DCB concentrations varied in the range of 3.2-5.9 min, 0.17-3.1 gm^{-3}, and 0.1-0.8 gm^{-3}, respectively. The agreement between model predictions and data was very satisfactory but not as good as in the case with single VOCs.

For removal of m-CB/o-DCB mixtures it has been shown that kinetic interference can be neglected because the expected VOC concentrations are low. Regarding oxygen, it was found that an oxygen-controlled zone exists in the BTF (close to the inlet of the polluted air) when the total VOC concentration is relatively high. For the hydrophobic compounds used in this study oxygen availability does not seem to play a crucial role. Model sensitivity studies have shown that at least two kinetic constants are important and thus, zero or first-order kinetic approximations cannot and should not be made.

The model developed in this study along with the computer code generated for solving the equations can be used in (at least preliminary) scale-up calculations for the design of BTFs.

REMOVAL OF VOLATILE ORGANIC COMPOUND (VOC) VAPORS IN BIOTRICKLING FILTERS: PROCESS MODELING AND VALIDATION WITH CHLORINATED AROMATIC COMPOUNDS

by
Christos J. Mpanias

A Dissertation
Submitted to the Faculty of
New Jersey Institute of Technology
in Partial Fulfillment of the Requirements for the Degree of
Doctor of Philosophy

Department of Chemical Engineering,
Chemistry, and Environmental Science

May 1998

APPROVAL PAGE

REMOVAL OF VOLATILE ORGANIC COMPOUND (VOC) VAPORS IN BIOTRICKLING FILTERS: PROCESS MODELING AND VALIDATION WITH CHLORINATED AROMATIC COMPOUNDS

Christos J. Mpanias

Dr. Basil C. Baltzis, Thesis Advisor — Date
Professor of Chemical Engineering, NJIT

Dr. Gordon A. Lewandowski, Committee Member — Date
Professor of Chemical Engineering, NJIT

Dr. Piero M. Armenante, Committee Member — Date
Professor of Chemical Engineering, NJIT

Dr. Robert G. Luo, Committee Member — Date
Assistant Professor of Chemical Engineering, NJIT

Dr. Richard Bartha, Committee Member — Date
Professor of Microbiology,
Department of Biochemistry and Microbiology,
Rutgers University (New Brunswick)

BIOGRAPHICAL SKETCH

Author: Christos J. Mpanias

Degree: Doctor of Philosophy

Date: May 1998

Undergraduate and Graduate Education:

- Doctor of Philosophy in Chemical Engineering
  New Jersey Institute of Technology, Newark, New Jersey, 1998

- Diploma in Chemical Engineering
  National Technical University of Athens, Athens, Greece, 1992

Major: Chemical Engineering

Publications and Presentations:

Mpanias, C.J. and Baltzis, B.C., "An Experimental and Modeling Study on the Removal of Mono-Chlorobenzene Vapor in Biotrickling Filters." *Biotechnology and Bioengineering* (in press).

Mpanias, C.J. and Baltzis, B.C., "Biocatalytic Removal of Mono-Chlorobenzene Vapor in Trickling Filters." *Catalysis Today*, 40, pp 113-120 (1998).

Mpanias, C.J. and Baltzis, B.C., "Modeling Single VOC Removal in Biotrickling Filters: Theory and Experimental Verification." *1997 AIChE Annual Meeting*, Los Angeles, CA (November 18-23, 1997).

Mpanias, C.J. and Baltzis, B.C., "Biodegradation of Chlorinated VOCs in Trickling Filters: Studies on the Effect of Physical, Biochemical and Operating Parameters on the Process." *1997 AIChE Annual Meeting*, Los Angeles, CA (November 18-23, 1997).

Mpanias, C.J. and Baltzis, B.C., "Chlorinated Solvent Vapor Removal in Biotrickling Filters", Presented at *9th Annual Symposium on Emerging Technologies in Hazardous Waste Management*, Pittsburgh, PA (September 15-17, 1997) and submitted for publication in book devoted to Biofiltration Trends (R.Covind, editor, September 1997).

Baltzis, B.C. and Mpanias, C.J., "Biotrickling Filter Design for Removal of Chlorobenzenes" *1996 AIChE Annual Meeting*, Chicago, IL (November 17-22, 1996).

Mpanias, C.J. and Baltzis, B.C., "Removal of Mono-Chlorobenzene Vapors in a Biotrickling Filter." pp 21-29, in *Proceedings of 1996 Conference on Biofiltration*, D.S. Hodge and F.E. Reynolds Jr. (eds), The Reynolds Group, Tustin, CA (October 24 & 25, 1996).

Baltzis, B.C., de la Cruz, D.S., and Mpanias, C.J., " Removal of VOC Vapors in Biotrickling Filters." pp 241-249, in *Proceedings on an International Conference: Protection and Restoration of the Environment III,*_Chania, Greece (August 28-30, 1996).

Mpanias, C.J., Oreopoulou, V., and Thomopoulos, C.D., "The Effect of Primary Antioxidants and Synergists on the Activity of Plants Extracts in Lard" *Journal of the American Oil Chemists' Society*, 69, no. 6, pp 520-525 (1992).

This dissertation is dedicated to
my mother Despina,
my father Ioannis,
my brother Efthimios,
and the Vasilopoulos family

ACKNOWLEDGMENT

The author would like to express his sincere gratitude to his dissertation advisor, Professor Basil Baltzis for his guidance, encouragement, and moral support throughout this research.

The author is grateful to Professors Gordon A. Lewandowski, Piero Armenante, Robert G. Luo, and Richard Bartha for serving as members of the committee.

The author appreciates the timely help and suggestions from his colleagues and friends Mr. Stefanos Papakirillou, Mr. Otute Atiti, Dr. Socrates Ioannides, Dr. Dionisis Karvelas, Dr. Charalambos Christou, Dr. Dilip Madal, Mr. Evangelos Tsumis, and Dr. Kung-Wei Wang.

Mr. Clint Brockway, and Ms. Gwen San Augustin provided timely and expert assistance with the experimental set-up and analytical instruments.

Departmental support, as well as financial support from the Hazardous Substance Management Research Center (HSMRC: A NSF Industry/University Co-operative Research Center) through funded research projects, are also greatly appreciated.

Finally, the author thanks all members of his family in Greece and USA, for their patience, support, and constant encouragement without which this work could not have been accomplished.

TABLE OF CONTENTS

Chapter Page

Chapter **Page**

LIST OF TABLES

Table **Page**

LIST OF FIGURES

Figure **Page**

LIST OF SYMBOLS

A_{Sj} : specific wetted biofilm area in a unit treating VOC j (m^{-1})

A_{Tj} : total specific surface area of packing used in treating VOC j (m^{-1})

b : biomass concentration in a serum bottle (gm^{-3})

b_0 : initial biomass concentration in a serum bottle (gm^{-3})

b_f : final biomass concentration in a serum bottle (gm^{-3})

C_{Gj} : concentration of VOC j in the gas phase in a serum bottle (gm^{-3})

C_{Gq} : concentration of compound q in the air at positicn h along the BTF (gm^{-3})

$\overline{C}_{Gq}$: dimensionless version of C_{Gq} defined as $\overline{C}_{Gq} = C_{Gq}/C_{Gqi}$

C_{Gqi} : value of C_{Gq} at the inlet of biofilter (gm^{-3})

C_{Lj} : concentration of VOC j in the liquid phase in a serum bottle (gm^{-3})

C_{Lp} : concentration of VOC p in the liquid phase in a serum bottle (gm^{-3})

C_{Lq} : concentration of compound q in the liquid at position h along the BTF (gm^{-3})

$\overline{C}_{Lq}$: dimensionless version of C_{Lq} defined as $\overline{C}_{Lq} = m_q C_{Lq}/C_{Gqi}$

D_{qG} : diffusion coefficient of compound q in the air (m^2h^{-1})

D_{qW} : diffusion coefficient of compound q in water (m^2h^{-1})

d_{Pj} : nominal diameter of packing used in a unit treating VOC j (m)

$f(X_v)$: ratio of diffusivity of a compound in the biofilm to that in water

g : gravitational constant (ms^{-2})

h : position in the column (m); h = 0 at the entrance, h = H at the exit for co-current flow; h = H at the entrance, h = 0 at the exit for counter-current flow; entrance and exit refer to the airstream

H : total height of biofilter bed (m)

K_{2j} : dimensionless kinetic constant expressing competitive inhibition of compound j removal from another compound

K_{Hgj} : constant for compound j in equation (5.21), g = 1,2 ($molL^{-1}$)

K_{Ij} : self-inhibition kinetic constant for biodegradation of VOC j (gm^{-3})

K_j : kinetic constant for biodegradation of VOC j (gm^{-3})

K_{Lq} : overall mass transfer coefficient for compound q (h^{-1})

K_O : kinetic constant for biodegradation of VOC j related to oxygen (gm^{-3})

k_{Gq} : gas phase mass transfer coefficient for compound q (mh^{-1})

k_{Lq} : liquid phase mass transfer coefficient for compound q (mh^{-1})

M_j : total mass of compound j in a serum bottle (g)

$M_{j,0}$: initial total mass of compound j in a serum bottle (g)

m_q : distribution coefficient between air and water for compound q

$pH_{j,opt}$: optimum pH for removal of compound j; calculated via equation (5.23)

Q_G : air flow rate through the BTF (m^3h^{-1})

Q_L : liquid flow rate through the BTF (m^3h^{-1})

R_{exp} : experimental removal rate of a VOC in a biotrickling filter (gm^{-3}-reactor h^{-1})

R_j : average specific rate of compound j removal in a serum bottle [(g j) (h^{-1}) (g^{-1} biomass)]

R_{pred} : model-predicted removal rate of a VOC in a biotrickling filter (gm^{-3}-reactor h^{-1})

S : cross-sectional area of biofilter column (m^2)

S_q : concentration of compound q at a position x in the biofilm (gm^{-3})

$\bar{S}_q$: dimensionless version of S_q defined as $\bar{S}_q = S_q / K_q$

S_q^* : normalized version of S_q defined as $S_q^* = S_q(\theta)/S_q(\theta = 0)$

t : time (h)

u_G : superficial air velocity in the biofilter defined as $u_G = Q_G/S$ (mh^{-1})

u_L : superficial liquid velocity in the biofilter defined as $u_L = Q_L/S$ (mh^{-1})

V_G : volume of gas phase (headspace) in a serum bottle (L)

V_L : volume of liquid phase in a serum bottle (L)

V_{Pj} : volume of biofilter treating VOC j (m^3)

V_{Sj} : liquid phase volume of compound j injected in a serum bottle(L)

X_v : biofilm density (kg dry cells m^{-3})

x : position in the biofilm (m)

Y_j : yield coefficient of a culture on VOC j (g-biomass g^{-1}-VOC j)

Y_{Oj} : yield coefficient of a culture on oxygen (g-biomass g^{-1}-oxygen) when VOC j is the carbon source

z : dimensionless position in the biofilter ($z = h/H$)

Greek Symbols

α_q : dimensionless quantity for compound q defined as $\alpha_q = C_{Gqi}/m_q K_q$

β : dimensionless quantity defined as $\beta = K_{LO}/K_{Lj}$

β_1 : dimensionless quantity defined as $\beta_1 = K_{LD}/K_{LC}$

β_2 : dimensionless quantity defined as $\beta_2 = K_{LO}/K_{LC}$

γ : inverse dimensionless inhibition constant ($\gamma = K_j/K_{Ij}$)

γ_1 : inverse dimensionless inhibition constant ($\gamma_1 = K_C/K_{IC}$)

γ_2 : inverse dimensionless inhibition constant ($\gamma_2 = K_D/K_{ID}$)

δ : effective biofilm thickness (m)

δ_j : constant for compound j in equation (5.21) (h^{-1})

ε : dimensionless quantity defined as $\varepsilon = m_j K_{LO}/m_O K_{Lj}$

ε_1 : dimensionless quantity defined as $\varepsilon_1 = m_C K_{LD}/m_D K_{LC}$

ε_2 : dimensionless quantity defined as $\varepsilon_2 = m_C K_{LO}/m_O K_{LC}$

η : dimensionless quantity defined as $\eta = f(X_v) D_{jW} A_{Sj} K_j m_j H/u_L \delta C_{Gji}$

η_C : dimensionless quantity defined as $\eta_C = f(X_v) D_{CW} A_S K_C m_C H/u_L \delta C_{GCi}$

θ : dimensionless position in the biofilm defined as $\theta = x/\delta$

λ : dimensionless quantity defined as $\lambda = D_{jW} K_j Y_j/D_{OW} K_O Y_{Oj}$

λ_1 : dimensionless quantity defined as $\lambda_1 = D_{CW} K_C Y_C/D_{OW} K_O Y_{OC}$

λ_2 : dimensionless quantity defined as $\lambda_2 = D_{DW} K_D Y_D/D_{OW} K_O Y_{OD}$

μ_G : gas (air) viscocity ($kgm^{-1}s^{-1}$)

μ_j^* : kinetic constant for the biodegradation of VOC j (h^{-1})

μ_j : specific growth rate for compound j (h^{-1})

μ_L : liquid (water) viscocity ($kgm^{-1}s^{-1}$)

$\mu_{max\,j}$: maximum specific growth rate for compound j (h^{-1})

ξ_j : correction factor in expression (6.36)

ξ_{1q} : correction factor in expression (6.38)

ξ_{2q} : correction factor in expression (6.39)

ρ : dimensionless quantity defined as $\rho = K_{Lj}H/u_G m_j$

ρ_C : dimensionless quantity defined as $\rho_C = K_{LC}H/u_G m_C$

ρ_G : air density (kgm^{-3})

ρ_L : liquid (water) density (kgm^{-3})

ρ_{Sj} : liquid density for compound j (gm^{-3})

σ_1 : dimensionless quantity defined as $\sigma_1 = K_{CD}K_D/K_C$

σ_2 : dimensionless quantity defined as $\sigma_2 = K_{DC}K_C/K_D$

σ_L : surface tension of liquid (Nm^{-1})

σ_P : surface tension of packing material (Nm^{-1})

ϕ^2 : dimensionless quantity defined as $\phi^2 = X_v\delta^2\mu_j^*/f(X_v)Y_jD_{jW}K_j$

ϕ_1^2 : dimensionless quantity defined as $\phi_1^2 = X_v\delta^2\mu_C^*/f(X_v)Y_CD_{CW}K_C$

ϕ_2^2 : dimensionless quantity defined as $\phi_2^2 = X_v\delta^2\mu_D^*/f(X_v)Y_DD_{DW}K_D$

ψ : dimensionless quantity defined as $\psi = K_{Lj}H/u_L$

ψ_C : dimensionless quantity defined as $\psi_C = K_{LC}H/u_L$

ω : dimensionless quantity defined as $\omega = C_{Gji}D_{OW}K_O m_O/C_{GOi}D_{jW}K_j m_j$

ω_1 : dimensionless quantity defined as $\omega_1 = C_{GCi}D_{DW}K_D m_D/C_{GDi}D_{CW}K_C m_C$

ω_2 : dimensionless quantity defined as $\omega_2 = C_{GCi}D_{OW}K_O m_O/C_{GOi}D_{CW}K_C m_C$

Special Subscripts

j = C : VOC j is m-CB

j = D : VOC j is o-DCB

q = C : compound is m-CB

q = D : compound is o-DCB

q = j : compound is either m-CB or o-DCB

q = O : compound is oxygen

j = 1 : VOC j is m-CB

j = 2 : VOC j is o-DCB

p = 1 : VOC p is m-CB

p = 2 : VOC p is o-DCB

CHAPTER 1

INTRODUCTION

The concerns of the public regarding the impacts of industrial pollution on the environment have resulted in a number of regulations and policies at the local, national and international level. These policies have, on one hand, bolstered research in pollution mitigation from the perspective of almost all physical and social sciences. On the other hand, the same policies have imposed enormous challenges to scientists and technologists who seek efficient, economic and publicly acceptable means to abate pollution and protect the environment. As a result, in the past two decades and in the present environmental research is actively pursued in both academic and industrial settings.

Among the many environmental problems, air pollution is one of the top issues being addressed by industrialized nations. It is also fast becoming a priority among developing countries. One of the most serious aspects of air pollution is the problem of volatile organic compound (VOC) emissions. Some of these compounds may have severe implications for human health as they are suspected carcinogens and for this reason, they are classified as hazardous air pollutants (HAPs). In general however, VOCs -whether HAPs or not- create problems related to either smog formation in the troposphere or ozone depletion in the stratosphere (Mukhopadhyay and Moretti, 1993).

Several industrial plants, such as the pharmaceutical industry, wastewater and sewage treatment works, and a few categories of the food industry, constitute a continuous source of emission of large volumes of waste gases containing volatile organic compounds (VOCs). Over the years, regulations regarding VOCs have become increasingly stringent both at national and international levels. Regulations are currently affecting industrial operations. The 1990 Clean Air Act Amendments (CAAA) require 90% reduction in specific hazardous air pollutants (HAPs) released from major emission sources by the year 2000. Under the CAAA, thousands of currently unregulated sources will be required to reduce or eliminate VOC emissions. In addition, sources that are currently regulated may seek to evaluate alternative VOC control strategies to meet stricter regulatory requirements such as the maximum achievable control technology (MACT) requirements of the CAAA.

In order to address the problem of VOC emissions, a number of different technologies employing physical, chemical and biological methods for treating contaminated air streams, have been developed. Among them, biological waste gas treatment has some specific advantages. It occurs at low (ambient) temperature and pressure, leads to pollutant destruction without requiring expensive catalysts and -if the microorganisms are properly selected- does not lead to formation of toxic by-products. In general, biological treatment is an environmentally friendly technology which is expected to be competitive due to relatively low capital and operation cost.

A biodegradation-based process for air pollution control which has attracted a lot of attention in the recent years is biofiltration. It is based on the biological destruction of

VOC vapors by microorganisms immobilized on a porous solid support material. These solids are placed in open or closed structures known as biofilters. When a contaminated airstream is passed through such a conventional or classical biofilter, the VOCs are transferred to the biofilms formed on the surface of the solids where they undergo biological oxidation. Thus, the airstream exiting a biofilter contains amounts of VOCs less than the stream entering the unit. Clearly, the ultimate objective is to design biofilters in ways which ensure that the exiting airstreams are pollutant-free.

However, biofiltration is not as simple as it appears, and design of biofilters should successfully meet certain requirements, otherwise biofiltration can end up being a very expensive and poorly performing process. These design considerations are extensively discussed by Leson and Winer (1991), and Bohn (1993). Basically, what should be considered in the biofilter design is the need to provide the microorganisms with a hospitable environment, and the optimum conditions for the oxidation of the carbon source. The packed bed configuration should fulfill certain requirements, the most important of which are proper temperature and pH levels, presence of needed oxygen and nutrients, low pressure drop, high surface area, and maintenance of adequate moisture levels.

Classical or conventional biofilters, although simple in operation, usually require large volumes of packing and they are efficient under low VOC concentrations and high volumetric flow rates of air (Mukhopadhyay and Moretti, 1993). In addition, their design is not easy due to the ill-defined nature of the packing and biomass. To overcome these problems, biotrickling filters have been investigated in the recent years. Biotrickling

filters use a well-specified non-porous inorganic packing material and involve a liquid phase which trickles through the bed. This liquid phase provides additional nutrients (non-carbon sources) to the biomass and allows for pH control. Control of pH is particularly important for the removal of chlorinated compounds from airstreams. Biotrickling filters are much more complex than classical biofilters. On the other hand, they are much better defined systems and thus their engineering design and optimization may be easier through control of various parameters. For this reason, biotrickling filters appear to be a very attractive alternative to conventional biofilters.

Although a lot of feasibility studies on biotrickling filters exist (see Chapter 2) the process is not yet fully understood. A fundamental process understanding is needed so that it is translated to appropriate mathematical models which can help with a rational and optimal design of industrial units.

The present study was undertaken with the intent to derive, numerically solve, and experimentally validate detailed engineering models of VOC removal in biotrickling filters. An emphasis was placed on the kinetics of biodegradation as was earlier done by Shareefdeen et al. (1993), Shareefdeen and Baltzis (1994), Shareefdeen (1994) with conventional biofilters. For the first time, the present study considered the effect of oxygen and that of kinetic interactions among pollutants for the case of biotrickling filters. In addition, the present study is the first to introduce detailed models allowing for prediction of VOC and oxygen profiles in the three phases (air, liquid, biofilm) encountered in biotrickling filters. Model validation was based on experiments with mono-chlorobenzene (m-CB) and ortho-dichlorobenzene (o-DCB). Experiments were

performed with biotrickling filters treating airstreams contaminated with m-CB alone, o-DCB alone, and m-CB/o-DCB mixtures. Selection of chlorinated compounds was guided by the fact that biotrickling filters appear to be particularly suited for hard to degrade, halogenated pollutants. The model compounds used here have never been used in the past in any engineering study on biotrickling filters. The effects of various parameters such as co-current versus counter-current flow of air and liquid, liquid and air flow rate, pH, frequency of medium replenishment, and inlet VOC concentration were studied experimentally and from the modeling point of view.

CHAPTER 2

LITERATURE REVIEW

2.1 Conventional and Trickling Biofilters

Among the biological exhaust gas purification methods, biofiltration has attracted a growing interest during the recent years. It occurs in biological reactors known as biofilters. These reactors involve packed bed of solids on the surface of which biofilms of microbial consortia are formed. The airstreams are passed through the reactor and are eventually transferred into the biofilms where they undergo biodegradation. With proper selection of biomass and operating conditions VOCs are completely mineralized as they are converted into carbon dioxide, water, biomass, and inorganic salts. Depending on the type of solid support for the biomass and the presence or absence of a continuous liquid phase in the reactor, biofilters can be classified into two distinct categories: conventional (or classical) biofilters and biotrickling filters.

Conventional biofilters consist of open or closed structures containing porous solids of an organic base (e.g., peatmoss, compost, etc.) along with a bulking agent (e.g., perlite). They do not involve a continuous liquid phase although water is retained within the pores of the solids. Conventional biofilters often depend on the microflora which is indigenous in the packing although specially selected and separately grown microbial populations are also used for inoculating the filter bed. Moisture is controlled via prehumidification of the polluted airstream and occasional spraying of the filter bed with

water. Additional nutrients for the biomass are usually not supplied and, as a result, no excess biomass formation is observed in conventional biofilters. Where needed, the pH is attempted to be controlled via amending the solids packing with substances such as calcium carbonate. A very large number of experimental studies with conventional biofilters have been published in the literature. Fewer are the systematic studies which also involve process modeling. Modeling varies in complexity and conditions, e.g., single or mixed VOCs, steady-state or transient conditions, (Baltzis et al., 1997; Deshusses et al., 1995a,b; Hodge and Devinny, 1995; Ottengraf and van den Oever, 1983; Shareefdeen et al., 1993; Shareefdeen and Baltzis, 1994).

Conventional biofilters have been found to be economically competitive under low VOC concentrations and high volumetric air flow rates (Mukhopadhyay and Moretti, 1993). Although simple in concept and operation conventional biofilters have a number of drawbacks. They usually achieve low pollutant removal rates and thus, require large volumes to treat a given load, they cannot easily handle compounds which are tough to biodegrade, and they do not allow for pH-control when it is necessary (as in the case of chlorinated VOCs).

Biofiltration in conventional units is anything but a simple process. The complexity of the issues which have not yet been resolved (microbiology, moisture content, biofilm coverage of packing, etc.), but also the intrinsic limitations of biofilters (e.g., pH-control for cases of chlorinated solvent emissions) have led to the initiation of efforts for modifying the process. The most important modification which has already led to applications is that of biotrickling filters or trickling biofilters.

Biotrickling filters (Figure 2.1) involve the use of a bed packed with inorganic non-porous solids (such as plastic or even ceramic monoliths) on the surface of which microorganisms are immobilized. A liquid stream is recirculated through the column

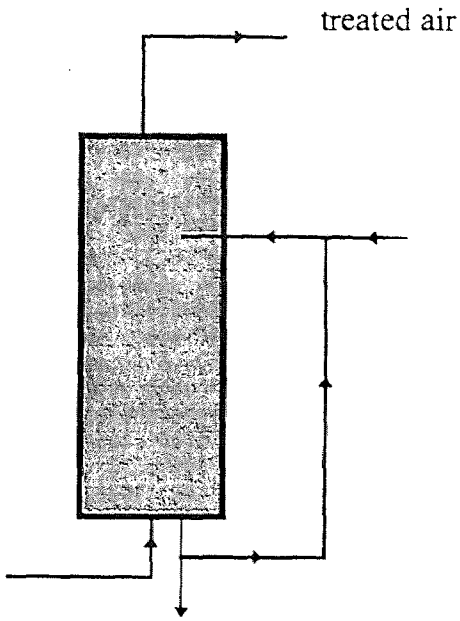

Figure 2.1 Schematic layout of a biotrickling filter

co-currently or counter-currently to the flow of contaminated air. The presence of a flowing liquid phase allows for supply of non-carbon nutrients to the microbes and for pH-control which is crucial for maintaining optimal performance.

Instrumentation and operating costs for biotrickling filters are higher than those for classical biofilters. However, because these systems are better defined their engineering and design is relatively easier to implement. Removal rates obtained with biotrickling filters are usually substantially higher than those obtained with conventional biofilters probably due to nutrients addition, pH control, and a larger air/liquid interfacial

area. These higher rates, which imply potentially substantially lower sizes and thus capital expenditure for industrial applications, have caused a shift in interest from conventional to trickling biofilters in the recent past.

Perhaps the most important problem with biotrickling filters is the production and accumulation of biomass due to nutrients supply. Occasional removal of biomaterial is required to avoid clogging and severe pressure drops. Biomass control strategies have been discussed in the literature (Smith et al., 1996). This problem is of higher concern when easily biodegradable compounds having high yield coefficients are treated in biotrickling filters. Classical biofilters once installed, require minimal supervision while biotrickling filters require frequent and specialized (engineering) attendance. Thus, applications of biotrickling filters are expected to be primarily within industrial settings and not at small business (bakeries, dry cleaners, etc.).

Biotrickling filters are particularly suitable for removal of chlorinated compounds which is the topic of the study reported here. Biodegradation of chlorinated compounds is not easy and leads to release of chloride ions with a concomitant change in the pH of the reaction environment. Consequently, proper selection of biomass is required, maintenance of biological activity via nutrient addition can be essential, and pH-control is certainly necessary. Furthermore, the usually low biomass yield on these compounds alleviates biomass accumulation problems. For all the foregoing reasons biotrickling filters appear to be ideal for chlorinated VOC removal.

2.2 Feasibility Studies on VOC Removal in Biotrickling Filters

As with conventional biofilters, the use of biotrickling filters for odor control purposes

was reported as early as 60 years ago (Mukhopadhyay and Moretti, 1993). However, biotrickling filters for removal of industrial VOCs and hazardous air pollutants (HAPs) started being investigated in the late 80's. Experimental results with biotrickling filters have been reported by various investigators, and a summary review is given in Table 2.1 and Table 2.2. These tables give information on the VOCs treated, the operating conditions used, the type of the packing employed, and the process performance achieved. Process performance is given in terms of percent VOC conversion and removal rate. In cases where the latter was not explicitly reported, it was calculated based on other reported experimental results.

2.3 Studies on Modeling of Biotrickling Filters

Biofiltration is a very complex process as it involves mass transfer and reaction of various substances as well as flow (hydrodynamic) characteristics. For this reason, modeling biofiltration is not an easy undertaking. On the other hand, mathematical models for biofiltration are essential both for optimal process design and for diagnostic purposes during process operation. Regarding biotrickling filters, modeling efforts have started but need further studying in conjunction with systematic experimental investigations.

The first model for biotrickling filters was proposed by Diks and Ottengraf (1991 a, b) who assumed a zero-order kinetic expression and negligible resistance for the transfer of the VOC from the gas (air) to the liquid phase. The model proved successful in describing their experimental results. This model was subsequently modified by

Table 2.1. VOC Removal in Biotrickling Filters as Reported in the Literature

Pollutant	[a]C_{Gji} (gm^{-3})	[b]τ (min)	[c]Q_L (Lh^{-1})	Reactor Size (d x L, cm x cm)	Packing Material	[d]X (%)	[e]R_{exp} ($gm^{-3}\,h^{-1}$)	pH	Reference
Toluene	2.5-5.0	0.67–2	0.83	14.6 x 112	[f]PEM	78-99	[g]68-112	7.7	A
Toluene	0.2-1.6	0.5–2.6	21-30	10 x 70	Steel Pall Rings	-	25-45	-	B
Styrene	1.5	1–1.5	-	-	-	90	[g]54-81	-	C
Isopentane	2.0	1–3	14	10 x 61	ceramic	60-93	[g]37-72	-	D
p-xylene	1.0-10.0	4	0.5	10 x 57	ceramic	46-98	[g]14.7-69	6.5	E
m-xylene	3.0-8.0	4	0.5	10 x 57	ceramic	94-96	[g]42-112	6.5	E
[h]MM	-	17.3	-	7.6 x 76.2	[i]PB	-	6.6-11	-	F

[a]inlet VOC concentration, [b]residence time based on empty reactor, [c]liquid flow rate, [d]percent removal, [e]experimentally determined removal rate, [f]peletized earth media, [g]calculated based on reported values, [h]mixture of methanes, [i]polypropylene rings, [A]Sorial et al. (1995), [B]Arcangeli and Arvin (1992), [C]Togna and Singh (1994a), [D]Togna and Singh (1994b), [E]Baltzis and de la Cruz (1996)), [F]Apel et al. (1990).

Table 2.2. VOC Removal in Biotrickling Filters as Reported in the Literature

Pollutant	[a]C_{Gji} (gm^{-3})	[b]τ (min)	[c]Q_L (Lh^{-1})	Reactor Size (d x L, cm x cm)	Packing Material	[d]X (%)	[e]R_{exp} ($gm^{-3}h^{-1}$)	pH	Reference
[J]TCM/TCE/T	-	2	0.6	2.5 x 60	activated carbon	25-80	-	-	G
[k]m-CB	1.2	1	0.04	5 x 20	perlite	-	5.1	6.9	H
[l]o-DCB	0.7	1.2	0.04	5 x 20	perlite	-	2.2	6.9	H
[j]TCM	2.0	-	-	-	oyster shells	92.1	-	6.9	G
[m]DCM	-	0.4	-	29 x 100	polypropylene	80-95	-	-	I
[m]DCM	0.5-10.0	0.5–1	450	40 x 270	ceramic	-	157	-	J

[a]inlet VOC concentration, [b]residence time based on empty reactor, [c]liquid flow rate, [d]percent removal, [e]experimentally determined removal rate, [j]trichloromethane, trichloroethylene,and toluene mixture, [k]mono-chlorobenzene, [l]ortho-dichlorobenzene, [m]dichloromethane, [G]Utgikar et al. (1991), [H]Oh and Bartha (1994), [I]Hartmans and Tramper (1991), [J]Diks and Ottengraf (1991a,b)

Ockeloen et al. (1992) who used Monod-type kinetics for the biodegradation of the VOC and performed numerical studies without experimental verification. They showed that VOC removal decreases as the solubility of the VOC in water decreases. They also showed that with less soluble compounds removal rates are higher under co-current rather than counter-current flow of the air and liquid streams. Diks and Ottengraf (1991 a, b) had concluded that differences in process performance due to co- or counter-current flow are insignificant.

Studying toluene removal in a biotrickling filter, Smith et al. (1995) have developed a more detailed model which assumes Monod kinetics and accounts for the effect of microbial growth on the hydrodynamics of the flow of process streams. These investigators also developed a relationship between the VOC flux into the biofilm and the biofilm thickness. This model involves more details of the process than earlier ones (Diks and Ottengraf, 1991 a, b; Ockeloen et al., 1992).

Hartmans and Tramper (1991) used a simplified approach to biotrickling filter modeling by simulating the filter bed with a series of perfectly stirred interconnected reactors, and they developed some relations based on macroscopic process characteristics (velocities, organic load, etc.). This is a model involving a much lesser degree of process details compared to the models discussed earlier.

Alonso et al. (1997) have proposed and validated a mathematical model that describes the biotreatment of toluene in a trickle-bed reactor. A new approach describing the variation in the biofilter specific surface area with microbial growth has been included. The most important conclusion is that the performance of the biofilter depends

not only on the amount of biomass but also on the amount of biomass that can be readily accessed by the diffusing contaminant.

None of the existing biotrickling filter models accounts for either inhibitory biodegradation kinetics with respect to the availability (concentration) of VOC or for potential kinetic limitations from the availability of oxygen in the biofilm. Kinetic self-inhibition and oxygen effects have been reported to be important for conventional biofilters (Baltzis et al., 1997; Shareefdeen et al., 1993; Shareefdeen and Baltzis, 1994). The same factors were accounted for in the present study and proved to be important as discussed in the following chapters.

CHAPTER 3

OBJECTIVES

This study was undertaken with the intent to gain a fundamental understanding of the removal of volatile organic compound (VOC) vapors in biotrickling filters. Issues regarding kinetics of VOC biodegradation, the effects of pH and oxygen, and mode of filter operation (co-current or counter-current flow of air and liquid) were to be addressed. The ultimate objective was to derive, numerically solve, and experimentally validate a general mathematical model describing removal of VOCs from airstreams in biotrickling filters. In order to meet this objective a number of sub-objectives were set.

First, it was decided to base the study on actual kinetic expressions concerning biodegradation of the model compounds rather than assuming simple zero- or first-order kinetics. Once mono-chlorobenzene (m-CB) and ortho-dichlorobenzene (o-DCB) were selected as model compounds a detailed kinetic investigation was undertaken. Experiments were performed with suspended cultures in closed serum bottles under conditions of oxygen abundance. This kinetic study, the results of which are presented in Chapter 5, involved experiments with each one of the two compounds alone and mixtures of the two compounds. It was found that both compounds, m-CB and o-DCB, follow Andrews (1968) self-inhibitory kinetics. In the case of biodegradation of mixtures it was found that in addition to self-inhibition, the two pollutants are involved in a cross-inhibitory kinetic interaction. In order to determine the optimal pH for the

process, a kinetic study under different pH-values was also undertaken and its results were also modeled (Chapter 5). In modeling VOC removal in biotrickling filters, it was assumed that the inherent biodegradation kinetics of a VOC are the same with a given biomass regardless of whether the biomass is suspended or immobilized in the form of biofilms. To test this assumption, kinetic experiments with m-CB were performed not only with the original consortium but also with biomass obtained from a biotrickling filter which was in continuous operation for 8 months. All the results regarding the sub-objectives concerning kinetics are presented in Chapter 5.

Second, and before the general case of mixtures was addressed, it was decided to undertake a systematic investigation with airstreams laden with a single VOC. Two experimental units were set-up. They were glass columns 80 cm in height and 15 cm in diameter. Their differences were in the type of packing material and the biomass used. The first unit operated with m-CB as model compound. It was packed with 3/4" non-porous Intalox ceramic saddles. The biomass used was capable of completely mineralizing m-CB using it as sole carbon and energy source. This consortium could not handle o-DCB. The second unit employed a consortium capable of mineralizing both o-DCB and m-CB. It operated with o-DCB only and was packed with 1/2" non-porous Intalox ceramic saddles. Detailed experiments with the two units helped meeting the following sub-objectives:

1. Evaluation of process performance under a variety of operating conditions concerning inlet pollutant concentration, flowrate (equivalently residence time) of the

airstream in the biotrickling filter, and flowrate of the liquid trickling through the filter bed.

2. Investigation of the effect of pH and frequency of liquid replenishment on the process.
3. Comparison of the two possible modes of operation of a biotrickling filter unit; namely, co-current and counter-current flow of the liquid and gas phases.

Simultaneously with the experimental work, a steady-state model describing removal of a single VOC under constant pH was developed. It considers three phases (air, liquid, and biofilm) and is based on principles of mass transfer and biodegradation kinetics. The model was numerically solved using the methods of orthogonal collocation and 4^{th}-order Runge-Kutta integrator and calibrated with some experimental data sets. Subsequently the predictive capabilities of the model were tested against data sets not used in the fitting approach. The model, once validated, helped selection of conditions for further experiments and was also subjected to numerical sensitivity studies. The latter have revealed the key parameters one needs to know relatively accurately in order to design a biotrickling filter unit with confidence. The results of the study with airstreams carrying one VOC only are presented in Chapter 6.

Once a good understanding of the process was obtained based on single VOC removal (Chapter 6) the ultimate objective of this thesis was addressed. A general model was written as an extension of the single VOC model introduced in Chapter 6. The only new feature is that the model is general enough to accommodate potential kinetic interactions among pollutants. This general model was then tested against experiments

with airstreams carrying two VOCs, namely m-CB and o-DCB. Experiments were performed with the culture which was used earlier in o-DCB removal only since it had the ability to also mineralize m-CB. Intalox ceramic saddles (1/2") were used again as packing. Experiments were performed in counter-current flow of air and liquid under a variety of conditions concerning residence time and relative VOC concentrations at the inlet conditions. In modeling the data, the general model was numerically solved for the case of a binary mixture. Kinetic interactions revealed in the kinetic studies (Chapter 5) were taken into consideration. Based on the calibration performed in Chapter 6 and without any further fitting, the model predicted the experimental results. Model sensitivity studies as well as calculations for comparing the performance of conventional and trickling biofilters were also performed. The results from the study on mixture removal are presented in Chapter 7.

CHAPTER 4

EXPERIMENTAL DESIGN AND PROCEDURES

4.1 Microbial Cultures

The biomass used in the experiments consisted of two microbial consortia which are called here the m-CB and o-DCB consortium. The m-CB consortium was capable of completely mineralizing mono-chlorobenzene (m-CB) by using it as its sole carbon and energy source. This consortium was incapable of using ortho-dichlorobenzene (o-DCB) as a substrate. The o-DCB consortium was capable of completely mineralizing both m-CB and o-DCB. Either substrate could serve as sole carbon and energy source for the o-DCB consortium. Inocula of the two consortia (in serum bottles) were provided by Professor R. Bartha (Microbiology Dept., Rutgers University, New Brunswick, NJ). The m-CB consortium was used in studies with m-CB while the o-DCB consortium was used in studies with both m-CB and o-DCB individually and in mixtures.

Inocula of the consortia were grown in 1 L flasks sealed with Teflon septa (Fisher Scientific Co., Springfield, NJ), on a nutrient medium consisting of a mixture of two solutions, A and B, at a B:A ratio of 1:99 by volume. Solution A contained the following chemicals, per liter of deionized water: 4.0 g Na_2HPO_4 (S374-500 Fisher Scientific Co., Springfield, NJ), 1.5 g KH_2PO_4 (P285-500 Fisher Scientific Co., Springfield, NJ), 1.0 g NH_4NO_3 (S441-500 Fisher Scientific Co., Springfield, NJ), and 0.2 g $MgSO_4 7H_2O$ (M63-500 Fisher Scientific Co., Springfield, NJ). Solution B contained 0.5 g $FeNH_4$-

citrate (I72-500 Fisher Scientific Co., Springfield, NJ) and 0.2 g $CaCl_2$ (C77-500 Fisher Scientific Co., Springfield, NJ) per liter of deionized water. The nutrient medium was a buffer of pH 7.0. Initially, an amount of 50 mL medium was placed in the flasks, inoculated with the consortium of interest, and provided with 5 μL liquid m-CB and/or 0.2 μL liquid o-DCB. After some initial serial transfers, part of the biomass was used in kinetic experiments and another part was used as inoculum for starting up the biotrickling filter experiments.

For the kinetic experiments serum bottles of 160 mL were used. All bottles received the same amount of medium (15 mL) and approximately the same amount of biomass (25 g m^{-3}). Each bottle was then sealed with aluminum crimp caps placed upon butyl Teflon-faced 20 mm-stoppers (Wheaton Manufactures, Millville, NJ). Each bottle was provided with a different amount of m-CB and/or o-DCB and was placed in an incubator shaker (200 rpm, 25°C). Experiments were monitored via GC analysis of air samples obtained through the septa via a 500 μL gas-tight syringe (Hamilton, Reno, NV). Air samples were obtained at a frequency of 30-60 min starting 2-3 h after the initiation of each experiment. This initial period of 2-3 h was found (from blank experiments involving the same amounts of medium and m-CB or o-DCB but no biomass) to be enough to ensure thermodynamic equilibrium distribution of m-CB or o-DCB between the medium and headspace of the closed bottle. The biomass concentration was measured only in the beginning and end of each kinetic run for determining the yield coefficient. In order to determine the optimal pH for culture growth, some experiments

were performed with the same medium to which amounts of either NaOH or HCl solutions were added to adjust its pH to a value other than 7.0.

Following the same methodology, kinetic experiments were also performed with inocula of the m-CB consortium obtained from the biotrickling filter treating m-CB after the filter bed had been in continuous operation for 8 months. This was done in order to check if the kinetic characteristics of the biomass change with time.

4.2 Biotrickling Filters

A schematic of the experimental biotrickling filter unit used in the study reported in this thesis is shown in Figure 4.1. The biotrickling filter itself was a custom-made glass column (ACE Glass, Vineland, NJ) of 15.2 cm diameter and 80 cm height, provided with sampling ports at its entrance, exit, and middle point. The column had a headtop and headbottom (ACE Glass, Vineland, NJ) made of glass and having various ports for liquid and air supply. For removal of m-CB vapor, the biotrickling filter was packed with 3/4" Intalox ceramic saddles (Norton Chemical Process Product Corp., Akron, OH) to a height of 74 cm. The void fraction of the bed was 0.64. For the removal of o-DCB and m-CB/o-DCB mixtures the columns were packed with 1/2" Intalox ceramic saddles (Norton Chemical Process Product Corp., Akron, OH). The bed height was 69 cm and 79 cm for o-DCB and mixture removal, respectively. In both cases the void fraction of the bed was 0.68. Operation of the filter bed involved downward flow of a liquid stream made of the same culture medium described in the preceding section, and an airstream laden with m-CB and/or o-DCB vapor. The airstream entering the bottom (counter-

current flow) or the top (co-current flow) of the filter bed was prepared by mixing two different airstreams. The main one consisted of pure air which was first completely humidified in a tower (column) packed with Intalox ceramic particles. This stream was

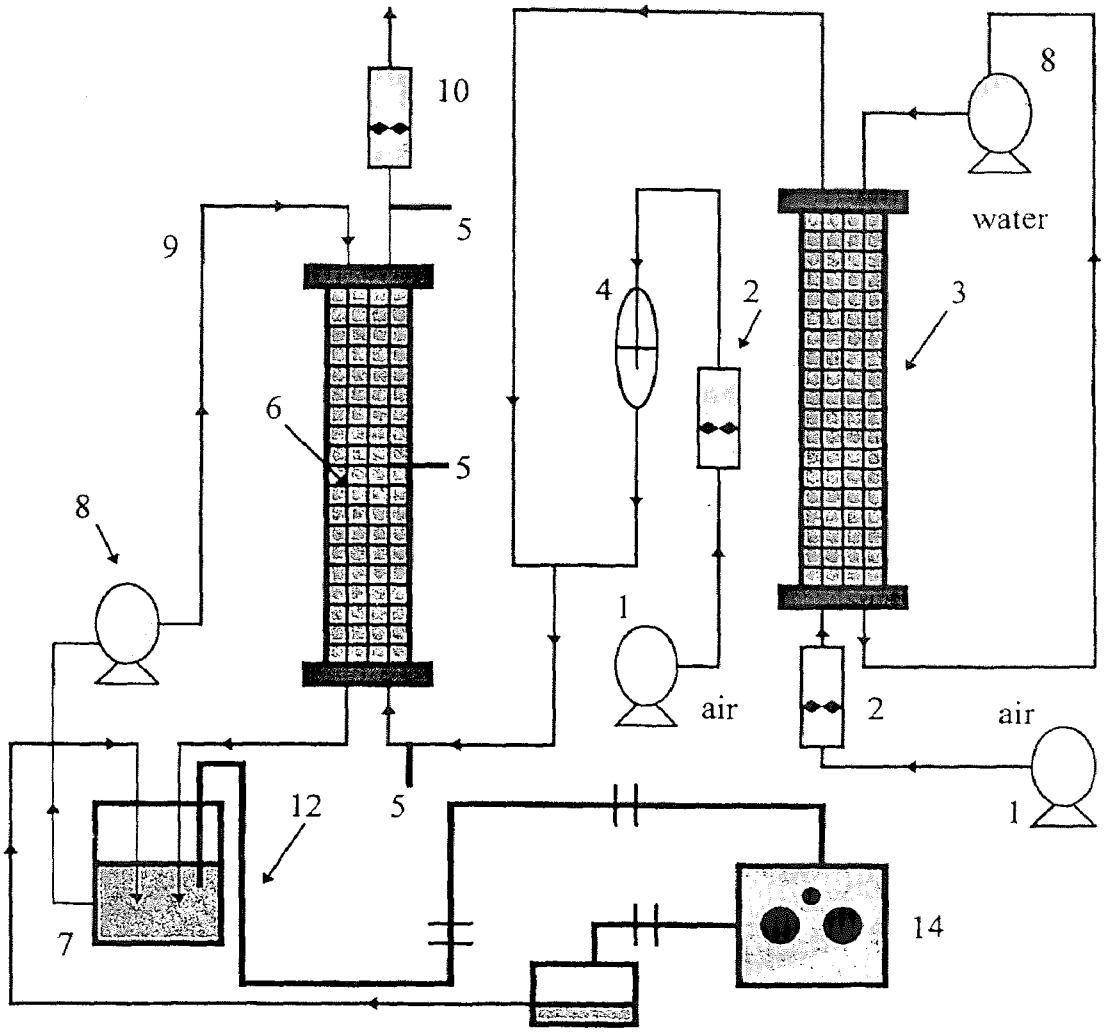

Figure 4.1: Schematic of the experimental biotrickling filter unit: (1) air pump, (2) rotameter assembly, (3) humidification tower, (4) solvent tank, (5) sampling port, (6) biotrickling filter, (7) tank for recirculating liquid, (8) peristaltic pump, (9) recirculating liquid line, (10) air flow meter, (11) exhaust,(12) pH-electrode, (13) NaOH solution tank, (14) pH-controller.

then mixed (see Figure 4.1) with a low flowrate airstream carrying the m-CB and/or o-DCB vapor obtained via bubbling through pure liquid solvents present in closed vessels.

Proper adjustment of the flowrates of the two airstreams allowed for variation, as desired, of the pollutant(s) concentration in the air supplied to the biofilter and the residence time of the air in the filter bed. A rotameter assembly (75-350, Gow-Mac Instrument Co., Bound Brook, NJ), was used to vary inlet solvent vapor concentrations independently, by directing a greater or smaller part of the airstream through the solvent vessels.

The liquid stream which trickled through the bed was recirculated after its pH was adjusted at the exit of the filter bed through automated NaOH solution addition using a pH-controller (Chemcadet model, Cole-Parmer Instrument Co., Niles, IL). The liquid, which also carried detached biomass, was discarded on a daily basis and replenished with an equal volume (4 L) of fresh medium. Some experiments, performed in order to determine the effect of the frequency of medium replenishment on the process, involved medium change at varying time intervals.

In order to ensure good liquid distribution in trickling filters it has been reported that the ratio of the bed diameter (d_C) to the particle diameter (d_p) should be at least equal to eight and the liquid should be supplied through at least 100 distributions points per m^2 of bed cross sectional area (Eckert, 1961, 1975). The d_C/d_p ratio for the m-CB unit used in this study was almost 8 (7.98 to be exact) and for the o-DCB and m-CB/o-DCB mixture units was 9. Six liquid distribution points were used. The aforementioned criterion suggested at least two distribution points.

Biomass produced during operation was practically removed during medium replenishment. In addition, at sparse intervals (15 days apart) an amount of 20 L of

medium was flushed through the column over a period of 10 min to ensure excess biomass removal. No difference in process performance was observed before and after the column was flushed with medium. The column operated without any detectable pressure drop.

Experiments were performed at room temperature (about 25°C) and each run under a given set of operating conditions (inlet pollutant concentration, liquid and air flow rate, etc.) lasted for a minimum of 24 h. Significant temperature variations in the laboratory were rare and when they occurred data were not collected.

Process start-up involved development of the filter bed as follows. Originally, the column contained no solid particles and was charged with 3 L of medium having the composition given earlier. The medium was inoculated with some biomass pregrown in closed flasks as described in the preceding section. The inoculated medium was bubbled with air containing solvent(s) vapor at a concentration of 2 g m^{-3} for about 2 days. By then, a noticeable change in optical density of the liquid had occurred , indicating growth of the culture. The column was then packed with ceramic saddles to a certain height and additional fresh culture medium was added so that the solids were entirely submerged. Air, carrying pollutant(s) at 2 gm^{-3}, was bubbled through the submerged filter. The column was drained every 2-3 days, aerated with pure air for about 1 h, and filled again with fresh medium before pollutant-laden air supply resumed. The procedure was repeated for about one month and led to development of biofilms on the surface of the solids. At that point, the liquid was drained off the column and the unit started being operated in the trickling mode.

4.3 Analytical Methods

The m-CB and o-DCB concentrations were monitored by subjecting air samples to gas chromatographic (GC) analysis. The GC unit used was a Hewlett-Packard model 5890 Series II (Hewlett-Packard, Paramus, NJ) equipped with a 6′ x 1/8″ stainless steel column packed with 80/100 Carbopack C/0.1% SP-1000 (Supelco Inc., Bellefonte, PA), and a flame ionization detector (FID). Nitrogen at 21 mL/min and 21 psig was used as carrier gas, while hydrogen at 26.3 mL/min and 14 psig was used for the detector. The injection port, oven, and detector of the GC unit were operated at 200°C. The retention time was 3.83 min for m-CB and 8.76 min for o-DCB. The area of the peaks in the chromatograms was determined by an HP3396A integrator (Hewlett-Packard, Paramus, NJ) to which the GC unit was connected. The GC calibration was repeated on a weekly basis.

Biomass concentration during kinetic runs was measured spectrophotometrically following procedures and calibrations described by Dikshitulu et al. (1993) and Wang et al. (1995).

CHAPTER 5

BIODEGRADATION KINETIC STUDIES

5.1 General Approach

The key-process in biofiltration is oxidation of pollutants by microorganisms. The microorganisms act as catalysts for the process and in many instances biomass is also a product of the reaction. Consequently, biofiltration is affected by reaction kinetics and type of catalyst (biomass). Once microorganisms capable of completely mineralizing the target VOCs have been isolated/developed, one needs to know the rate at which they are capable of destroying these VOCs. These reaction rates (kinetics) depend on the level of VOC presence, oxygen, other nutrients, pH, and temperature (Baltzis, 1998).

In this chapter the results of a detailed kinetic study of biodegradation of chlorinated VOCs namely, mono-chlorobenzene (m-CB) and ortho-dichlorobenzene (o-DCB) and their mixtures are presented. The study involved experiments with suspended cultures in closed serum bottles. The kinetic expressions revealed based on these experiments were subsequently used in describing removal of m-CB and o-DCB vapors in biotrickling filters. This was done based on the commonly made assumption, discussed by Karel et al (1985), that the inherent biodegradation kinetics are the same regardless of whether the microbial cells are suspended in nutrient medium or immobilized on a solid support as in the case of biotrickling filters.

The general experimental protocol was as follows. The first group of experiments involved two series of runs under a constant temperature of 30 °C and a pH of 7.0±0.1. In the first series, biodegradation experiments involving m-CB were performed by using a m-CB utilizing consortium. The second series involved experiments with m-CB at various concentrations using (again in suspension) biomass obtained from a biotrickling filter which had been used for removal of m-CB vapor over a period of 8 months. The filter bed was originally inoculated with the m-CB utilizing consortium used in the first series of kinetic experiments mentioned above. The second series of experiments was performed as a means of indirectly finding out whether the biomass undergoes changes over time when used in a filter bed and in order to, also indirectly, determining whether intrinsic kinetics are the same in suspensions and biofilms.

The first group of experiments was performed with a consortium which could not utilize o-DCB. A second consortium capable of completely mineralizing both m-CB and o-DCB was used in the second group of kinetic experiments. For distinction with the first consortium the second one will be referred to as the o-DCB utilizing consortium. As with the first group, the second group of experiments also involved two series of runs under a constant temperature and a pH of 7.0±0.1. The first series involved experiments with m-CB at various concentrations. In the second, biodegradation experiments involving o-DCB at various concentrations were performed.

The third group of experiments was performed with the o-DCB consortium and media containing both m-CB and o-DCB at different relative concentrations. The major

objective of the study with mixtures was to determine whether there is a kinetic interference from o-DCB on m-CB and vice versa.

Finally, a fourth group of experiments involved investigation of the effect of pH. There were two series of runs. The first involved media containing m-CB only and the catalyst was a m-CB utilizing consortium, and the second was with media containing o-DCB only and the experiments were performed with the o-DCB consortium.

5.2. Modeling of Kinetics of Individual VOCs Under Constant pH

Determination of the specific growth rate μ, of a population on a particular substrate from well shaken serum bottle experiments is based on the assumption that μ remains constant during the run when biomass maintenance requirements can be neglected.

From the equation:

$$\frac{db}{dt} = \mu_j(C_{Lj})b \tag{5.1}$$

one can get upon integration

$$\ln\frac{b}{b_0} = \mu_j(C_{Lj})t \tag{5.2}$$

Equation (5.2) implies that when biomass data are plotted versus time on a semilogarithmic scale, they should be on a straight line of slope $\mu_j(C_{Lj})$. This slope is taken as the specific growth rate of the population at the substrate concentration value in the beginning of the run. From experiments at different initial substrate concentrations one can generate $\mu_j(C_{Lj})$ values at various C_{Lj}. Each $\mu_j(C_{Lj})$ value requires a semilogarithmic plot as discussed above. For the biodegradation of volatile compounds,

collection of a large number of biomass data during a run is problematic. This is due to the fact that the flask needs to be sealed and the liquid volume small relative to the airspace so that oxygen limitation is avoided. Frequent sampling is much simpler in the gas phase. Air samples generate concentration values, C_{Gj}, of the volatile substrate in the gas phase and these data can be equivalently used for determination of specific growth rates as follows. Let M_j be the total mass of the volatile substrate in the flask, both in the gas and liquid phase. One can write the following mass balances

$$\frac{dM_j}{dt} = -\frac{1}{Y_j}\mu_j(C_{Lj})bV_L \tag{5.3}$$

$$M_j = V_L C_{Lj} + V_G C_{Gj} \tag{5.4}$$

Furthermore, assuming that the volatile substrate is distributed between the two phases as dictated by thermodynamic equilibrium (Henry's law), one has

$$C_{Gj} = m_j C_{Lj} \tag{5.5}$$

When, as was done in the present study, the liquid phase is sampled only in the beginning and end of the run, V_L and V_G can be taken as constant and then combination of equations (5.3)-(5.5) leads to

$$\frac{dC_{Gj}}{dt} = -\frac{m_j V_L}{V_L + m_j V_G}\frac{1}{Y_j}\mu_j(C_{Lj})b \tag{5.6}$$

Combining equations (5.1) and (5.6) one gets

$$\frac{dC_{Gj}}{dt} = -\frac{m_j V_L}{V_L + m_j V_G}\frac{1}{Y_j}\frac{db}{dt} \tag{5.7}$$

which upon integration yields

$$Y_j = \frac{m_j(b - b_0)V_L}{(C_{Gj,0} - C_{Gj})(V_L + m_j V_G)} \tag{5.8}$$

Combining equations (5.4) and (5.5) one gets

$$M_j = C_{Gj}\left(\frac{m_j V_G + V_L}{m_j}\right) \tag{5.9}$$

which when evaluated at t = 0 yields

$$M_{j,0} = C_{Gj,0}\left(\frac{m_j V_G + V_L}{m_j}\right) \tag{5.10}$$

Combining equations (5.8) and (5.10) one gets

$$Y_j = \frac{(b - b_0)V_L}{M_{j,0} - \frac{C_{Gj}(V_L + m_j V_G)}{m_j}} \tag{5.11}$$

which can be also written as

$$b = b_0 + \frac{Y_j M_{j,0}}{V_L} - \frac{Y_j(V_L + m_j V_G)}{m_j V_L} C_{Gj} \tag{5.12}$$

Equation (5.12) can be used for converting gas phase VOC concentration measurements (C_{Gj}) to biomass values provided that the yield coefficient is known.

Equation (5.11) allows for Y_j determination from two data points on biomass concentration. If an experiment is allowed to run over a long period of time so that the entire amount of the pollutant has been used (5.11) becomes

$$Y_j = \frac{(b_f - b_0)V_L}{M_{j,0}} \tag{5.13}$$

Equation (5.13) was used for determining the yield coefficient in this study. The mass of solvent used in each run ($M_{j,0}$) was determined from the liquid volume (V_{Sj}) injected in the serum bottle and the liquid density of the pollutant (ρ_{Sj}) as follows.

$$M_{j,0} = \rho_{Sj} V_{Sj} \tag{5.14}$$

During each experimental run involving a single compound, the headspace of the serum bottle was frequently sampled. After GC analysis of each sample the C_{Gj} value was determined and from it -via equation (5.12)- the corresponding value of b. The logarithm of b values was then taken and the resulting values, as a function of time, were regressed to a straight line using a least squares method for error minimization. The slope of the regressed line determines, according to equation (5.2), the value of $\mu_j(C_{Lj})$ at the liquid phase substrate concentration of the particular experimental run (where the regression starts). Both in the m-CB and o-DCB case, when the $\mu_j(C_{Lj})$ versus C_{Lj} data were plotted, it was clear that $\mu_j(C_{Lj})$ drops at high C_{Lj} values. For this reason, the data were regressed to the Andrews (1968) expression

$$\mu_j(C_{Lj}) = \frac{\mu_j^* C_{Lj}}{K_j + C_{Lj} + \frac{C_{Lj}^2}{K_{Ij}}} \tag{5.15}$$

by using a non-linear regression routine for error minimization.

Expression (5.15) involves three kinetic constants which do not really have a physical significance; K_j and K_{Ij}, have units of concentration-same as C_{Lj}- and μ^*_j has units of inverse time; constant K_{Ij} is known as the inhibition constant. In many instances, μ^*_j is

referred to in the literature as the maximum specific growth rate; this is not correct. In fact, expression (5.15) predicts a maximum specific growth rate given by

$$\mu_j\left(C_{Lj}^{*}\right) = \mu_{max\,j} = \frac{\mu_j^{*}}{1+2\sqrt{\frac{K_j}{K_{Ij}}}} \qquad \text{where} \qquad C_{Lj}^{*} = \sqrt{K_j K_{Ij}} \tag{5.16}$$

Expression (5.15) implies that high substrate concentrations inhibit growth, and according to Shuler and Kargi (1992), it could imply a noncompetitive substrate inhibition pattern when $K_{Ij} >> K_j$.

5.3. Modeling of Kinetics of VOC Mixtures Under Constant pH

When modeling mixtures, the first task is to experimentally determine whether there is kinetic interference between the two substrates. For this reason, and using the methodology of Wang et al. (1996), the data were first used in determining an average value for the specific (i.e. per unit amount of biomass) removal rate of substrate 1 (R_1) and 2 (R_2). The values of R_j, j = 1,2 were calculated using the equation

$$R_j = \frac{(C_{Lj,0} - C_{Lj,n})\sum_{\kappa=0}^{n} t_\kappa}{(t_n - t_0)\sum_{\kappa=0}^{n} t_\kappa b_\kappa}, \; j = 1,2 \tag{5.17}$$

Quantities R_j were only used in order to qualitatively determine the type of interaction between the two substrates. Once it was determined that the two substrates were involved in cross-inhibition, the time concentration profiles were used in revealing the type of cross-inhibition and the values of the corresponding interaction constants.

For the case of two volatile compounds, each one of which can serve as primary carbon and/or energy source for the culture employed, the following mass balances can be written when the process occurs in a closed vessel:

$$\frac{dC_{Gj}}{dt} = -\frac{m_j V_L}{V_L + m_j V_G}\frac{1}{Y_j}\mu_j(C_{Lj}, C_{Lp})b, \qquad j,p = 1,2, \quad j \neq p \tag{5.18}$$

Equation (5.18) is a version of equation (5.6) for the case of mixtures of two VOCs involved in kinetic interactions. Expressions μ_j (C_{Lj}, C_{Lp}) represent the specific growth rate of the biomass on substrate j and are functions of the availability (concentration) of both resources. As has been shown by Oh et al. (1994), gas phase substrate concentration data can be converted to biomass concentration through the following expression

$$b = b_0 + \frac{1}{V_L}\sum_{j=1}^{2}\left[Y_j M_{j,0} - \frac{Y_j(V_L + m_j V_G)}{m_j}C_{Gj}\right] \tag{5.19}$$

The functional form of μ_j (C_{Lj}, C_{Lp}) used in this study is

$$\mu_j(C_{Lj}, C_{Lp}) = \frac{\mu_j^{\bullet} C_{Lj}}{K_j + C_{Lj} + \frac{C_{Lj}^2}{K_{Ij}} + K_{2j}C_{Lp}}, \qquad j,p = 1,2, \quad j \neq p \tag{5.20}$$

Expression (5.20) expresses competitive inhibition between two substrates. Constants K_{2j}, are dimensionless and can be called cross-inhibition constants; their magnitude indicates the intensity of the kinetic interaction between the two substrates. As discussed by Wang et al. (1996); if one of the K_{2j} values is equal to zero we have competitive partial inhibition. If both of K_{2j} are equal to zero, expressions (5.20) reduce to the Andrews model.

Determination of the K_{2j}; j = 1,2 values was done as follows. It was first assumed that the values of all parameters (except K_{2j}) in expressions (5.20) are those obtained from the kinetic studies with each one of the two compounds individually. With this assumption; gas phase time concentration profiles of the two compounds obtained from GC analysis of headspace samples were fitted to the solution of equations (5.18)-(5.20) using a 4^{th}-order Runge-Kutta algorithm and attempting to minimize the square of the errors via a trial and error approach.

5.4 pH Effects

During the course of this study experiments were performed at different pH values in order to reveal and quantify the dependence of the specific growth rate on pH. The data from runs at a given value of substrate concentration were modeled by drawing an analogy between enzyme kinetics and kinetics of microbial growth as had been done earlier by Antoniou et al. (1990) and Wang et al. (1995). The expression used is the following:

$$\mu_j = \frac{\delta_j}{1 + \frac{[H^+]}{K_{H1j}} + \frac{K_{H2j}}{[H^+]}} \tag{5.21}$$

Using the expression above, one can show that it becomes maximum when

$$[H^+] = \sqrt{K_{H1j} K_{H2j}} \tag{5.22}$$

Expression (5.22) implies that

$$pH_{j,opt} = \frac{1}{2}\left(pK_{H1j} + pK_{H2j}\right) \tag{5.23}$$

5.5 Results and Discussion

Following are the results from the kinetic studies and their modeling based on the equations discussed in Sections 5.2-5.4.

5.5.1 Biodegradation Kinetics of Individual Chlorinated VOCs at constant pH

A number of runs were performed with each compound (m-CB and o-DCB) and with initial liquid phase concentrations of up to 70 gm^{-3}. In all experiments the initial biomass concentration was kept bellow 40 gm^{-3}. In analyzing the data, the values used for the distribution coefficients (Henry's constants) were 0.167 for m-CB, and 0.119 for o-DCB. The biomass concentration data from each experimental run were plotted semilogarithmically versus time as shown in Figure 5.1 [(a): m-CB substrate, m-CB consortium,; (b): o-DCB substrate, o-DCB consortium]. The initial points (after equilibrium was attained in the bottle) in the lnb versus t plane were regressed to a straight line by using the method of least squares. The slope of the line was taken as the specific growth rate μ_j at the initial m-CB or o-DCB liquid phase concentration of the run. The values for the specific growth rate were plotted versus the corresponding substrate concentration values as shown in Figures 5.2-5.4. Both consortia exhibited a qualitatively similar behavior toward each one of the two substrates. As can be seen from the figures, after an initial increase, the specific growth rate drops at high substrate concentrations, i.e. the data suggested substrate inhibition kinetics. The data were then regressed to the Andrews expression (5.15). Regression was performed by using a numerical routine based on the Gauss and Marquardt methods and performs optimal

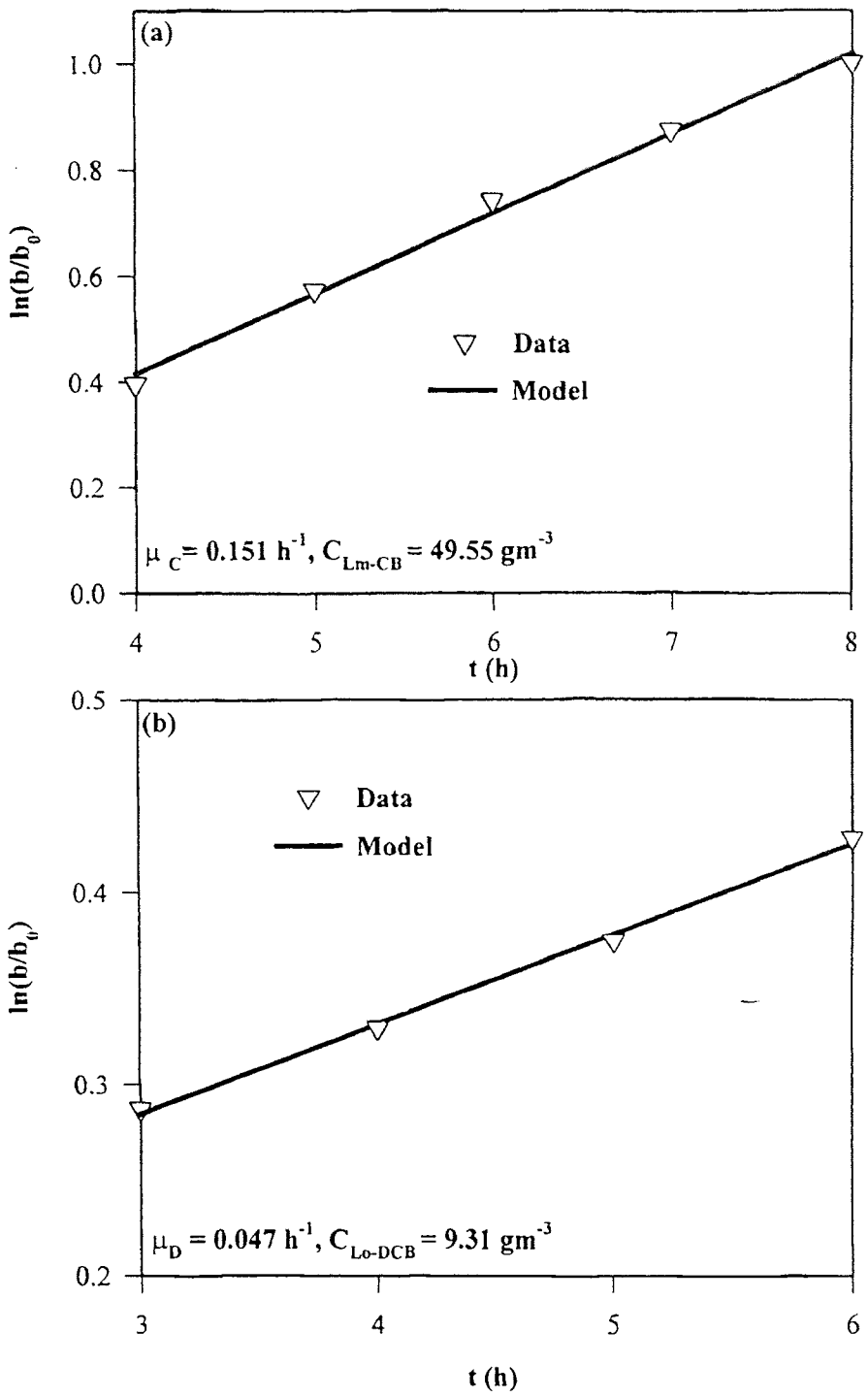

Figure 5.1 Biomass concentration versus time on a semilogarithmic scale. The slope of the straight line is taken as the specific growth rate of the population at the substrate concentration in the beginning of the run. Used consortium, substrate, and initial biomass concentration are (a): m-CB, m-CB, and 27.9 gm^{-3} and (b): o-DCB, o-DCB, and 26.5 gm^{-3}.

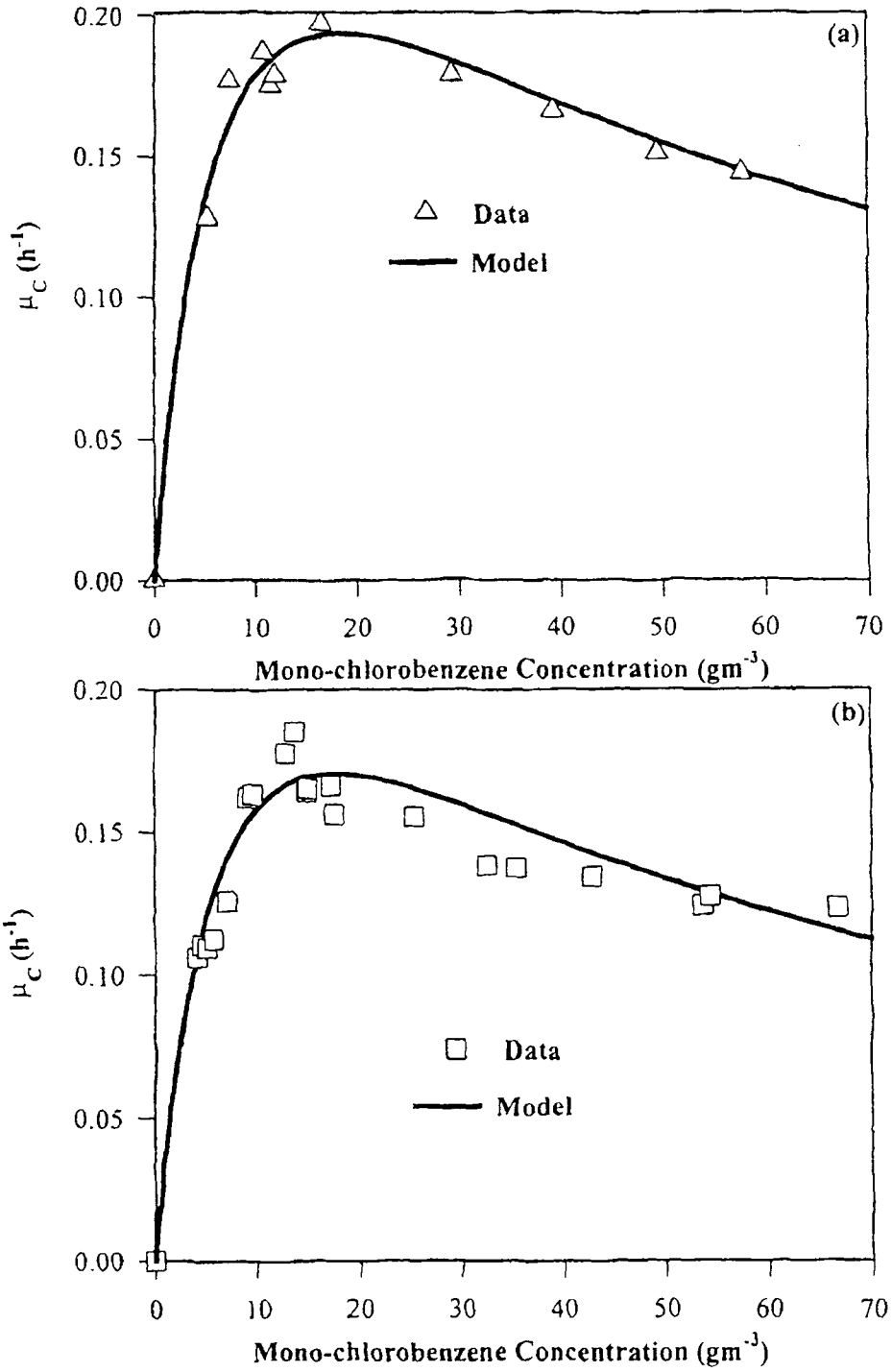

Figure 5.2 Specific growth rate of (a) original biomass (m-CB consortium) and (b) column culture as a function of mono-chlorobenzene concentration in the liquid medium. Data (symbols) from suspended culture experiments at pH = 7.0 have been fitted to the Andrews model (curves).

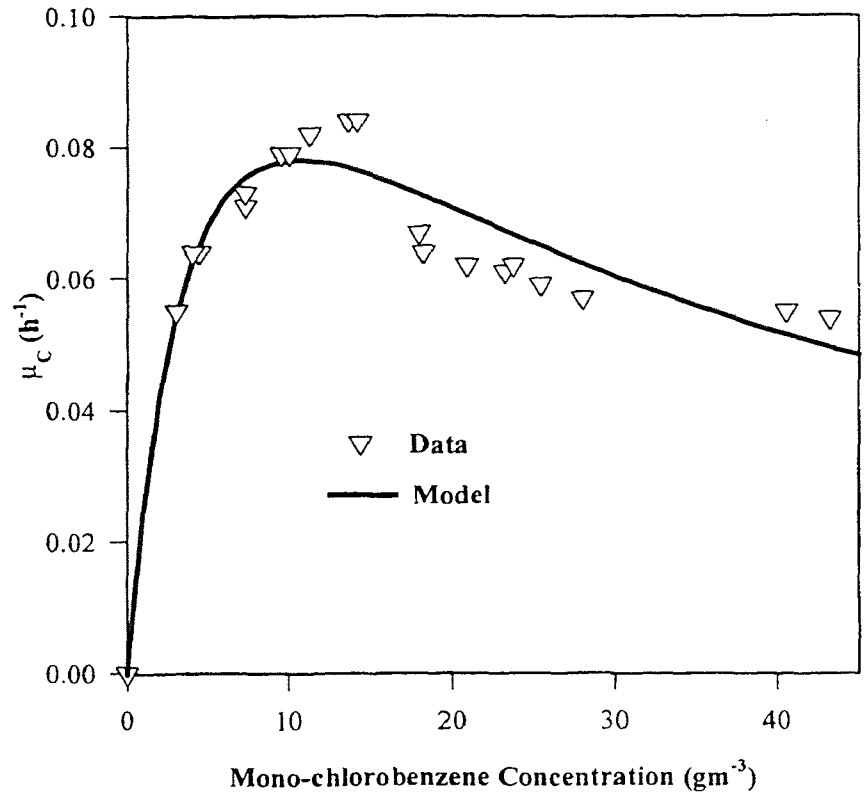

Figure 5.3 Specific growth rate of original biomass (o-DCB consortium) as a function of mono-chlorobenzene concentration in the liquid medium. Data (symbols) from suspended culture experiments at pH = 7.0 have been fitted to the Andrews model (curve).

parameter search in a VAX/VMS platform. The values obtained for the three constants appearing in expression (5.15) are shown in Table 5.1 for m-CB and in Table 5.2 for o-DCB substrate, respectively. Based on these constants, the curves representing the specific growth rate have been generated and are plotted in Figures 5.2-5.4. As can be seen from these graphs there is very good agreement between fitted curves and data. It should be mentioned that convergence to the reported values was obtained regardless of the values used as initial guesses. The maximum specific growth rates on m-CB (Table 5.1) and o-DCB (Table 5.2) were calculated using equation (5.16). The values of the yield coefficients reported in Tables 5.1 and 5.2 were obtained via equations (5.13)

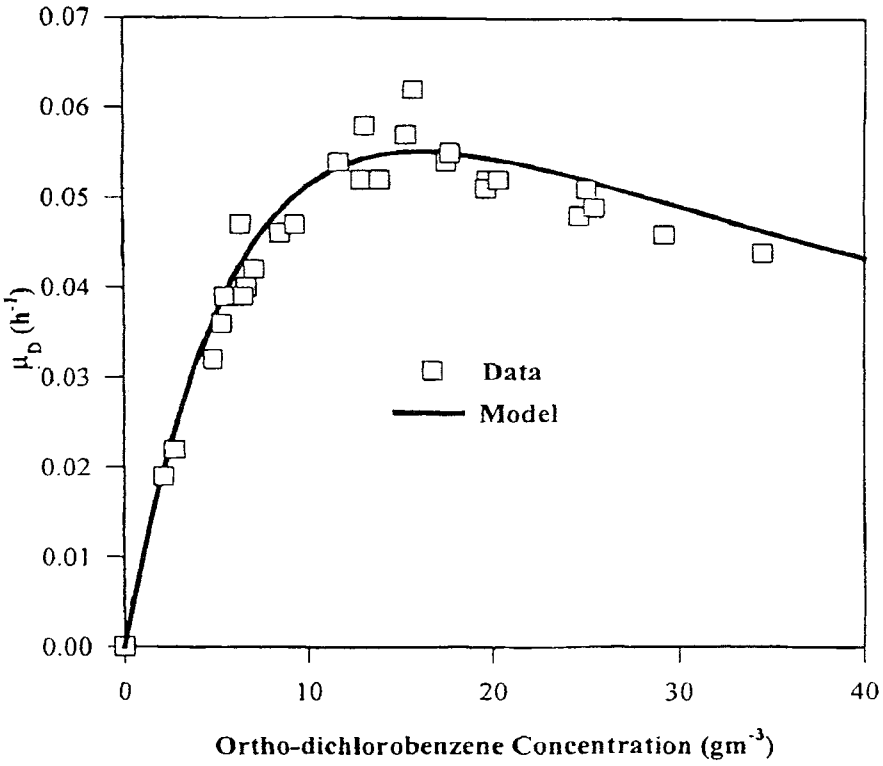

Figure 5.4 Specific growth rate of original biomass (o-DCB consortium) as a function of ortho-dichlorobenzene concentration in the liquid medium. Data (symbols) from suspended culture experiments at pH = 7.0 have been fitted to the Andrews model (curves).

Table 5.1. Growth characteristics and parameters of the mono-chlorobenzene and ortho-dichlorobenzene consortium on mono-chlorobenzene.

Mono-chlorobenzene (Andrews Kinetics)			
	m-CB consortium	suspension from BTF	o-DCB consortium
Kinetic Parameters			
μ^*_C (h^{-1})	0.352	0.320	0.154
K_C (gm^{-3})	7.437	7.782	5.140
K_{IC} (gm^{-3})	44.419	40.076	21.883
Maximum specific growth rate (h^{-1})	0.194	0.171	0.078
Yield Coefficient (gg^{-1})	0.579	0.579	0.553

Table 5.2. Growth characteristics and parameters of the ortho-dichlorobenzene consortium on ortho-dichlorobenzene.

Ortho-dichlorobenzene (Andrews Kinetics)	
Kinetic parameters	
μ^*_D (h^{-1})	0.146
K_D (gm^{-3})	13.389
K_{ID} (gm^{-3})	19.657
Maximum specific growth rate (h^{-1})	0.055
Yield Coefficient (gg^{-1})	0.398

and (5.14). Once the kinetic constants were determined, equation (5.6) was numerically integrated while simultaneously using equations (5.12) and (5.15). A fourth-order Runge-Kutta routine was used for the integration. The numerically obtained time concentration profiles agreed nicely with the experimental data. Examples are given in Figures 5.5-5.8.

Based on the results obtained from the kinetic studies the following conclusions can be reached.

1. The maximum specific growth rate of the m-CB consortium on m-CB is considerably (almost 2.5 times) higher than that of the o-DCB consortium on m-CB. Taking into account (Table 5.1) the fact that the yield coefficients of both consortia on m-CB are almost equal one can easily conclude that at the same initial biomass and substrate concentration, the biodegradation rate of m-CB when the m-CB consortium is used is much higher than that obtained with o-DCB consortium. With simple calculations one can also see that the ratio of the specific growth rates of the m-CB consortium to

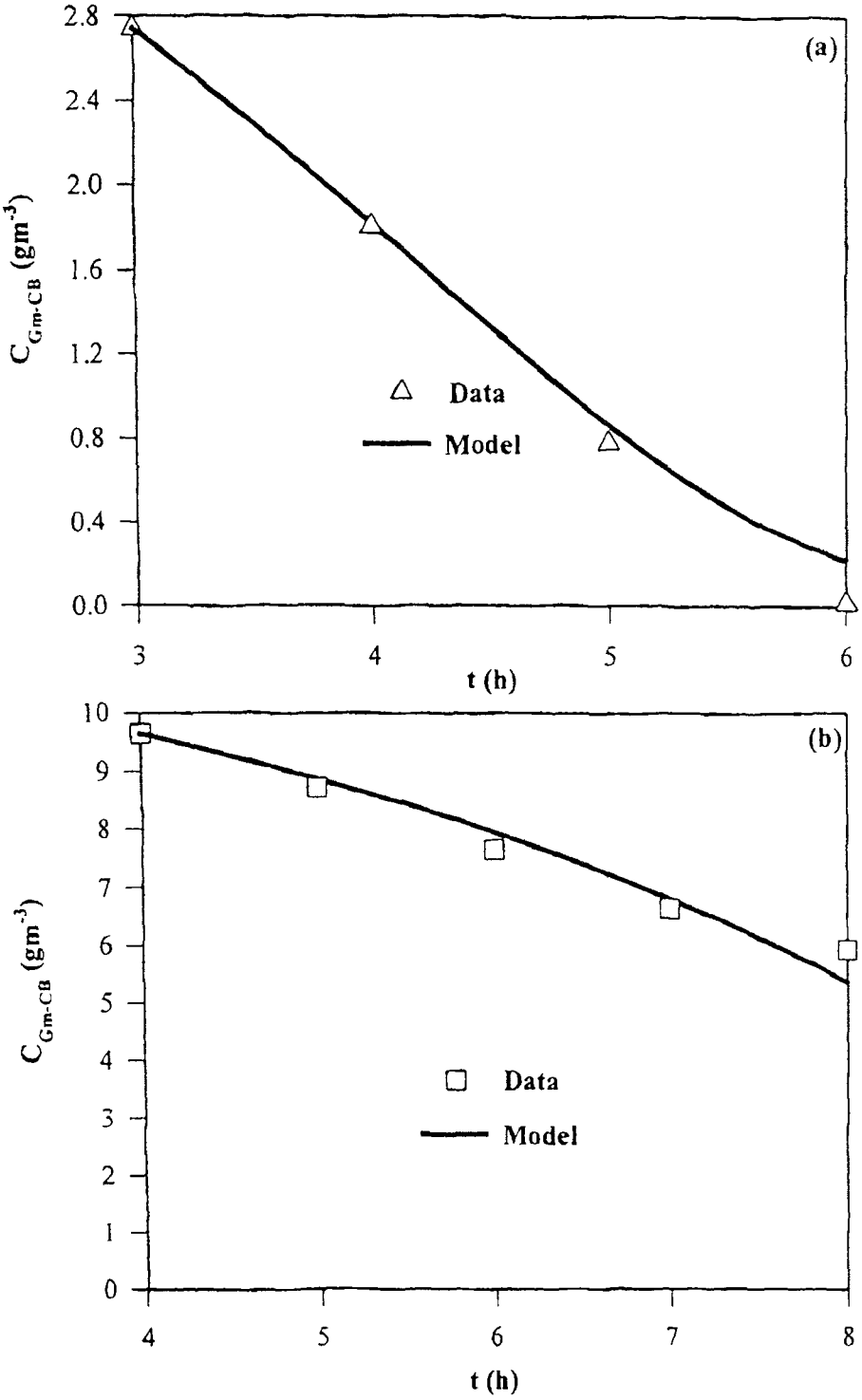

Figure 5.5 Comparison between experimental data (symbols) and model predicted concentration profiles for m-CB when the m-CB consortium is used. Initial liquid phase m-CB and biomass concentrations are (a): 16.4 and 23.3 gm^{-3} and (b): 57.8 and 28.6 gm^{-3}, respectively.

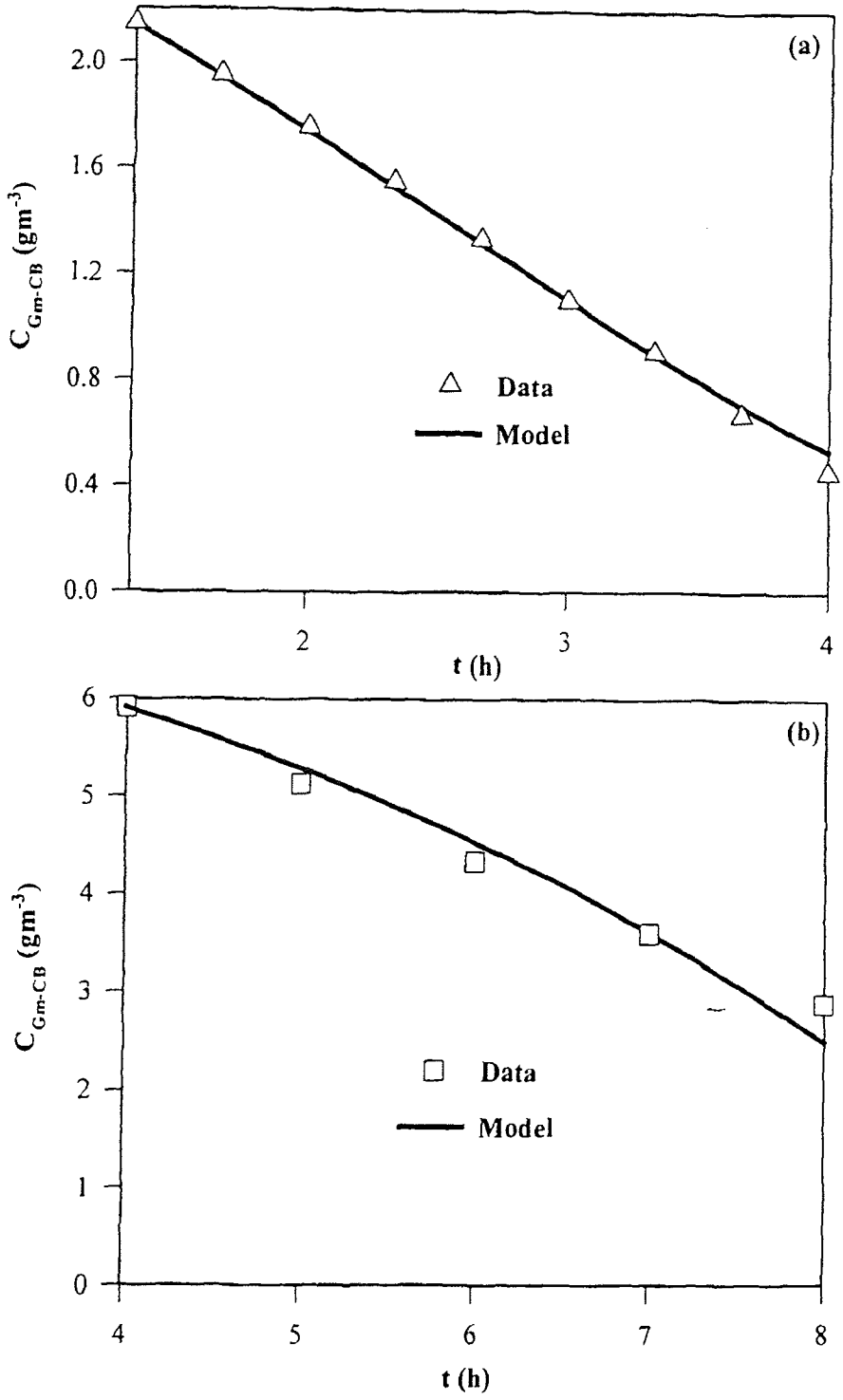

Figure 5.6 Comparison between experimental data (symbols) and model predicted concentration profiles for m-CB when the column culture is used. Initial liquid phase m-CB and biomass concentrations are (a): 12.9 and 34.2 gm^{-3} and (b): 35.4 and 19.2 gm^{-3}, respectively.

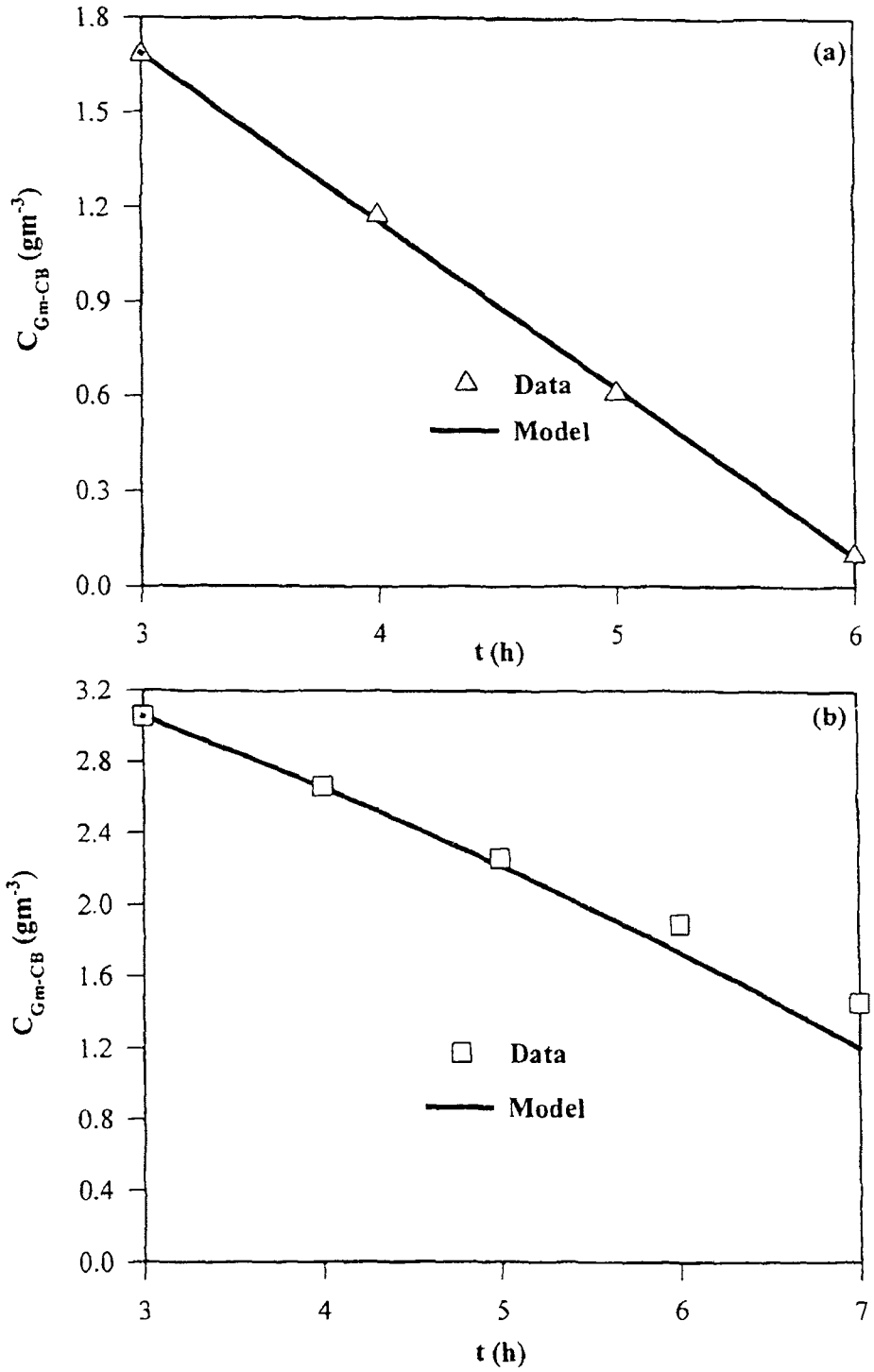

Figure 5.7 Comparison between experimental data (symbols) and model predicted concentration profiles for m-CB when the o-DCB consortium is used. Initial liquid phase m-CB and biomass concentrations are (a): 10.1 and 39.2 gm^{-3} and (b): 18.3 and 30.5 gm^{-3}, respectively.

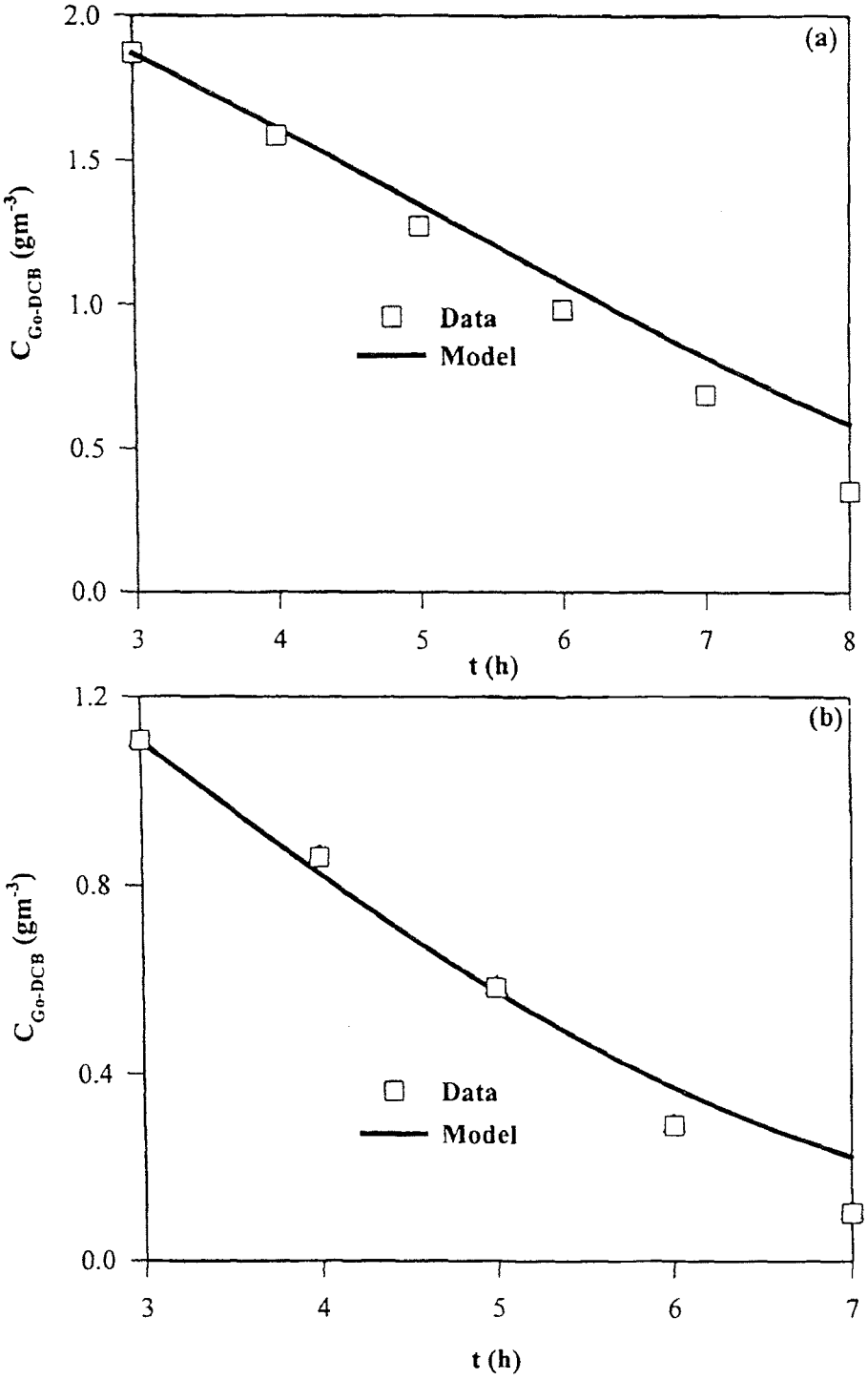

Figure 5.8 Comparison between experimental data (symbols) and model predicted concentration profiles for o-DCB when the o-DCB consortium is used. Initial liquid phase o-DCB and biomass concentrations are (a): 15.7 and 18.6 gm^{-3} and (b): 9.3 and 26.5 gm^{-3}, respectively.

that of the o-DCB consortium increases with the m-CB concentration. This ratio for example, is 2.2 at an m-CB concentration of 10 gm^{-3} and becomes 3.3 at 50 gm^{-3}. This implies that the o-DCB consortium is inhibited more than the m-CB consortium at elevated m-CB concentrations.

2. Regarding the o-DCB consortium, its maximum specific growth rate on o-DCB is much lower when compared to the maximum specific growth rate of the same consortium on m-CB (0.055 versus 0.078 h^{-1}). On the other hand, the same consortium is a more

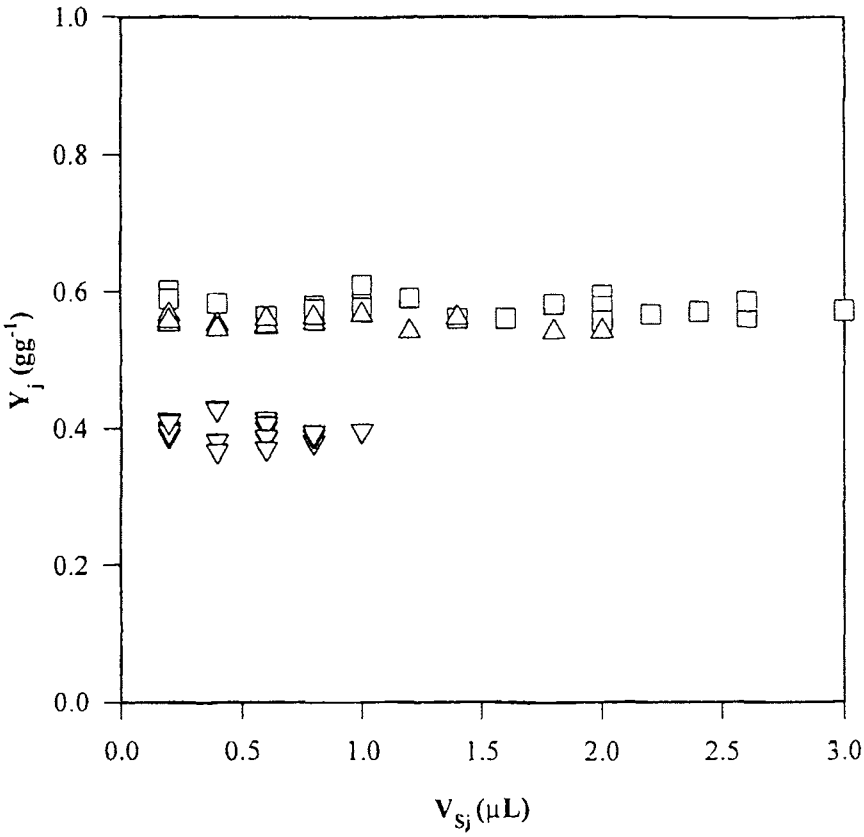

Figure 5.9 Experimentally measured yield coefficients as a function of liquid VOC volume injected in the serum bottles. Mono-chlorobenzene data with the m-CB consortium are shown as □, mono-chlorobenzene data with the o-DCB consortium are shown as Δ and ortho-dichlorobenzene data with the o-DCB consortium are shown as ∇.

efficient user of o-DCB as refllected by the higher yield coefficient. Using the kinetic constants and the yield coefficient values one can easily calculate biodegradation rates at various substrate concentration values. For comparisons, one can calculate m-CB and o-DCB degradation rates using the same biomass and substrate concentration values. Such calculations show that the o-DCB degradation is slightly faster than that of m-CB. The ratio of such rates is 1.05 at a substrate concentration of 10 gm^{-3} and increases to 1.28 when the concentration reaches 50 gm^{-3}.

It was assumed, as stated in Section 5.2, that biomass maintenance requirements are negligible. The implication of this assumption is that the yield coefficient is constant and not a function of substrate concentration. This assumption is well justified by the data, as shown in Figure 5.9. Yield coefficients were calculated via equations (5.13) and (5.14), and less than a 5% variation around an average value was observed in all cases.

5.5.2 Biodegradation Kinetics of Chlorinated VOC Mixtures

As mentioned earlier, kinetic experiments with mixtures of the two substrates (m-CB and o-DCB) were performed by using the o-DCB consortium which is capable of utilizing both m-CB and o-DCB as sole carbon and energy sources. The first important finding from these experiments was that the two substrates were simultaneously used by the biomass. In order to determine whether the two substrates are involved in kinetic interactions a number of experimental runs were designed and carried out. These runs were performed with the same volume of liquid medium and can be classified into two

categories. In the first category (see Table 5.3) the initial m-CB concentration (equivalently, the initial volume of liquid m-CB injected into the serum bottles) was kept

Table 5.3. Average specific rate of m-CB removal (R_1) by the o-DCB consortium in the presence of o-DCB.

Experiment	$V_{Sm\text{-}CB}$ (μL)	$V_{So\text{-}DCB}$ (μL)	R_1 (g-m-CB h^{-1} g^{-1}-biomass)
1	1.0	1.0	0.0333
2	1.0	0.6	0.0353
3	1.0	0.2	0.0445
4	1.0	0.0	0.0536
5	0.6	1.0	0.0395
6	0.6	0.6	0.0460
7	0.6	0.2	0.0544
8	0.6	0.0	0.0630
9	0.2	1.0	0.0239
10	0.2	0.6	0.0247
11	0.2	0.2	0.0278
12	0.2	0.0	0.0393

constant whereas the initial o-DCB concentration was varied. In the second category (see Table 5.4) the opposite happened. For each run the values of average specific rates of substrate removal (R_j) were calculated using equation (5.17) in conjunction with equation (5.19). Values of R_1 and R_2 are shown in Tables 5.3 and 5.4. From Table 5.3, it is obvious that when the initial m-CB concentration remains constant and that of o-DCB decreases the specific rate of m-CB removal increases. Hence, o-DCB exerts inhibition on m-CB removal. Similarly, from Table 5.4 one can see that for a given initial o-DCB concentration the specific rate of o-DCB removal increases as the m-CB presence

decreases. Hence, one can conclude that the two substrates interact at the kinetic level via a cross-inhibitory pattern.

Due to the structural similarity of the two substrates, it was assumed that their

Table 5.4. Average specific rate of o-DCB removal (R_2) by the o-DCB consortium in the presence of m-CB.

Experiment	$V_{So\text{-}DCB}$ (μL)	$V_{Sm\text{-}CB}$ (μL)	R_2 (g-o-DCB h^{-1} g^{-1}-biomass)
1	1.0	1.0	0.0315
5	1.0	0.6	0.0385
9	1.0	0.2	0.0488
13	1.0	0.0	0.0586
2	0.6	1.0	0.0305
6	0.6	0.6	0.0372
10	0.6	0.2	0.0463
14	0.6	0.0	0.0564
3	0.2	1.0	0.0190
7	0.2	0.6	0.0196
11	0.2	0.2	0.0240
15	0.2	0.0	0.0411

cross-inhibitory interaction is of the competitive type and thus, specific growth rates can be described by expression (5.20). The m-CB and o-DCB data from experiments 2, 5, 7, and 11 (Tables 5.3 and 5.4) were used for determining the values of the interaction constants K_{2j}, j = 1,2. This was done by fitting the data to the solution of equations (5.18)-(5.20). A 4^{th}-order Runge-Kutta algorithm was used. With all parameters except K_{2j} known from the single substrate experiments (Section 5.5.1), values for K_{2j} were assumed, the equations were integrated and the computer generated concentration profiles were compared to the experimental data. The values of 0.75 and 1.32 for K_{21} and K_{22},

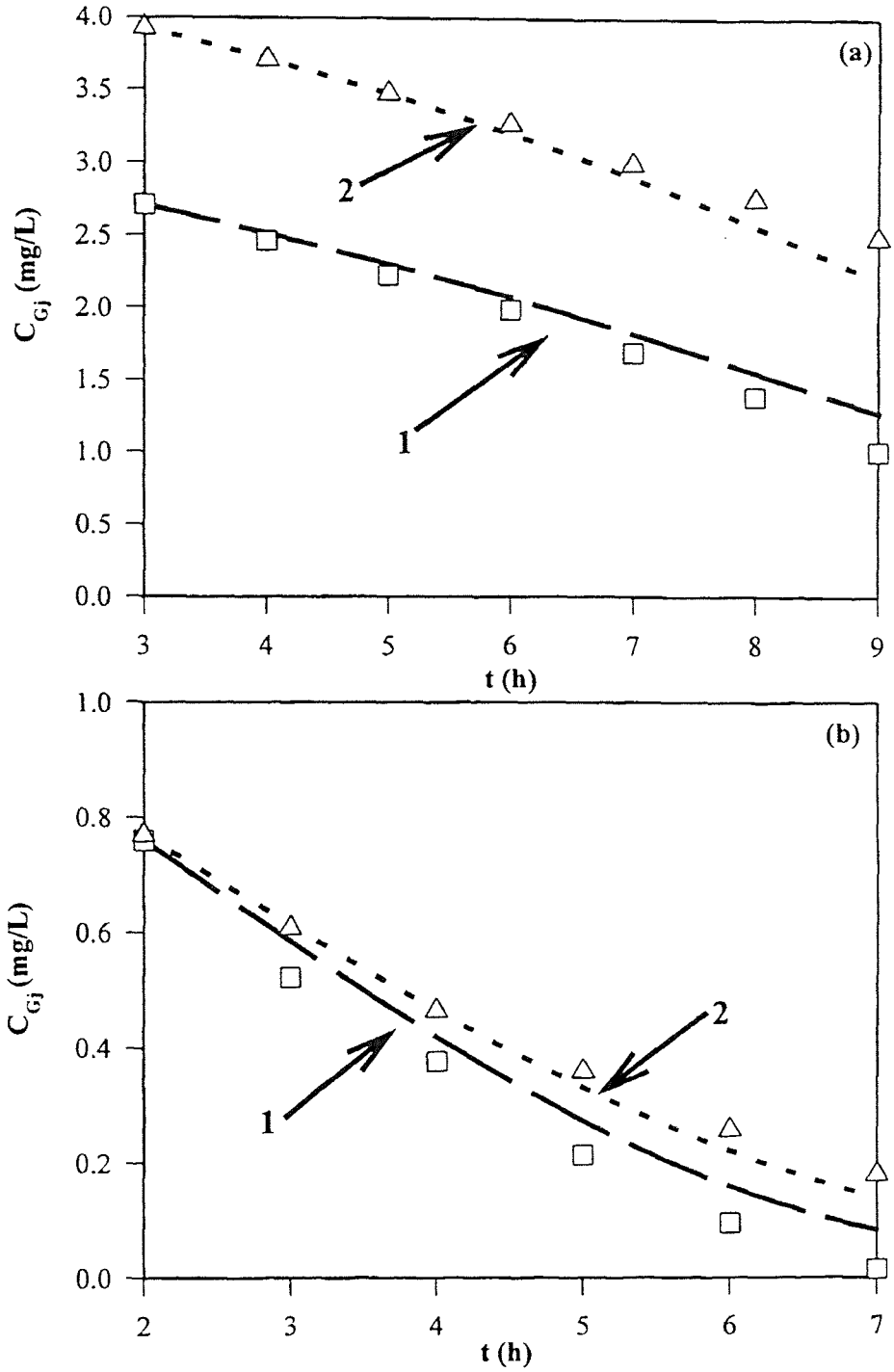

Figure 5.10 Comparison of fitted concentration profiles and experimental data from experiments with m-CB/o-DCB mixtures. Figures (a) and (b) are for experiments 5 and 11, respectively. For conditions see Table 5.3. Curves 1 and 2 are for m-CB (data shown as □) and o-DCB (data shown as Δ), respectively.

respectively, gave the best fit. Two examples are shown in Figure 5.10. The aforementioned values for K_{2j} were subsequently used in predicting (without any further fitting) the data of 12 kinetic experiments. In all cases the agreement between model predicted concentration profiles and data was very good as shown in the two examples of Figure 5.11.

The importance of kinetic interference can be seen from Figure 5.11(b) where predictions (curves) have been prepared by taking into consideration the interaction (dotted curves) and neglecting it (solid curves). It is clear that the data cannot be described when cross-inhibition is neglected.

Constant K_{21} expresses and quantifies the inhibition exerted on m-CB removal by the presence of o-DCB. Similarly, K_{22} indicates the inhibition exerted on o-DCB removal by the presence of m-CB. The K_{22} value is 1.7 times the K_{21} value and this suggests that the presence of m-CB has a stronger effect on o-DCB removal than the presence of o-DCB on the removal of m-CB.

Cross-inhibition can be either competitive as discussed above or non-competitive. Non-competitive cross-inhibition can be described by a modification of expression (5.20) as discussed by Wang et al. (1996) who studied glucose/phenol mixtures. The data from the experiments performed in the present study could not be described when non-competitive cross-inhibition was assumed. This is not surprising since m-CB and o-DCB are structurally similar whereas glucose and phenol are structurally dissimilar compounds. Oh et al. (1994) have also shown that benzene and toluene, which are

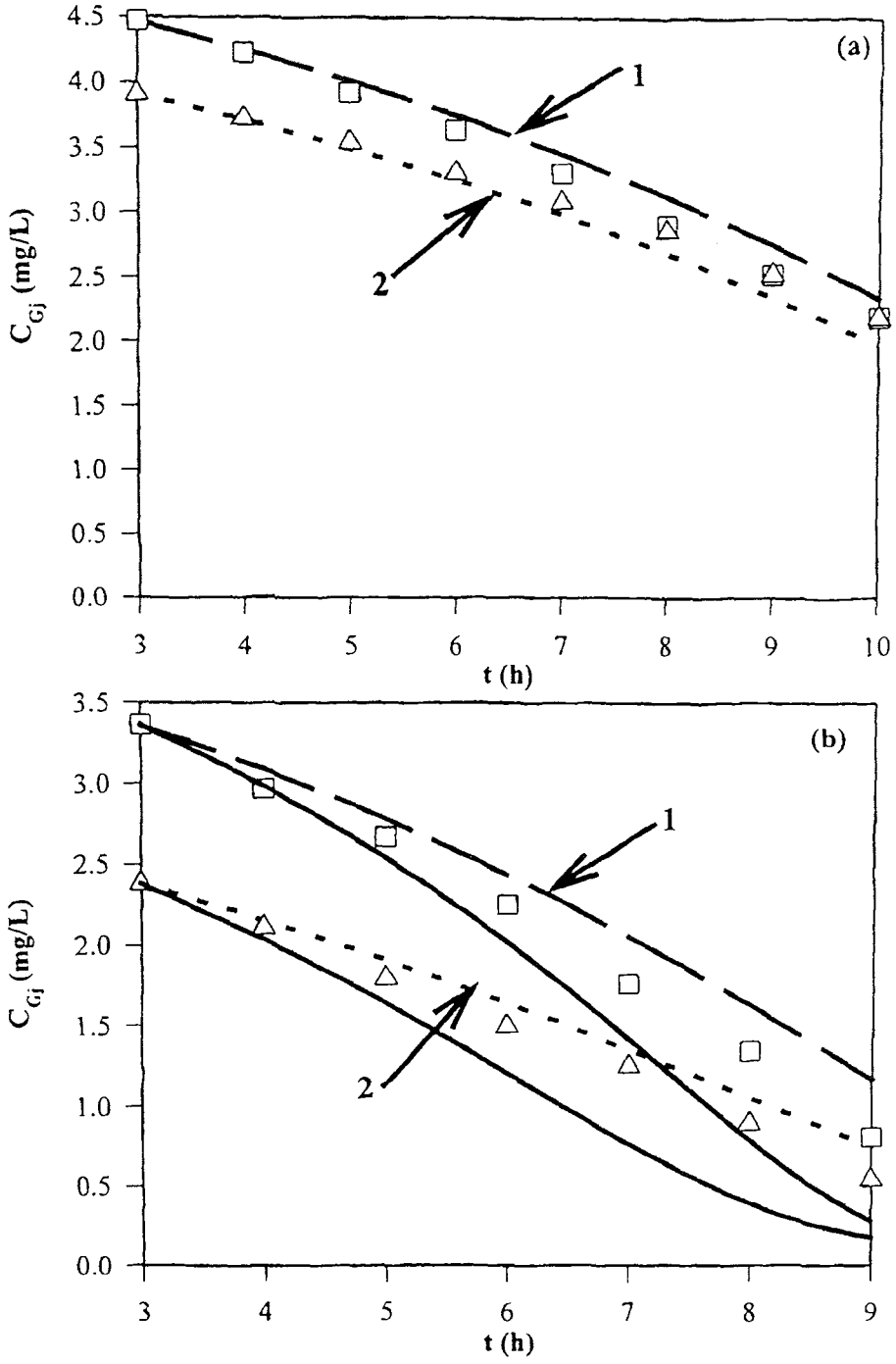

Figure 5.11 Comparison of model predictions and experimental data from two biodegradation experiments with m-CB/o-DCB mixtures. In (a) the conditions are those of experiment 1 (Table 5.3). In (b) 0.8 μL of m-CB and 0.6 μL of o-DCB were added to the serum bottle. Curves 1 and 2 are for m-CB (data shown as □) and o-DCB (data shown as Δ), respectively. Solid curves in (b) represent model predictions assuming no kinetic interactions.

structurally similar, are also involved in a competitive cross-interaction during their biodegradation.

5.5.3 pH Effects

The study on the effect of pH on the biodegradation kinetics of m-CB and o-DCB involved three groups of experiments. The first group involved the m-CB consortium and two series of experiments were performed one at initial m-CB concentration of 16.6 gm^{-3} and one at initial m-CB concentration of 22.6 gm^{-3}. The second group involved experiments with the o-DCB consortium at an initial m-CB concentration of 14.2 gm^{-3}. The third group involved the o-DCB consortium and o-DCB as the substrate. Two series of experiments were performed one at 6.5 gm^{-3} and one at 24.5 gm^{-3} of initial o-DCB concentration.

With each initial substrate concentration a number of experiments were performed at various pH values. From each experiment, the data were analyzed as discussed in Section 5.2 and the value of the specific growth rate was determined. The data from each series of experiments were fitted to equation (5.21) using the non-linear curve fitting approach discussed by Wang et al. (1995). The constants obtained are reported in Tables 5.5 and 5.6 for m-CB and o-DCB, respectively. The optimum pH values, determined via equation (5.23) are also reported in the tables.

Data on specific growth rate values as function of pH along with the fitted curves are presented in Figures 5.12 through 5.14. As can be seen, a nice fitting was obtained in all cases.

Table 5.5. Parameter values for expression (5.21) describing the pH-dependence of the specific growth rates of m-CB and o-DCB consortium on m-CB.

$\delta_{m\text{-}CB}$ (h^{-1})	$K_{H1\ m\text{-}CB}$ (mol/L)	$K_{H2\ m\text{-}CB}$ (mol/L)	pH_{opt}
	m-CB consortium, $C_{L,AVE}$ = 16.58 gm^{-3}		
0.188	1.75 X 10^{-5}	1.8 X 10^{-5}	6.75
	m-CB consortium, $C_{L,AVE}$ = 22.58 gm^{-3}		
0.199	1.75 X 10^{-5}	1.8 X 10^{-5}	6.75
	o-DCB consortium, $C_{L,AVE}$ = 14.21 gm^{-3}		
0.090	2.9 X 10^{-6}	1.5 X 10^{-9}	7.18

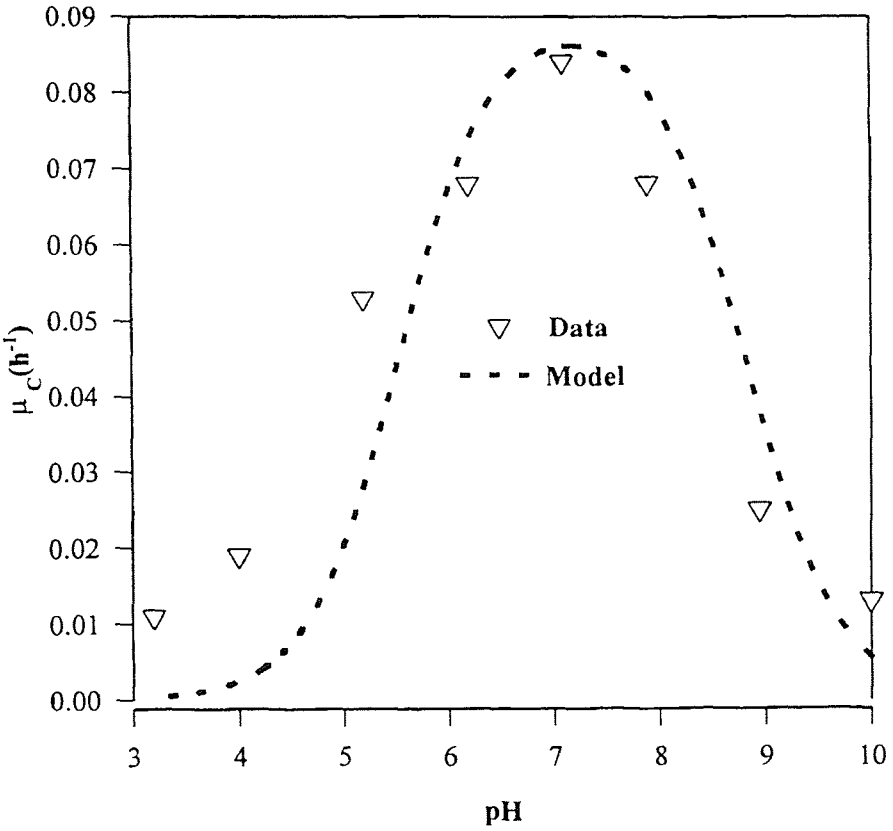

Figure 5.12 Dependence of the specific growth rate of the o-DCB consortium on pH when the m-CB concentration in the medium is 14.2 gm^{-3}. Data from suspended culture experiments are shown as symbols. Curves represent fitting of data to expression (5.21).

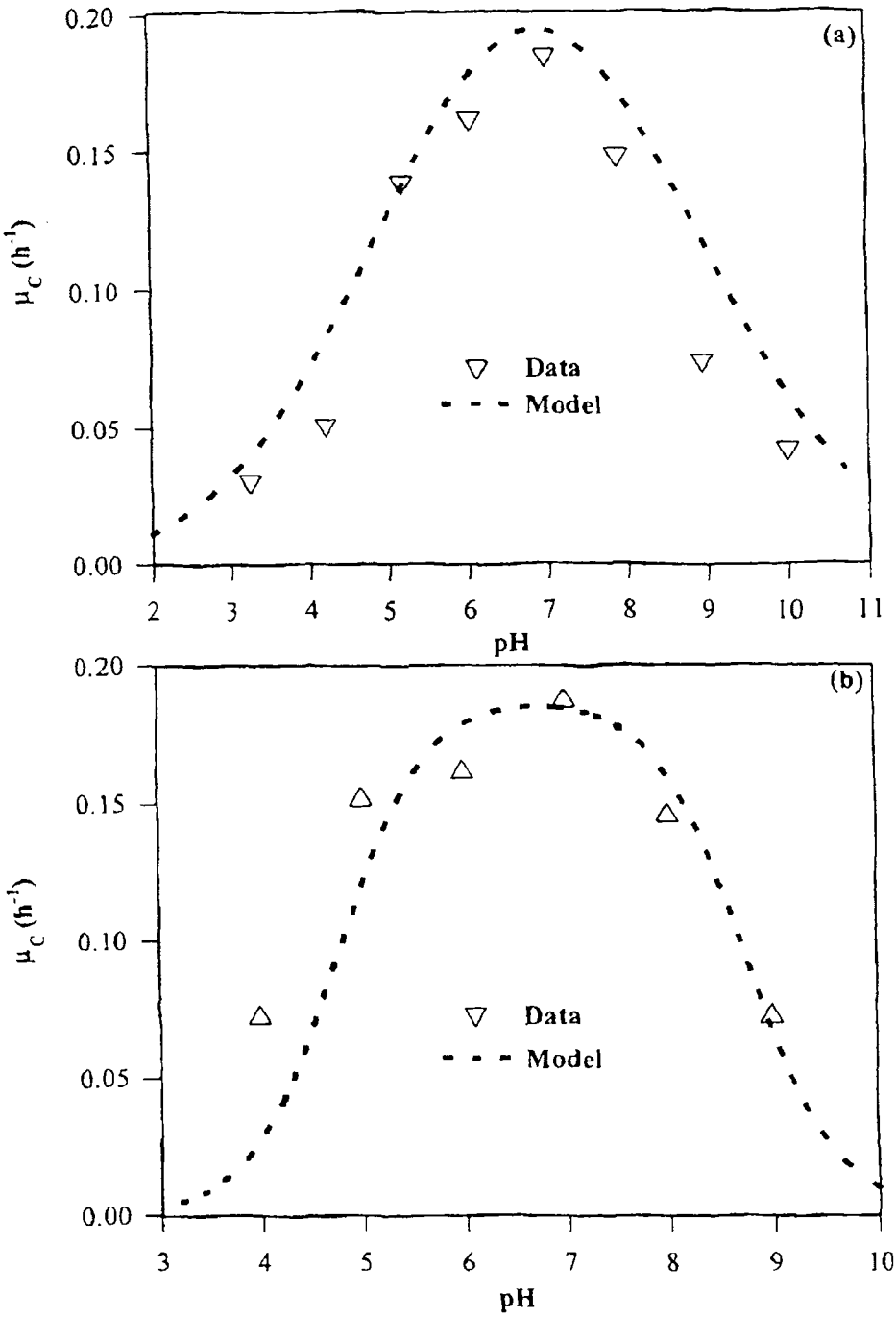

Figure 5.13 Dependence of the specific growth rate of the m-CB consortium on pH when the m-CB concentration in the medium is (a) 16.6 gm^{-3} and (b) 22.6 gm^{-3}. Data from suspended culture experiments are shown as symbols. Curves represent fitting of data to expression (5.21).

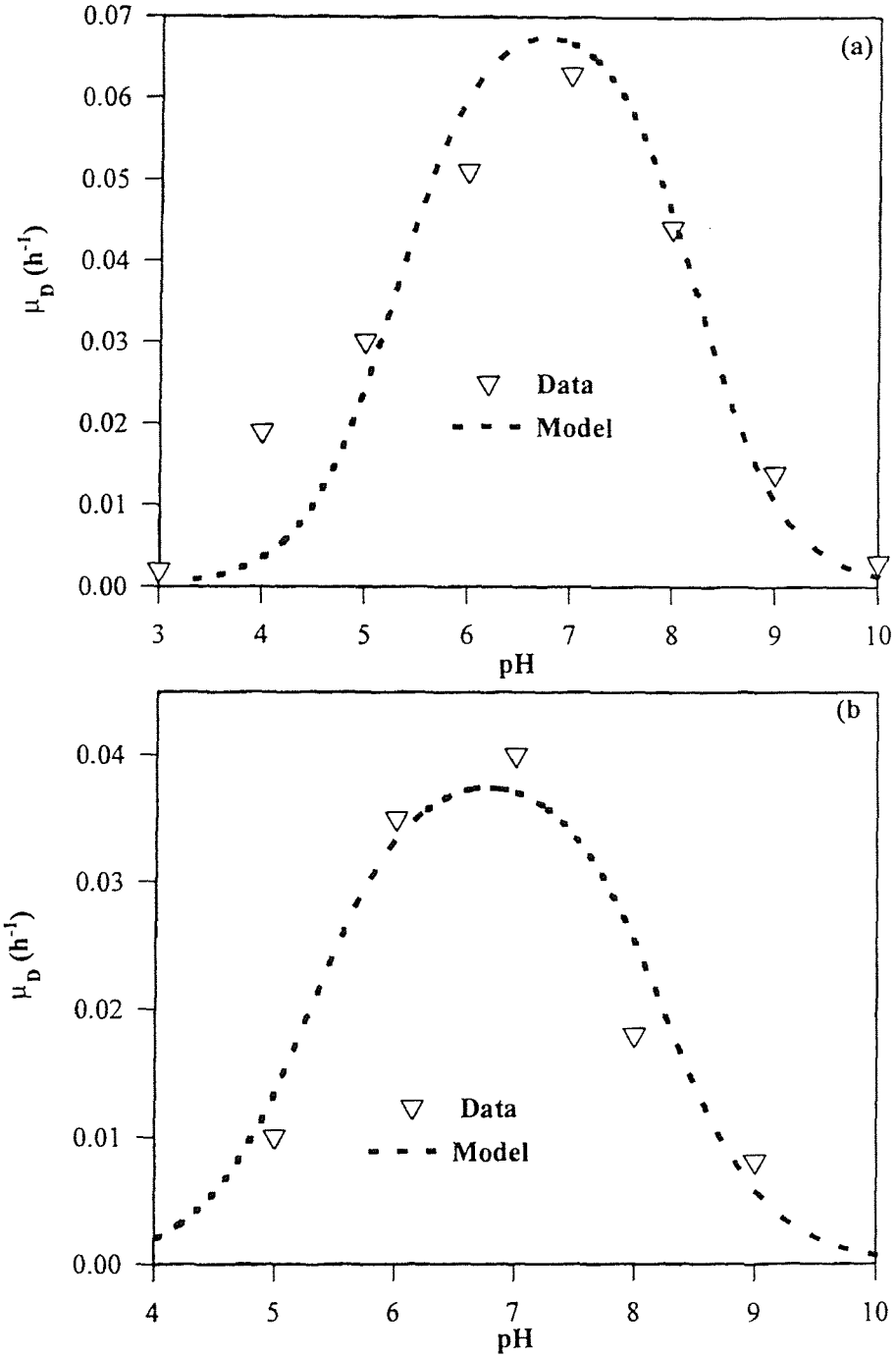

Figure 5.14 Dependence of the specific growth rate of the o-DCB consortium on pH when the o-DCB concentration in the medium is (a) 24.5 gm^{-3} and (b) 6.5 gm^{-3}. Data from suspended culture experiments are shown as symbols. Curves represent fitting of data to expression (5.21).

Table 5.6. Parameter values for expression (5.21) describing the pH-dependence of the specific growth rates of o-DCB consortium on o-DCB.

$\delta_{o\text{-DCB}}$ (h^{-1})	$K_{H1\ o\text{-DCB}}$ (mol/L)	$K_{H2\ o\text{-DCB}}$ (mol/L)	pH_{opt}
	$C_{L,AVE} = 6.48\ gm^{-3}$		
0.040	5.1×10^{-6}	5.8×10^{-9}	6.76
	$C_{L,AVE} = 24.52\ gm^{-3}$		
0.072	5.1×10^{-5}	5.8×10^{-9}	6.76

For m-CB biodegradation when the o-DCB consortium is used, the optimum pH value is slightly higher than that when the m-CB consortium is employed as can be seen from Table 5.5. In all cases, however, it was found that the optimal pH is very close to the neutral value of 7. Knowing the optimal pH values from this study, a value of 6.8 ± 0.2 was used in the great majority of experiments with biotrickling filters described in Chapters 6 and 7 of this thesis.

It should be mentioned here that the same consortia had been earlier used by Oh and Bartha (1994) in experiments, without modeling, for determination of the optimal pH. Their data agree nicely with the results obtained here.

CHAPTER 6

STEADY-STATE REMOVAL OF SINGLE VOCs IN BIOTRICKLING FILTERS

In this chapter, the results from the studies on single VOC removal are reported. These studies involved the development of a detailed mathematical model, its numerical solution and validation with data obtained from the experimental unit described in Chapter 4. Airstreams laden with either m-CB or o-DCB were used in the experiments discussed in the present chapter.

The model describes VOC vapor removal under steady state conditions and conceptually is shown in Figure 6.1. Liquid and air are flowing either counter-currently (as shown in Figure 6.1) or co-currently around the solids of the packing material. The surface of the packing is either completely covered by biofilm or partially covered by biofilm patches. The VOC and oxygen are transferred first from the gas to the liquid phase wetting the biofilm and subsequently to the biofilm itself where the actual biodegradation process takes place.

6.1 Mathematical Description of the Process

In deriving the model equations, for the removal of a VOC j, the following assumptions have been made.

1. The concentration of VOC j and oxygen are the only variables affecting the reaction rate.

2. The reaction rate is directly related to the specific growth rate of biomass which is described via an interactive model in the sense of Bader (1982).

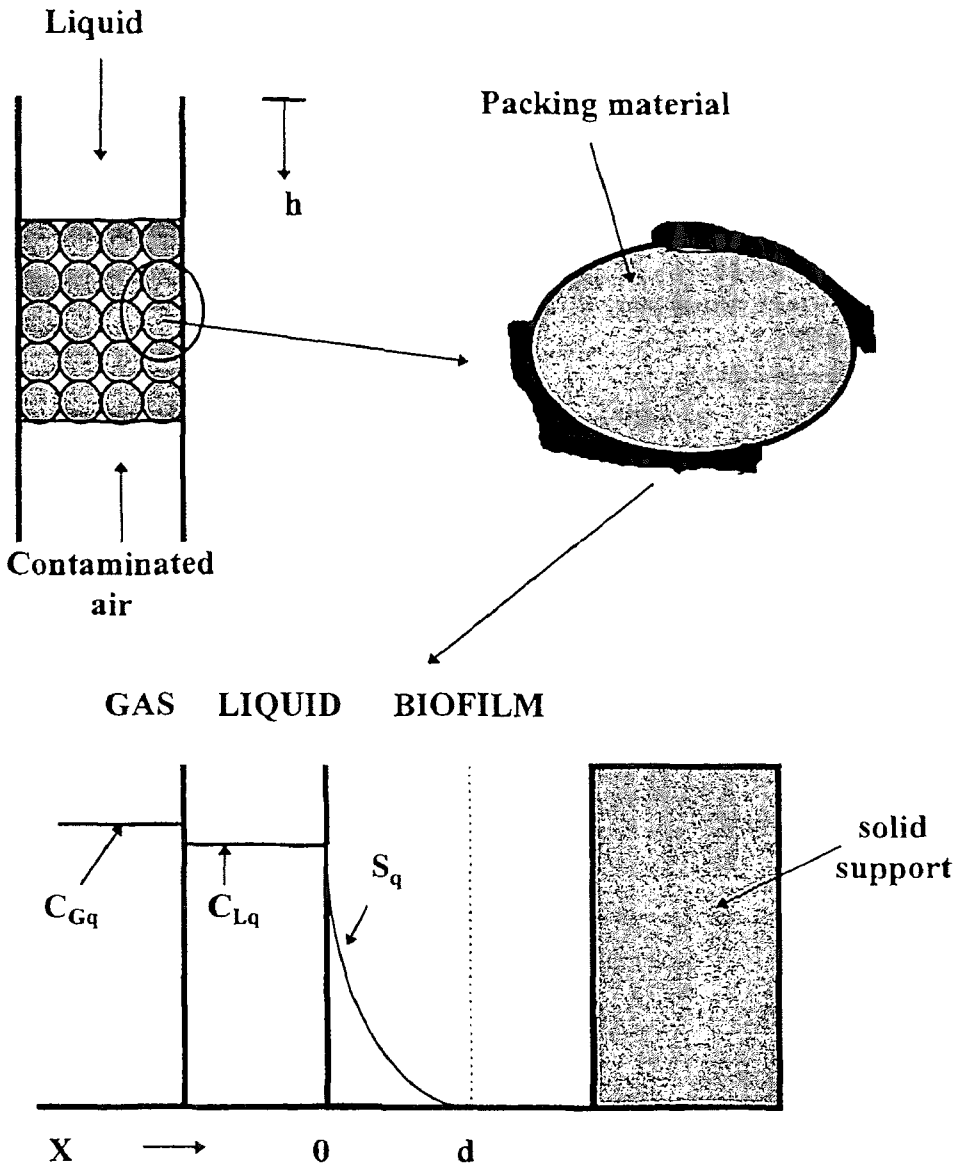

Figure 6.1 Schematic representation of the model concept at a cross-section of the biotrickling filter column. VOC j and oxygen are transferred from the air (gas) to the liquid and then to the biofilm where reaction occurs.

3. The specific growth rate of biomass immobilized on the surface of the packing is the same with that of the same culture when it is suspended in growth medium.

4. When the surface of the solid packing is not completely covered with biofilm, the extent (surface) of the biofilm patch is much larger than its depth. Consequently, VOC and oxygen transfer into the biofilm through the side surfaces of the patch can be neglected, and diffusion/reaction in the biofilm can be described by using only the direction which is perpendicular to the main surface of the patch.

5. Reaction occurs only in a fraction of the biofilm called effective biofilm (or biolayer). The thickness of the effective biofilm can vary with the position in the filter bed and is determined by the depletion of either the VOC or oxygen.

6. If the effective biofilm thickness is determined via depletion of oxygen, anaerobic degradation of the VOC in the remaining part of the biofilm does not take place.

7. The thickness of the effective biolayer is very small relative to the main curvature of the solid particles and thus, planar geometry can be used.

8. There are no radial gradients of either concentration or velocity in the airstream passing through the filter bed (plug flow).

9. There is no boundary layer close to the air/liquid interface and there is thermodynamic equilibrium for both VOC and oxygen at that interface. The concentrations of VOC and oxygen in the two phases of the air/liquid interface are related via Henry's law.

10. At every cross-section of the filter bed there are neither velocity nor concentration gradients in the liquid phase. Constant VOC and oxygen concentrations in the liquid imply no biodegradation in the liquid phase and negligible resistance to mass transfer from the bulk liquid to the liquid/biofilm interface.

11. The concentrations of VOC and oxygen in the biofilm at the liquid/biofilm interface are equal to those in liquid phase.

12. Diffusivities of VOC and oxygen in the biofilm are equal to those in water multiplied by a correction factor determined via the correlation of Fan et al. (1987,1990).

13. The density of the biofilm (X_v) is constant throughout the biotrickling filter at all times.

14. The void fraction of the filter bed is constant implying that the amount of biomass produced is sloughed off into the liquid and then discarded from the system during medium replenishment. Thus, a biomass balance is not needed for a complete system description.

15. The liquid trickling through the bed is recirculated in the unit.

Under the assumptions above, removal of VOC j in a biotrickling filter can be described by six mass balances, three on VOC j and three on oxygen, as follows.

I. Mass balances in the biofilm, at a position h along the column,

$$f(X_v)D_{jw}\frac{d^2S_j}{dx^2} = \frac{X_v}{Y_j}\mu_j(S_j)f(S_O) \tag{6.1}$$

$$f(X_v)D_{Ow}\frac{d^2S_O}{dx^2} = \frac{X_v}{Y_{Oj}}\mu_j(S_j)f(S_O) \tag{6.2}$$

with corresponding boundary conditions

$$S_j = C_{Lj} \quad \text{at} \quad x = 0 \tag{6.3}$$

$$\frac{dS_j}{dx} = 0 \quad \text{at} \quad x = \delta \tag{6.4}$$

$$S_O = C_{LO} \qquad \text{at} \qquad x = 0 \tag{6.5}$$

$$\frac{dS_O}{dx} = 0 \qquad \text{at} \qquad x = \delta \tag{6.6}$$

II. Mass balances in the liquid phase along the column,

$$u_L \frac{dC_{Lj}}{dh} = K_{Lj}\left(\frac{C_{Gj}}{m_j} - C_{Lj}\right) + f(X_v) D_{jW} A_{Sj}\left[\frac{dS_j}{dx}\right]_{x=0} \tag{6.7}$$

$$u_L \frac{dC_{LO}}{dh} = K_{LO}\left(\frac{C_{GO}}{m_O} - C_{LO}\right) + f(X_v) D_{OW} A_{Sj}\left[\frac{dS_O}{dx}\right]_{x=0} \tag{6.8}$$

with corresponding boundary conditions

$$C_{Lj}(h = 0) = C_{Lj}(h = H) \tag{6.9}$$

$$C_{LO}(h = 0) = C_{LO}(h = H) \tag{6.10}$$

Note that conditions (6.9) and (6.10) reflect assumptions 10 and 15, i.e., that the liquid is recirculated through the biotrickling filter bed as well as the assumption that no reaction occurs in the liquid phase.

III. Mass balances in the gas phase (airstream) along the biofilter column,

$$u_G \frac{dC_{Gj}}{dh} = \pm K_{Lj}\left(\frac{C_{Gj}}{m_j} - C_{Lj}\right) \tag{6.11}$$

$$u_G \frac{dC_{GO}}{dh} = \pm K_{LO}\left(\frac{C_{GO}}{m_O} - C_{LO}\right) \tag{6.12}$$

Equations (6.11) and (6.12) taken with the plus (+) sign describe counter-current flow of the airstream and the liquid stream, whereas when taken with the minus (-) sign describe co-current flow of the two phases. Depending on the mode of operation, the corresponding boundary conditions for equations (6.11) and (6.12) are as follows.

IIIa. Under counter-current conditions

$$C_{Gj} = C_{Gji} \quad \text{at} \quad h = H \tag{6.13}$$

$$C_{GO} = C_{GOi} \quad \text{at} \quad h = H \tag{6.14}$$

IIIb. Under co-current conditions

$$C_{Gj} = C_{Gji} \quad \text{at} \quad h = 0 \tag{6.15}$$

$$C_{GO} = C_{GOi} \quad \text{at} \quad h = 0 \tag{6.16}$$

The product of functions $\mu_j(S_j)$ and $f(S_O)$ appearing in equations (6.1) and (6.2) represents the specific growth rate of the biomass and reflects assumptions 1 and 2 introduced earlier. The explicit forms of these functions are given by

$$\mu_j(S_j) = \frac{\mu_j^* S_j}{K_j + S_j + \frac{S_j^2}{K_{Ij}}} \tag{6.17}$$

$$f(S_O) = \frac{S_O}{K_O + S_O} \tag{6.18}$$

When K_{Ij} is very large, expressions (6.17) and (6.18) imply that the specific growth rate and, consequently, the rates of VOC degradation and oxygen consumption have a Monod (1942) type dependence on the availability of VOC j and oxygen. On the other hand, if K_{Ij} is finite and relatively small, the specific growth rate has an Andrews (1968) type dependence on the concentration of VOC j and a Monod type dependence on oxygen.

When the following dimensionless quantities are introduced,

$$\bar{S}_j = \frac{S_j}{K_j}, \qquad \bar{S}_O = \frac{S_O}{K_O}, \qquad \bar{C}_{Lj} = \frac{m_j C_{Lj}}{C_{Gji}}, \qquad \bar{C}_{LO} = \frac{m_O C_{LO}}{C_{GOi}},$$

$$\bar{C}_{Gj} = \frac{C_{Gj}}{C_{Gji}}, \qquad \bar{C}_{GO} = \frac{C_{GO}}{C_{GOi}}, \qquad \alpha_j = \frac{C_{Gji}}{m_j K_j}, \qquad \alpha_O = \frac{C_{GOi}}{m_O K_O},$$

$$\theta = \frac{x}{\delta}, \qquad z = \frac{h}{H}, \qquad \gamma = \frac{K_j}{K_{Ij}}, \qquad \lambda = \frac{D_{jW} Y_j K_j}{D_{OW} Y_{Oj} K_O},$$

$$\phi^2 = \frac{X_v \delta^2 \mu_j^*}{f(X_v) Y_j D_{jW} K_j}, \qquad \psi = \frac{K_{Lj} H}{u_L}, \qquad \beta = \frac{K_{LO}}{K_{Lj}}, \qquad \rho = \frac{K_{Lj} H}{u_G m_j},$$

$$\eta = \frac{f(X_v) D_{jW} A_{Sj} K_j m_j H}{u_L \delta C_{Gji}}, \qquad \omega = \frac{C_{Gji} D_{OW} K_O m_O}{C_{GOi} D_{jW} K_j m_j}, \qquad \varepsilon = \frac{m_j K_{LO}}{m_O K_{Lj}},$$

equations (6.1)-(6.16), when expressions (6.17) and (6.18) are also used, can be written in dimensionless form as follows.

$$\frac{d^2 \bar{S}_j}{d\theta^2} = \phi^2 \frac{\bar{S}_j \bar{S}_O}{\left(1 + \bar{S}_j + \gamma \bar{S}_j^2\right)\left(1 + \bar{S}_O\right)} \tag{6.19}$$

$$\frac{d^2 \bar{S}_O}{d\theta^2} = \lambda \phi^2 \frac{\bar{S}_j \bar{S}_O}{\left(1 + \bar{S}_j + \gamma \bar{S}_j^2\right)\left(1 + \bar{S}_O\right)} \tag{6.20}$$

$$\frac{d\bar{S}_j}{d\theta} = \frac{d\bar{S}_O}{d\theta} = 0 \quad \text{at} \quad \theta = 1 \tag{6.21}$$

$$\bar{S}_j = \alpha_j \bar{C}_{Lj} \quad \text{at} \quad \theta = 0 \tag{6.22}$$

$$\bar{S}_O = \alpha_O \bar{C}_{LO} \quad \text{at} \quad \theta = 0 \tag{6.23}$$

$$\frac{d\bar{C}_{Lj}}{dz} = \psi\left(\bar{C}_{Gj} - \bar{C}_{Lj}\right) + \eta\left[\frac{d\bar{S}_j}{d\theta}\right]_{\theta=0} \tag{6.24}$$

$$\frac{d\bar{C}_{LO}}{dz} = \psi\beta\left(\bar{C}_{GO} - \bar{C}_{LO}\right) + \eta\omega\left[\frac{d\bar{S}_O}{d\theta}\right]_{\theta=0} \tag{6.25}$$

$$\bar{C}_{Lj}(z = 0) = \bar{C}_{Lj}(z = 1) \tag{6.26}$$

$$\bar{C}_{LO}(z=0) = \bar{C}_{LO}(z=1) \tag{6.27}$$

$$\frac{d\bar{C}_{Gj}}{dz} = \pm\rho\left(\bar{C}_{Gj} - \bar{C}_{Lj}\right) \tag{6.28}$$

$$\frac{d\bar{C}_{GO}}{dz} = \pm\rho\varepsilon\left(\bar{C}_{GO} - \bar{C}_{LO}\right) \tag{6.29}$$

$$\bar{C}_{Gj} = \bar{C}_{GO} = 1 \quad \text{at} \quad z = 1 \quad \text{(for counter-current flow)} \tag{6.30}$$

$$\bar{C}_{Gj} = \bar{C}_{GO} = 1 \quad \text{at} \quad z = 0 \quad \text{(for co-current flow)} \tag{6.31}$$

Equations (6.19) and (6.20) along with boundary conditions (6.21)-(6.23) yield

$$\bar{S}_O = \lambda\left(\bar{S}_j - \alpha_j \bar{C}_{Lj}\right) + \alpha_O \bar{C}_{LO} \tag{6.32}$$

or

$$\bar{S}_j = \frac{1}{\lambda}\left(\bar{S}_O - \alpha_O \bar{C}_{LO}\right) + \alpha_j \bar{C}_{Lj} \tag{6.33}$$

Because of relations (6.32) and (6.33), instead of solving the original set of equations (6.19)-(6.31) one can equivalently solve either one of the following sets of equations. Set 1: Equations (6.19), (6.22), (6.24)-(6.31) and from (6.21) only the condition concerning $\bar{S}_j$. In this case, relation (6.32) needs to be substituted for $\bar{S}_O$ in equation (6.19). Set 2: Equations (6.20), (6.23), (6.24)-(6.31) and from (6.21) only the condition concerning $\bar{S}_O$. In this case, relation (6.33) needs to be substituted for $\bar{S}_j$ in equation (6.20). Each one of the aforementioned sets of equations constitutes a non-linear and coupled boundary value problem in two directions, x and z. Solving this problem requires a trial and error approach because of boundary conditions (6.26) and (6.27).

6.2 Numerical Methodology

A computer code has been developed for solving the model equations (see Appendix A) and [based on equations of Set 1 discussed in Section 6.1] works as follows. An initial guess is made for the values of the VOC and oxygen concentrations in the liquid phase at $z = 0$. Equation (6.19) is solved at $z = 0$ with an assumed value of δ (which determines ϕ^2). The value of δ is adjusted until boundary condition (6.21) is satisfied and, additionally, either $\bar{S}_j(\theta = 1) = 0$ or $\bar{S}_O(\theta = 1) = 0$ in order to satisfy assumption 5 of the model. For every value of δ, the orthogonal collocation method (Finlayson, 1980; Villadsen and Michelsen, 1978) with 10 points is employed. When the right value of δ is determined, concentration slopes at $\theta = 0$ are calculated and the 4^{th}-order Runge-Kutta method is used for determining VOC and oxygen concentrations in the liquid and airstream at a position Δz away from $z = 0$. At this position, equation (6.19) is solved again and repeatedly till the right value of δ is determined. Slopes are determined at $\theta = 0$ and the procedure is repeated in Δz increments till z becomes equal to 1. The value of Δz used is 1/600 implying that the procedure is repeated 600 times and each time equation (6.19) is solved a number of times till δ is properly determined. This methodology leads to determination of liquid and gas phase concentrations of VOC and oxygen along the biofilter bed. If the liquid phase concentrations at $z = 1$ match the ones assumed at the very beginning of the procedure, conditions (6.26) and (6.27) are satisfied and the solution has been found. If conditions (6.26) and (6.27) are not satisfied, a new initial guess is made and the whole procedure is repeated again.

In cases where the VOC is consumed in the biofilm faster than oxygen the equations of Set 1 (Section 6.1) need to be solved. If oxygen is depleted before the VOC in the biofilm, then equations of Set 2 (Section 6.1) need to be solved. This introduces a further complication as it is not known a priori which substance is depleted first in the biolayer. Consequently, the same code is written twice (for Set 1 and Set 2) and which version is used is determined as the program runs. In fact, as discussed later in the results, there are operating conditions under which concentration profiles are determined via solving Set 1 only and others where both Set 1 and Set 2 are needed. In the latter case, zones of oxygen control and VOC control are formed in the biotrickling filter bed.

6.3 Parameter Determination

6.3.1 Kinetic Constants

The values of the kinetic constants appearing in expression (6.17) were determined from suspended culture, closed shake serum bottle experiments as discussed in Chapter 5. Using these constants in describing VOC vapor removal reflects assumption 3 of the model (see Section 6.1).

For the constant appearing in expression (6.18) the value used in other studies with conventional biofilters (Baltzis et al., 1997; Shareefdeen et al., 1993; Shareefdeen and Baltzis, 1994) was used here as well due to lack of a better estimate. However, model sensitivity studies (as discussed later in this chapter) show that the results remain unchanged even when the value of K_O changes by one order of magnitude. The value of K_O is reported in Table 6.1.

6.3.2 Yield Coefficients

For the yield coefficients of the biomass on the carbon source, the values used were those determined from the kinetic runs discussed in Chapter 5. The values of the yield coefficient of the biomass on oxygen were calculated via reaction stoichiometry following the method also discussed by Shareefdeen et al. (1993). The stoichiometries for m-CB and o-DCB when biomass composition is taken as $CH_{1.8}O_{0.5}N_{0.2}$ (Shuler and Kargi, 1992) and NH_4NO_3 serves as nitrogen source (see Chapter 5) are as follows.

For mono-chlorobenzene (m-CB) degradation,

$$C_6H_5Cl + 3.69\,O_2 + 0.265\,NH_4NO_3 \longrightarrow$$

$$2.65\,CH_{1.8}O_{0.5}N_{0.2} + 0.15\,H_2O + 3.35\,CO_2 + HCl \qquad (6.34)$$

Similarly for ortho-dichlorobenzene (o-DCB) degradation,

$$C_6H_4Cl_2 + 4.20\,O_2 + 0.237\,NH_4NO_3 \longrightarrow$$

$$2.37\,CH_{1.8}O_{0.5}N_{0.2} + 0.66\,H_2O + 3.63\,CO_2 + 2HCl \qquad (6.35)$$

Based on equations (6.34) and (6.35) the values of the yield coefficients on oxygen were calculated and are reported in Table 6.1.

6.3.3 Wetted Area and Mass Transfer Coefficients

The specific wetted surface area of the biofilm was determined via the following equation,

$$\frac{A_{Sj}}{\xi_j A_{Tj}} = 1 - \exp\left\{-1.45\left(\frac{\sigma_P}{\sigma_L}\right)^{0.75}\left(\frac{Q_L\rho_L}{SA_{Tj}\mu_L}\right)^{0.1}\left(\frac{A_{Tj}}{\rho_L^2 g}\right)^{-0.05}\left[\left(\frac{Q_L\rho_L}{S}\right)^2\frac{1}{\rho_L\sigma_L A_{Tj}}\right]^{0.2}\right\} \qquad (6.36)$$

and the overall mass transfer coefficients K_{Lq} (q = O for oxygen, q = C for m-CB, q = D for o-DCB) from the equation,

$$\frac{1}{K_{Lq}} = \frac{1}{m_q k_{Gq} A_{Sj}} + \frac{1}{k_{Lq} A_{Sj}} \tag{6.37}$$

The values of the gas and liquid phase mass transfer coefficients (k_{Gq}, k_{Lq}) appearing in equation (6.37) were determined from the following correlations,

$$\frac{\xi_{1q} k_{Gq}}{A_{Tj} D_{qG}} = 5.23 \left(\frac{Q_G \rho_G}{SA_{Sj} \mu_G} \right)^{0.7} \left(\frac{\mu_G}{\rho_G D_{qG}} \right)^{1/3} \left(A_{Tj} d_{Pj} \right)^{-2} \tag{6.38}$$

$$\xi_{2q} k_{Lq} \left(\frac{\rho_L}{\mu_L g} \right)^{1/3} = 0.0051 \left(\frac{Q_L \rho_L}{SA_{Sj} \mu_G} \right)^{2/3} \left(\frac{\mu_L}{\rho_L D_{qW}} \right)^{-0.5} \left(A_{Tj} d_{Pj} \right)^{-0.4} \tag{6.39}$$

With the exception of the volumetric flowrates of air (Q_G) and liquid medium (Q_L) which varied among experiments, the values of all parameters appearing in expressions (6.36)-(6.39) are given in Tables 6.1, 6.2 and 6.3.

When $\xi_j = \xi_{1q} = \xi_{2q} = 1$, expressions (6.36), (6.38) and (6.39) are the well known Onda correlations (Djebbar and Narbaitz, 1995; Kavanaugh and Trussell, 1980; Lamarche and Droste, 1989; Onda et al., 1968). The numerical coefficients in the right hand side of expressions (6.38) and (6.39) reflect the physical characteristics of the packing material used in this study (Bolles and Fair, 1982; Eckert, 1961, 1975).

Coefficients ξ_j, ξ_{1q} and ξ_{2q} were determined during the course of this study through fitting of some data sets from biotrickling filter experiments to the solution of the model equations. The values of ξ_{1q} and ξ_{2q} determined and used here lead to values

for the overall mass transfer coefficient of m-CB and o-DCB which are close to those experimentally determined for toluene in a biotrickling filter operating under flow conditions similar to those used in the present study (Pedersen and Arvin, 1995). These values are also similar to those found by Turek and Lange (1981) who studied mass transfer in non-biological trickle-bed reactors operating at low Reynolds numbers as is also the case in the present study. For oxygen, the value of m_O is very large implying, from equation (6.37), that the contribution of gas phase mass transfer resistance to the overall mass transfer coefficient for oxygen is negligible. For this reason, the value of ξ_{lO} was taken as zero.

A correction factor (ξ_j) in correlation (6.36) has been also used by other investigators who worked with biotrickling filters. A value of $\xi_j = 2$ has been reported by Diks and Ottengraf (1991 a, b) and a value of $\xi_j = 6$ can be inferred from the results of Pedersen and Arvin (1995) who speculated that the enlarged contact area between the air and the biofilm may be due to the irregular (rough) surface of the biofilm. The value of ξ_j determined in the present study is 4.5 for m-CB and 2.4 for o-DCB.

6.3.4 Effective Biolayer Thickness

As also done earlier by Shareefdeen et al. (1993), the value of the effective biofilm thickness in this study is determined by the computer code. At each position in the biotrickling filter a trial and error approach is incorporated in the code to determine δ as the thickness which leads to 99% reduction in the concentration of either oxygen or the pollutant (whichever happens first) present at the liquid/biolayer interface.

Table 6.1. Model parameter values common for m-CB and o-DCB biofiltration.

Model Parameter	Numerical Value	Unit	Reference
		Biofilm	
X_v	75	kgm^{-3}	Present study
$f(X_v)$	0.253	-	Fan et al. (1987, 1990)
		Physical Parameters for Oxygen	
m_O	34.4	-	Shareefdeen et al. (1993)
D_{OW}	2.39×10^{-9}	m^2s^{-1}	Perry and Green (1984)
D_{OG}	2.03×10^{-5}	m^2s^{-1}	Perry and Green (1984)
C_{GOi}	275	gm^{-3}	Shareefdeen et al. (1993)
		Kinetic Parameters for Oxygen	
K_O	0.26	gm^{-3}	Shareefdeen et al. (1993)
Y_{OC}	0.551	gg^{-1}	Present study
Y_{OD}	0.363	gg^{-1}	Present study
		Physical Parameters for Air	
μ_G	0.018×10^{-3}	$kgm^{-1}s^{-1}$	Perry and Green (1984)
ρ_G	1.193	kgm^{-3}	Perry and Green (1984)
		Physical Parameters for Water	
μ_L	0.982×10^{-3}	$kgm^{-1}s^{-1}$	Perry and Green (1984)
ρ_L	997.85	kgm^{-3}	Perry and Green(1984)
σ_L	72×10^{-3}	Nm^{-1}	Heggen (1983)

Table 6.2. Model parameter values for m-CB biofiltration[a].

Model Parameter	Numerical Value	Unit	Reference
	Physical Parameters for m-CB		
m_C	0.167	-	Yurteri et al. (1987)
D_{CW}	0.81×10^{-9}	m^2s^{-1}	Perry and Green (1984)
D_{CG}	0.78×10^{-5}	m^2s^{-1}	Fuller et al. (1966)
	Column Dimensions		
S	1.82×10^{-2}	m^2	Present study
V_{PC}	1.32×10^{-3}	m^3	Present study
	Packing Characteristics		
A_{TC}	334.65	m^{-1}	Eckert (1961, 1975)
d_{PC}	0.019	m	Eckert (1961, 1975)
σ_P	61×10^{-3}	Nm^{-1}	Bolles and Fair (1982)
	Other Parameters		
ξ_C	4.50	-	Present study
ξ_{1C}	4.40	-	Present study
ξ_{2C}	4.40	-	Present study
ξ_{1O}	0	-	Present study
ξ_{2O}	35	-	Present study

[a]Kinetic parameter values are those in the second column of Table 5.1

Table 6.3. Model parameter values for o-DCB biofiltration[a].

Model Parameter	Numerical Value	Unit	Reference
	Physical Parameters for o-DCB		
m_D	0.119	-	Yurteri et al. (1987)
D_{DW}	0.78×10^{-9}	m^2s^{-1}	Perry and Green (1984)
D_{DG}	0.69×10^{-5}	m^2s^{-1}	Fuller et al. (1966)
	Column Dimensions		
S	1.82×10^{-2}	m^2	Present study
V_{PD}	1.26×10^{-3}	m^3	Present study
	Packing Characteristics		
A_{TD}	623.36	m^{-1}	Eckert (1961, 1975)
d_{PD}	0.0127	m	Eckert (1961, 1975)
σ_P	61×10^{-3}	Nm^{-1}	Bolles and Fair (1982)
	Other Parameters		
ξ_D	2.36	-	Present study
ξ_{1D}	2.55	-	Present study
ξ_{2D}	2.55	-	Present study
ξ_{1O}	0	-	Present study
ξ_{2O}	7.12	-	Present study

[a]Kinetic parameter values are given in Table 5.2

6.3.5 Other Parameters

The values of all other model parameters that have not been discussed earlier have been taken from the literature and are given in Tables 6.1, 6.2, and 6.3.

The values of the distribution coefficients of m-CB and o-DCB between air and water (m_C and m_D) were taken from the literature but were also confirmed from experiments with close serum bottles in which uninoculated liquid medium was placed and then spiked with various amounts of m-CB or o-DCB.

The value of the biofilm density (X_v) used in this study is lower than the value used in conventional biofilters because in biotrickling filters thick biofilms are formed. Ranges of reported X_v values and the relation between X_v and biofilm thickness have been reviewed and discussed by Shareefdeen et al. (1993).

6.4 Biofiltration of Mono-chlorobenzene (m-CB)

A large number of experiments were performed with the biotrickling filter unit shown in Figure 4.1. Among experiments, the volumetric flow rate of the air supplied to the biofilter (Q_G) and thus the air residence time $\tau = V_P/Q_G$, the m-CB vapor concentration in the air supplied to the biotrickling filter (C_{GCi}), and the flow rate of the liquid (Q_L) were varied. All data sets were analyzed with the model presented in Section 6.1. With the exception of four experiments the data of which were used in determining parameters ξ_C, ξ_{1q} and ξ_{2q}, all experiments were described with the model without fitting the data and thus the predictive capabilities of the model were examined.

The first detailed series of runs involved experiments at a constant value of the air residence time (τ) and counter-current flow of air and liquid. The results are reported in Tables 6.4 and 6.5. These tables show not only the usual results of percent removal and removal rate but also the experimental and model-predicted m-CB concentrations in the air, as well as their comparison, at the exit and one point (about the middle) along the filter bed. Looking at the experimental data in Tables 6.4 and 6.5 one can conclude that for constant τ and C_{GCi} values the percent removal and, consequently, the removal rate increase as the value of Q_L increases. This is probably due to an increased value of A_{SC} obtained at higher Q_L values. One can also observe that the positive effect of increased Q_L is more pronounced at higher C_{GCi} values. For example, when Q_L changes from 1.7 to 5.7 Lh^{-1}, an extra 11% removal is observed at C_{GCi} = 0.46 gm^{-3} whereas at C_{GCi} of 1.7 and 2.7 gm^{-3} the extra removal is 13.5 and 21.5%, respectively. Similar conclusions can be reached from the data at C_{GCi} of 1.2 and 3.1 gm^{-3} for a change in Q_L from 2.7 to 5.7 Lh^{-1}.

The experimental removal rate values are very substantial and can reach levels of about 60 gm^{-3}-reactor h^{-1}. These values are very interesting when one compares them to conventional biofilter performance. With the latter, a maximum removal rate of about 20 gm^{-3}-reactor h^{-1} has been reported for toluene, a compound which is much more easily biodegraded than m-CB. Although performance of biofilters is usually judged based on removal rate (also called removal efficiency) an equally, if not more, important factor is the percent removal. Values exceeding 70% removal have been obtained in almost all cases reported in Tables 6.4 and 6.5 and in some instances values above 90% were

Table 6.4. Experimental data and model predictions for biofiltration of mono-chlorobenzene (m-CB) at constant air residence time ($\tau = 3.8 \pm 0.2$ min) and pH = 6.8 ± 0.2. Air and liquid in counter-current flow.

[a]Q_L (Lh^{-1})	[b]$C_{GCm,1}$ (gm^{-3})	[c]$C_{GCm,2}$ (gm^{-3})	[d]E_1 (%)	[e]$C_{GCe,1}$ (gm^{-3})	[f]$C_{GCe,2}$ (gm^{-3})	[g]E_2 (%)	[h]X (%)	[i]R_{exp} (gm^{-3}-reactor h^{-1})	[j]R_{pred} (gm^{-3}-reactor h^{-1})	[k]E_3 (%)
					[l]$C_{GCi} = 0.46$ gm^{-3}					
1.7	0.22	0.23	+4.55	0.08	0.12	+50.00	82.61	5.56	4.97	-10.61
5.7	0.14	0.15	+7.14	0.03	0.07	+133.33	93.48	6.68	6.06	-9.28
					[l]$C_{GCi} = 0.90$ gm^{-3}					
2.2	0.44	0.41	-6.82	0.14	0.21	+50.00	84.44	11.11	10.09	-9.18
3.9	0.32	0.35	+9.38	0.06	0.16	+166.66	93.33	12.72	11.21	-11.87
					[l]$C_{GCi} = 1.20$ gm^{-3}					
2.7	0.52	0.53	+1.92	0.18	0.26	+44.44	85.00	14.91	13.74	-8.52
5.7	0.43	0.41	-4.65	0.09	0.18	+100.00	92.50	17.24	15.84	-8.12

[a]liquid flow rate, [b]experimental m-CB concentration in air at z = 0.48, [c]model-predicted m-CB concentration in air at z = 0.48, [d]percent error in predicted m-CB concentration at z = 0.48 defined as 100 x $(C_{GCm,2} - C_{GCm,1})/C_{GCm,1}$, [e]experimental m-CB concentration in the air exiting the biofilter bed, [f]model-predicted m-CB concentration in the air exiting the biofilter bed, [g]percent error in predicted exit m-CB concentration defined as 100 x $(C_{GCe,2} - C_{GCe,1})/C_{GCe,1}$, [h]percent m-CB vapor removal based on experimental values and defined as 100 x $(C_{GCi} - C_{GCe,1})/C_{GCi}$, [i]experimentally obtained m-CB vapor removal rate defined as $(C_{GCi} - C_{GCe,1})/\tau$, [j]model-predicted m-CB vapor removal rate defined as $(C_{GCi} - C_{GCe,2})/\tau$, [k]percent error in predicted m-CB removal rate defined as 100 x $(R_{pred} - R_{exp})/R_{exp}$, [l]m-CB vapor concentration in the air entering the biofilter

Table 6.5. Experimental data and model predictions for biofiltration of mono-chlorobenzene (m-CB) at constant air residence time ($\tau = 3.8 \pm 0.2$ min) and pH = 6.8 ± 0.2. Air and liquid in counter-current flow[a].

Q_L (Lh^{-1})	$C_{GCm,1}$ (gm^{-3})	$C_{GCm,2}$ (gm^{-3})	E_1 (%)	$C_{GCe,1}$ (gm^{-3})	$C_{GCe,2}$ (gm^{-3})	E_2 (%)	X (%)	R_{exp} (gm^{-3}-reactor h^{-1})	R_{pred} (gm^{-3}-reactor h^{-1})	E_3 (%)
					$C_{GCi} = 1.70\ gm^{-3}$					
1.7	0.85	0.88	+3.53	0.37	0.48	+29.73	78.23	19.45	17.84	-8.28
5.7	0.58	0.59	+1.72	0.14	0.28	+100.00	91.70	24.23	22.05	-9.00
					$C_{GCi} = 2.70\ gm^{-3}$					
1.7	1.41	1.46	+3.42	0.87	0.82	-5.74	67.77	26.76	27.49	+2.73
3.0	1.32	1.39	+5.30	0.57	0.77	+35.09	78.89	34.69	31.10	-10.35
5.7	1.00	0.97	-3.00	0.31	0.47	+51.61	89.14	38.02	35.48	-6.68
					$C_{GCi} = 3.10\ gm^{-3}$					
2.7	1.65	1.62	+1.82	0.76	0.87	+14.47	75.48	35.99	34.29	-4.72
5.7	1.48	1.24	-16.22	0.47	0.61	+29.78	85.10	44.83	41.42	-7.59
					$C_{GCi} = 3.60\ gm^{-3}$					
3.9	1.94	1.81	+6.70	0.87	0.97	+11.49	73.05	46.53	44.83	-3.65
5.7	1.69	1.53	+9.47	0.72	0.79	+9.72	80.01	49.09	47.89	-2.44
					$C_{GCi} = 4.40\ gm^{-3}$					
3.0	2.65	2.44	+7.92	1.38	1.45	+5.07	68.63	49.18	47.95	-2.50
5.7	2.18	1.88	+13.76	1.12	1.00	-10.71	74.54	55.91	57.95	+3.65

[a]All symbols as defined in Table 6.4

observed. These values are very good when one considers the relatively high inlet m-CB concentration values used in this study and the reasonable residence time under which the experiments of Tables 6.4 and 6.5 were performed.

The agreement between experimental and model-predicted values for the removal rate is extremely good (less than 10% in the majority of cases) as can be seen from Tables 6.4 and 6.5. The agreement is also very good between experimental and model-predicted m-CB concentration values at about the middle ($z = 0.48$) of the filter bed. The agreement is much less satisfactory, and often poor, between experimental and model-predicted values for the m-CB concentration at the exit of the unit. It should be mentioned, however, that the poor agreement is on a percent basis and is observed at very low concentration values. On an absolute basis, the model predicts the exit concentration within no more than 0.1 gm^{-3} in almost all cases.

Some experimental results from runs under constant C_{GCi} and Q_L but varying values of τ are shown in Table 6.6. As expected, the percent removal increases as the

Table 6.6. Experimental data and model predictions for biofiltration of mono-chlorobenzene at pH = 6.8±0.2 as a function of air residence time (τ)[a].

τ (min)	X (%)	R_{exp} (gm^{-3}-reactor h^{-1})	R_{pred} (gm^{-3}-reactor h^{-1})	E (%)
	$C_{GCi} = 1.0\ gm^{-3}, Q_L = 2.2\ Lh^{-1}$			
4.1	84.4	12.34	11.28	-8.59
5.6	96.2	10.28	8.99	-12.55
	$C_{GCi} = 3.0\ gm^{-3}, Q_L = 3.9\ Lh^{-1}$			
2.8	66.6	42.81	44.38	-13.99
3.9	81.5	37.62	37.11	-1.36

[a]All symbols as defined in Table 6.4; counter-current flow of air and liquid

value of τ increases. However, the removal rate decreases which implies that, overall, the process does not behave as a zero-order one.

The effect that Q_L and τ have on the process, when all other operating conditions are constant, is the same with regard to percent conversion. More specifically, as can be seen from Tables 6.4 through 6.6 the conversion of m-CB increases when either Q_L or τ increases. Consequently, a desired conversion can be achieved with various pairs of Q_L and τ values, provided that one decreases when the other increases. This can be

Table 6.7. Experimental data and model predictions for biofiltration of mono-chlorobenzene at pH = 6.8±0.2 as a function of liquid flowrate (Q_L) and air residence time (τ). Counter-current flow of air and liquid[a].

Q_L (Lh^{-1})	τ (min)	X (%)	R_{exp} (gm^{-3}-reactor h^{-1})	R_{pred} (gm^{-3}-reactor h^{-1})	E (%)
			$C_{GCi} = 1.0\ gm^{-3}$		
2.2	5.6	96.2	10.28	8.99	-12.55
3.9	3.9	93.3	14.35	12.32	-14.14
			$C_{GCi} = 1.6\ gm^{-3}$		
0.7	8.8	96.3	10.51	9.03	-14.08
3.9	3.9	91.5	22.52	19.54	-13.23
			$C_{GCi} = 1.9\ gm^{-3}$		
0.7	8.8	90.1	11.67	10.68	-8.48
3.9	3.9	91.5	26.74	23.11	-13.58
			$C_{GCi} = 2.6\ gm^{-3}$		
0.7	8.8	92.9	16.47	14.32	-13.05
3.9	3.9	85.6	34.24	31.33	-8.50
			$C_{GCi} = 3.1\ gm^{-3}$		
2.2	5.4	79.3	27.31	27.76	-1.65
5.7	3.6	86.2	44.53	41.42	-7.59
			$C_{GCi} = 3.6\ gm^{-3}$		
0.7	8.8	83.5	20.50	19.36	-5.56
5.7	3.6	80.0	49.09	47.89	-2.44

[a]All symbols as defined in Table 6.4

observed from the data shown in Table 6.7. From a process design point of view, the implication is that when a specified (e.g., by environmental regulations) pollutant conversion is desired it can be achieved with a smaller unit operating at a higher Q_L.

As in the data sets reported in Tables 6.4 and 6.5, the agreement between experimentally obtained and model-predicted values for the removal rate is also very good for the data sets reported in Tables 6.6 and 6.7.

Figure 6.2 shows model-predicted m-CB concentration profiles in the air along the biofilter bed and experimental data from the three ports on the column. In all cases the

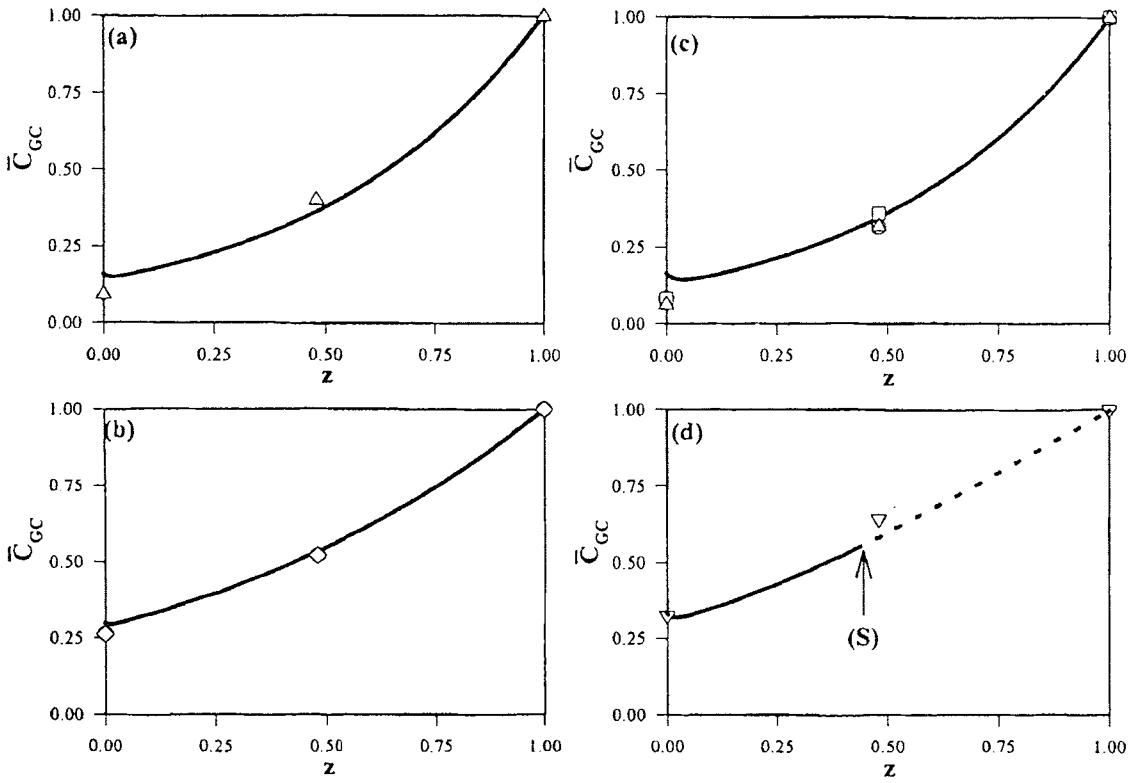

Figure 6.2 Model-predicted mono-chlorobenzene concentration profiles (curves) in the air along the biotrickling filter. Experimental concentration values are given by symbols. Values of C_{GCi} (gm^{-3}), Q_L (Lh^{-1}) and τ (min), respectively, are (a) 1.0, 2.2, and 5.5; (b) 2.6, 1.7, and 4.0; (c) 1.5, 5.7, and 3.7; (d) 4.4, 3.0, and 3.9. Dotted curves imply oxygen control ending at point (S). Air and liquid in counter-current flow.

agreement is very good. The diagram of Figure 6.2(c) is particularly interesting because it shows data from three runs under the same operating conditions, performed months apart one from the other. Clearly, there is an excellent reproducibility of data which has been also observed in all cases in which experiments were repeated. For the cases shown in graphs (a)-(c) of Figure 6.2 the model predicts that m-CB is depleted before oxygen in the biofilm throughout the biotrickling filter. For the case shown in Figure 6.2(d) there are two zones separated at point (S). In the zone which is close to the entrance of the airstream and exit of the liquid stream ($z = 1$) oxygen is depleted before m-CB in the biolayer and the reverse occurs in the zone away from $z = 1$.

The importance of oxygen for the process can be better seen from the diagrams of Figures 6.3 and 6.4. Figure 6.3 shows concentration profiles of m-CB and oxygen, both in air and the liquid along the biotrickling filter, for two sets of operating conditions as predicted by the model. The measured values of m-CB concentration in the air are also shown for comparison purposes. Observe again the excellent reproducibility of data. The oxygen concentration in the air (curve 3) is always very close to the saturation value. However, the oxygen concentration in the liquid (curve 4) can be very high (above 90%) throughout the column as shown in Figure 6.3(b1) or can vary considerably along the column reaching below 50% of the saturation level in segments of the column, as shown in Figure 6.3(b2). For the case shown in graphs (a1) and (b1) m-CB is depleted before oxygen throughout the column and one could argue that the process could had been described equally well with a model which neglects the effect of oxygen. The foregoing argument cannot be made for the case shown in graphs (a2) and (b2) of Figure 6.3. In

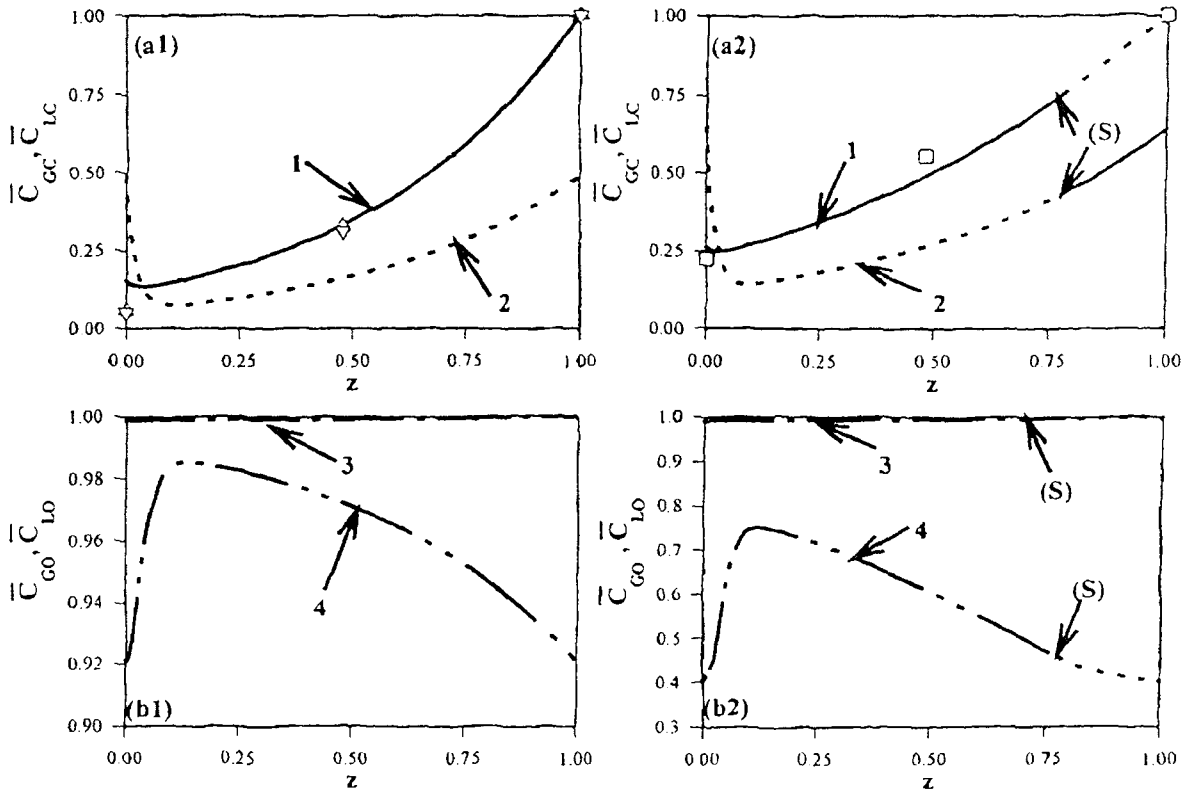

Figure 6.3 Model-predicted concentration profiles of mono-chlorobenzene (curves 1: air, curves 2: liquid) and oxygen (curves 3: air, curves 4: liquid) along the biotrickling filter when the values of C_{GCi} (gm^{-3}), Q_L (Lh^{-1}) and τ (min), respectively, are (a1, b1) 0.46, 5.7, and 3.9; (a2, b2) 3.7, 3.9, and 3.9. Point (S) on curves indicates switching from oxygen limitation close to z = 1 to VOC limitation toward $z = 0$. Symbols represent experimentally measured mono-chlorobenzene concentrations in the air. Air and liquid in counter-current flow.

this case, as in Figure 6.2(d), there are two zones [separated by point (S)] and the one close to z = 1 is essentially oxygen-controlled as oxygen is depleted before m-CB in the biofilm which is the reaction environment.

Oxygen and m-CB concentration profiles in the biofilm, as predicted by the model, are shown in Figure 6.4. This is again a case where there are two zones in the biotrickling filter bed. At low values of z (close to the exit of the airstream) m-CB is depleted before oxygen which stays at very high levels as shown in Figure 6.4(a). As z

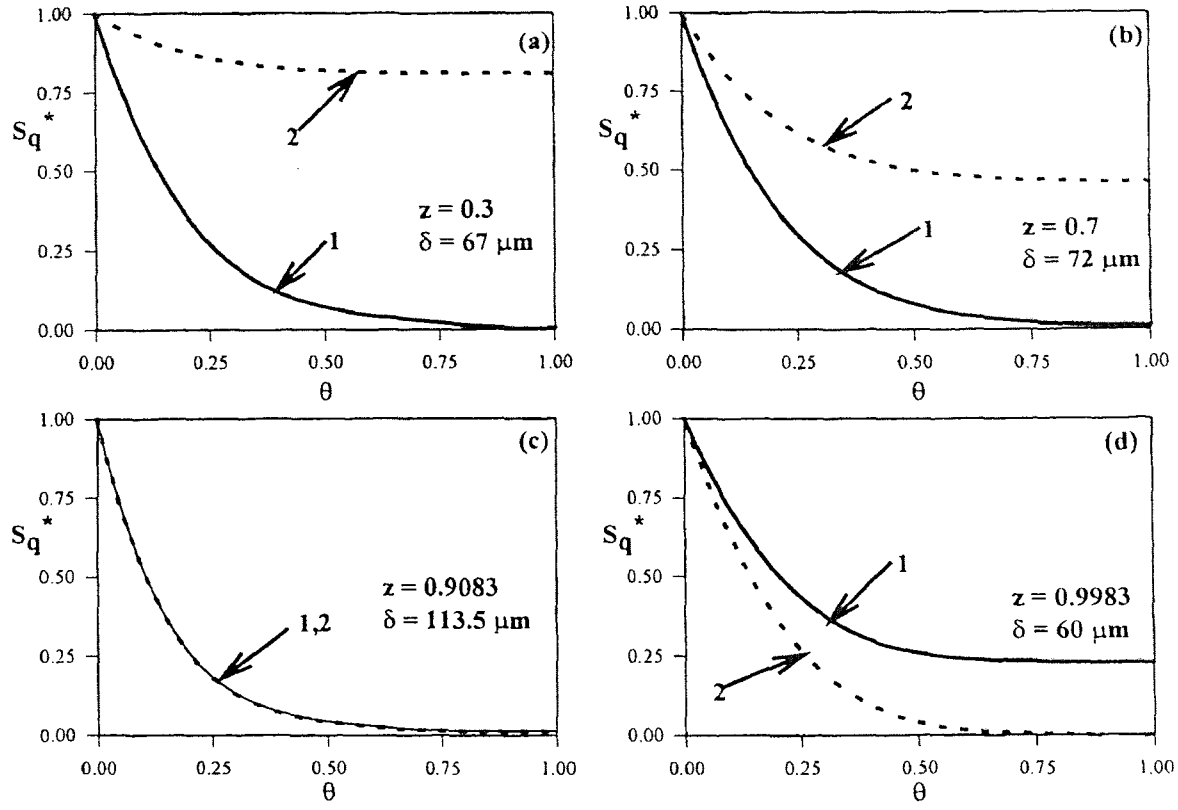

Figure 6.4 Model-predicted normalized concentration profiles in the active biofilm for mono-chlorobenzene (curves 1) and oxygen (curves 2) at four locations along the biotrickling filter column when C_{GCi} = 3.6 gm^{-3}, Q_L = 5.7 Lh^{-1}, and τ = 3.6 min. The effective biofilm thickness (δ) is predicted to vary significantly with z. Air and liquid flow counter-currently.

increases, Figure 6.4(b), m-CB is still depleted first but there is a considerable change in the oxygen concentration along the biolayer depth. As z increases further, it reaches a critical value [point (S) in Figures 6.2 and 6.3] where the normalized m-CB and oxygen concentration profiles are identical as shown in Figure 6.4(c). After the critical value of z, and as one moves toward the bottom of the filter bed, oxygen is depleted before m-CB in the biofilm as shown in Figure 6.4(d).

The structure of the model is such that it allows for determination of the effective biolayer thickness (δ) at every location along the filter bed. The results indicate that

depending on the operating conditions, δ may be essentially constant (curve 2) or vary slightly (curve 1) as shown in Figure 6.5(a), but it can also vary substantially along the column as shown in Figure 6.5(b). The variations of δ along the biotrickling filter bed which have been found during the course of this study are much larger than those found in conventional biofilters (Baltzis et al., 1997; Shareefdeen et al., 1993; Shareefdeen and Baltzis, 1994). However, calculations show that even in cases with large variations in δ, such as the one shown in Figure 6.5(b), using an average value of δ as constant throughout the column does not lead to more than 2% error in the predicted removal rate. This seems to justify the assumption of constant δ made by other investigators who have modeled biotrickling filters (Diks and Ottengraf, 1991 a, b; Ockeloen et al., 1992).

As discussed in Chapter 4, most of the experiments were performed under liquid replenishment with fresh medium on a daily basis. This was the case with all data sets reported in Tables 6.4 through 6.7 and everywhere else in this thesis unless specified otherwise. From experiments performed under less frequent changes of the recirculating liquid with fresh medium, it was found that the percent m-CB removal and the removal rate drop. This can be seen from the experimental data reported in Table 6.8. From this table it can be observed that when the liquid is replenished every two days the percent m-CB removal, relative to that obtained under daily liquid change, drops by 2.5, 5.8, and 8.7 percentage points for inlet m-CB concentrations of 2.4, 3.3, and 4.3 gm^{-3}, respectively. Similarly, at inlet m-CB concentrations of 1.7 and 4.3 gm^{-3} there is a drop by 9 and 18.5 percentage points, respectively, when the liquid is replenished every three days instead of daily. These observations suggest that the higher is the inlet m-CB concentration the

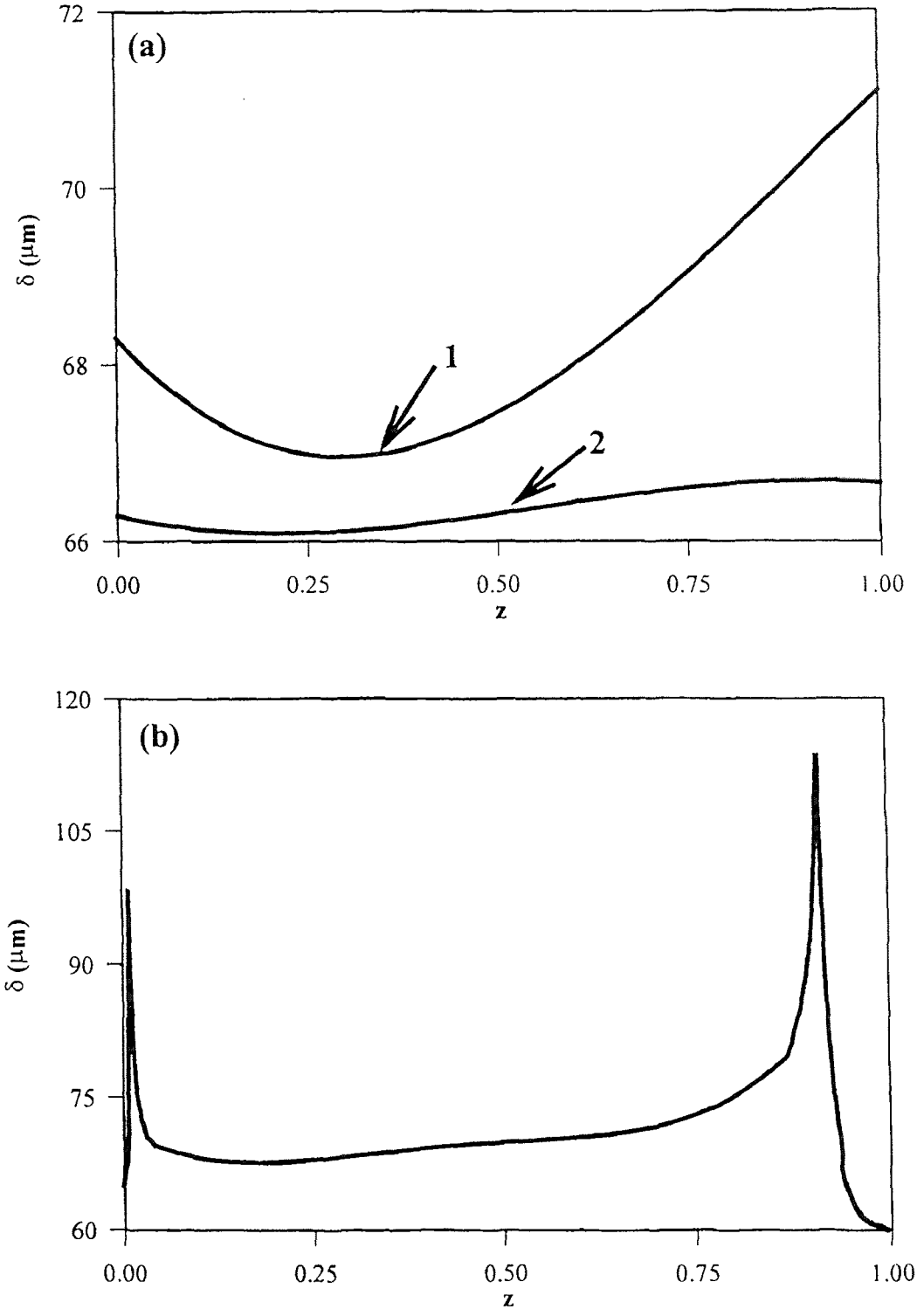

Figure 6.5 Model-predicted variation of the effective biofilm thickness (δ) along the biotrickling filter column when Q_L = 5.7 Lh^{-1}, τ = 3.6 min, and C_{GCi} (gm^{-3}) is (a, curve 1) 2.1, (a, curve 2) 0.46, (b) 3.6. Air and liquid in counter-current flow.

more important is the timely change of the liquid in order to maintain high percent removal and removal rate. This could be explained by the fact that the higher is the inlet m-CB concentration the more amounts of additional nutrients are required. Another possibility is that the drop in removal is related to elevated salt (NaCl) levels as has been reported by Diks and Ottengraf (1991 a, b) as well as Oh and Bartha (1994). The NaCl presence increases with the inlet m-CB concentration since more chloride ions are released and thus, more sodium hydroxide is used for pH adjustment.

Table 6.8. Experimental data for biofiltration of mono-chlorobenzene at pH = 6.8±0.2 and τ = 3.9 min as a function of frequency of medium replenishment[a].

Day	X (%)	R_{exp} (gm^{-3}-reactor h^{-1})
	C_{GCi} = 1.7 gm^{-3}, Q_L = 3.9 Lh^{-1}	
1	91.5	23.93
3	82.5	21.57
	C_{GCi} = 2.4 gm^{-3}, Q_L = 3.9 Lh^{-1}	
1	88.7	32.75
2	86.2	31.83
	C_{GGi} = 3.3 gm^{-3}, Q_L = 3.9 Lh^{-1}	
1	79.3	40.26
2	73.5	37.31
	C_{GCi} = 4.3 gm^{-3}, Q_L = 3.9 Lh^{-1}	
1	71.9	47.56
2	63.2	41.81
3	53.4	35.33

[a]All symbols as defined in Table 6.4; Counter-current flow of air and liquid

With regard to the present study, the diagram of Figure 6.6 shows that the removal rate of m-CB, both at high and low inlet m-CB concentrations, remains constant for the first 25-30 h after the liquid is replenished with fresh medium. Thus, the frequency

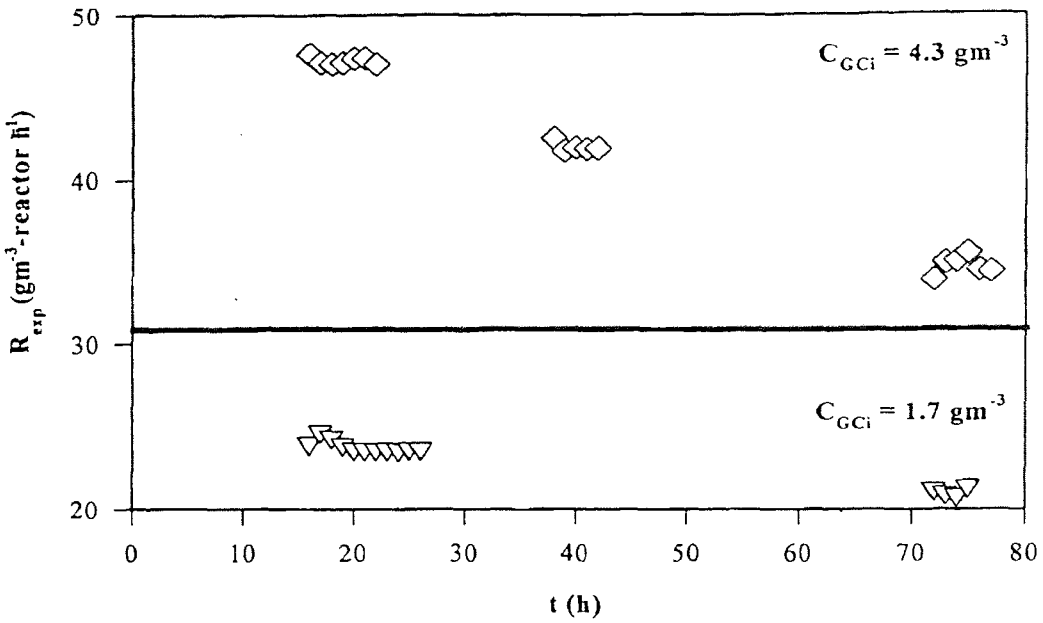

Figure 6.6 Experimentally determined mono-chlorobenzene removal rates as a function of time when Q_L = 3.7 Lh^{-1} and τ = 3.9 min. Fresh medium was used at t = 0 and was not replenished during the course of the measurements shown; counter-current flow of air and liquid.

of liquid replenishment used here was such that it ensured collection of data under steady state conditions which could then be described by a steady state model.

The data reported in Tables 6.3 through 6.8 as well as the kinetic constants reported in Table 5.1 were obtained from experiments performed at pH of about 7. This was the optimal pH value as can be seen from the diagrams of Figure 5.13 which show experimental specific growth rate values as a function of pH for two m-CB concentrations. These are kinetic results obtained from suspended culture experiments in closed serum bottles. The graphs show an almost linear change of the specific growth rate with pH when the latter is out of the 6-7 range. The drop in μ at pH less than 6 observed in suspended culture experiments should also imply a decrease in performance of biotrickling filters operated at pH less than 6. This does in fact occur as shown by the

Table 6.9. Experimental data for biofiltration of mono-chlorobenzene as a function of pH under counter-current flow of air and liquid[a].

C_{GCi} (gm^{-3})	X (%)	R_{exp} (gm^{-3}-reactor h^{-1})	pH
	$Q_L = 2.7\ Lh^{-1}, \tau = 4.1$ min		
1.6	80.6	18.9	6.3±0.1
1.6	70.6	16.5	5.1±0.2
4.2	68.9	42.3	6.8±0.2
4.2	56.7	34.8	5.1±0.1
	$Q_L = 3.9\ Lh^{-1}, \tau = 3.8$ min		
2.2	87.7	30.5	6.8±0.3
2.2	84.2	29.3	5.8±0.1
3.7	73.2	42.8	6.6±0.2
3.7	60.9	35.6	4.3±0.2

[a]All symbols as defined in Table 6.4

data reported in Table 6.9. However, the drop in removal rate observed is no way near the drop in μ observed in suspended cultures. Even at very low pH values a very respectable removal rate of m-CB vapor is obtained. This seems to suggest that the pH measured in the liquid exiting the biotrickling filter is not necessarily that in the reaction environment (biofilms). Although this is an issue which needs further and systematic study, it should be mentioned here that the data reported in Table 6.9 were not obtained under pH control. Data were obtained at various instants of time as the biofilter operated without pH adjustment of the recirculating liquid. Hence, it is yet unknown if long term operation of the biotrickling filter under low pH will yield removal rates as high as those shown in Table 6.9.

Experiments on m-CB vapor removal were also performed under co-current flow of the air and the liquid, and the results are presented in Table 6.10. For comparison purposes, results on m-CB removal under counter-current flow of air and liquid reported in earlier tables are also presented in Table 6.10. The first thing to be observed is that the

Table 6.10. Removal of mono-chlorobenzene vapor in a biotrickling filter under co- and counter-current flow of air and liquid[a].

	C_{GCi} (gm^{-3})	Q_L (Lh^{-1})	τ (min)	X (%)	R_{exp} (gm^{-3}-reactor h^{-1})	R_{pred} (gm^{-3}-reactor h^{-1})	E (%)
+[b]	0.60	2.4	3.65	86.44	8.36	7.26	-13.16
-[c]	0.45	1.7	4.00	82.61	5.56	4.97	-10.61
+	0.90	2.4	3.65	88.13	13.00	11.95	-13.46
-	0.90	2.2	3.80	84.44	11.11	10.09	-9.18
+	2.70	2.4	3.65	83.88	36.85	31.64	-14.14
-	2.70	2.9	3.65	78.89	34.69	31.43	-9.40
+	0.65	4.8	3.65	94.12	10.18	8.96	-11.98
-	0.45	5.6	3.85	93.48	6.68	6.06	-9.28
+	0.90	4.8	3.65	94.51	13.95	12.18	-12.69
-	1.10	5.6	3.85	92.90	15.92	14.41	-9.48
+	1.80	4.8	3.65	93.27	27.83	24.35	-12.50
-	1.75	5.6	3.85	92.70	25.28	22.75	-10.01

[a]All symbols as defined in Table 6.4;[b]co-current flow; [c]counter-current flow

percent removal of m-CB is always high, often exceeding 90%. For co-current flow, under the same values of C_{GCi} and τ (e.g., 0.60 gm^{-3} and 3.65 min, or 0.90 gm^{-3} and 3.65 min) the percent removal, as well as the removal rate, increases when the liquid flow rate increases (from 2.4 to 4.8 Lh^{-1}). The same observation was made from data under

counter-current flow of air and liquid. As also discussed earlier, this is probably due to an increased specific wetted biofilm area (A_{SC}) obtained at higher Q_L values. The data of Table 6.10 also show that co-current flow of air and liquid is better than counter-current flow in the sense that for the same C_{GCi}, Q_L, and τ the percent removal and removal rate of m-CB are higher under co-current flow. This can be seen, for example, at $C_{GCi} = 2.70$ gm^{-3} and $\tau = 3.65$ min where co-current flow leads to better performance although the Q_L is lower than that for counter-current flow. Similarly, at inlet concentration of 1.80 gm^{-3} using lower values for both Q_L and τ under co-current conditions one still gets a slightly better performance than under counter-current conditions where the higher Q_L and τ values should help obtaining better results.

The better performance of the biotrickling filter under co-current flow of air and liquid could be explained by the fact that a higher concentration differential exists between the two phases especially at the inlet of the airstream. This enhances the mass transfer of the pollutant from the air to the liquid and consequently to the biofilm which is the actual reaction environment. Enhanced performance under co-current operation is also predicted by the model describing the process. Similar predictions are made by the model of Diks and Ottengraf (1991a,b) although these investigators did not experimentally observe such differences.

As can be seen from Table 6.10 the model does an equally good job predicting the performance under co-current and counter-current flow of air and liquid. A sample of model-predicted concentration profiles for m-CB and oxygen for co-current operation is given in Figure 6.7. Observe that the m-CB concentration values in the air (curves 1 in

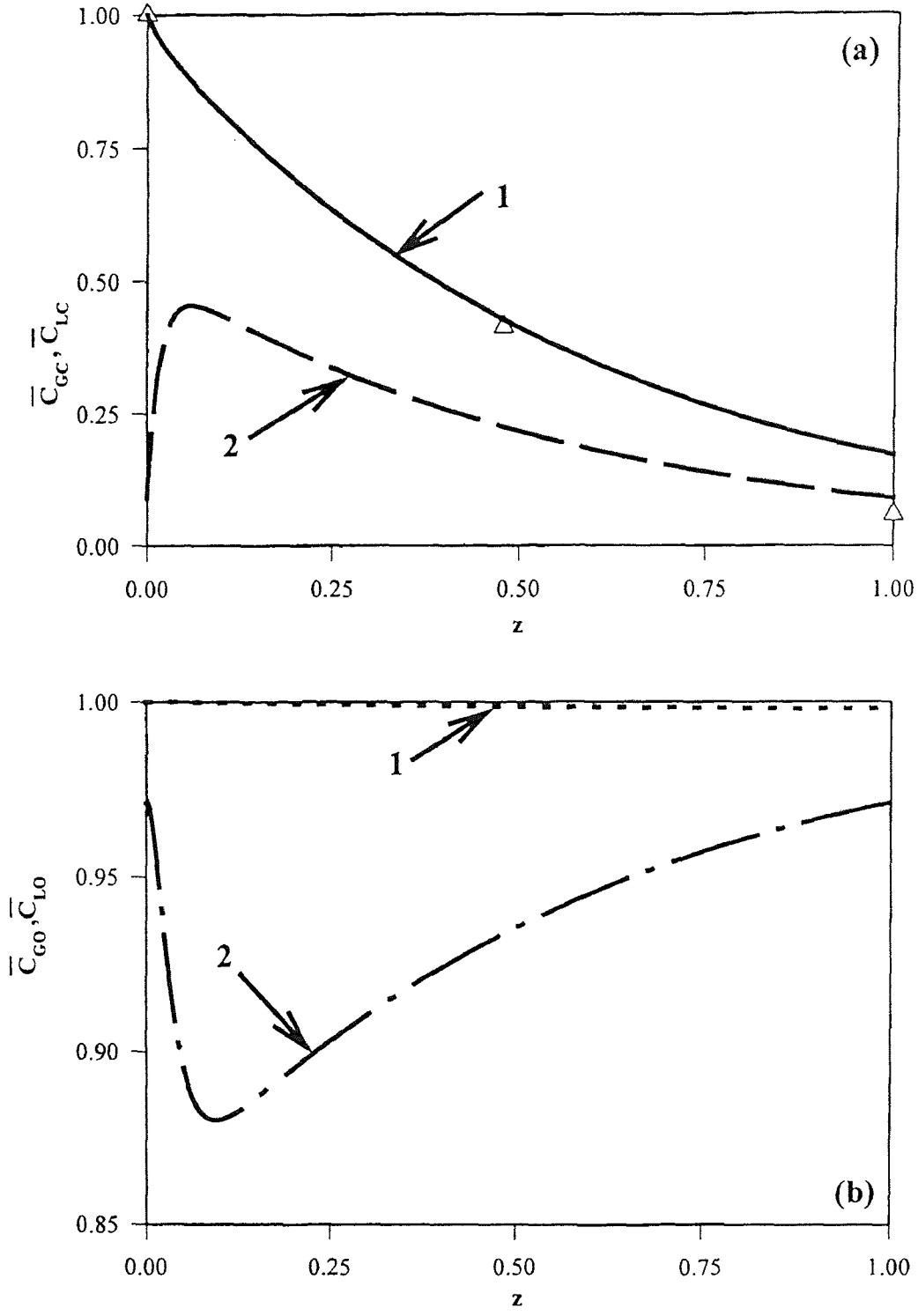

Figure 6.7 Model-predicted dimensionless concentration profiles of (a) m-CB and (b) oxygen along the biotrickling filter. Curves 1 and 2 are for the gas and liquid phase, respectively. Symbols represent data from the gas phase (air). Experimental conditions: co-current flow of air and liquid; C_{GCi} = 0.65 gm^{-3}; Q_L = 4.8 Lh^{-1}; τ = 3.65 min.

Figure 6.7a) is in excellent agreement with data obtained from the middle point of the column. At the exit, the model overpredicts the pollutant concentration although it should be mentioned that exit concentrations are very low and the likelihood of an error in measurement is much higher. From Figure 6.7a it is worth observing the predicted concentration differential between air and liquid (curves 1 and 2, respectively) at the entrance of the air in the biotrickling filter (z = 0 in Figure 6.7a). Under co-current conditions (Figure 6.7a) this difference is much larger and leads to enhanced mass transfer as discussed earlier. Regarding oxygen, one can observe from Figure 6.7b that the concentration in the air (curve 1) remains, as expected, essentially constant. In the liquid phase though (curve 2), there is a variation which is not significant. At inlet m-CB concentrations much higher than the one used in Figure 6.7b the model predicts a considerable variation in the oxygen concentration in the liquid phase. This is the same result as the one discussed earlier regarding counter-current flow of air and liquid.

6.5 Biofiltration of Ortho-dichlorobenzene (o-DCB)

Table 6.11 shows results from o-DCB vapor removal under counter-current flow of the air and liquid phases. It is clear (especially from the percent removal values) that removal of o-DCB is more difficult when compared to m-CB. This is due to the fact that o-DCB is a more recalcitrant compound and in fact, as discussed in Chapter 5, o-DCB biodegradation kinetics are much slower than m-CB kinetics. Percent removal of o-DCB in the 90% range is not impossible, but would require very large reactor volumes and/or flows of the liquid. On the other hand, low o-DCB levels are more likely to occur in

practical applications and thus, removal complying with environmental regulations could be achieved with units of reasonable size.

From Table 6.11 one can see that the agreement between experimental and model-predicted removal rates for o-DCB is very good. In fact, the agreement in the o-DCB case

Table 6.11. Experimental data and model predictions for biofiltration of ortho-dichlorobenzene (o-DCB) at pH = 6.8±0.2 as a function of air residence time (τ) and liquid flowrate (Q_L)[a].

C_{GDi} (gm^{-3})	X (%)	R_{exp} (gm^{-3}-reactor h^{-1})	R_{pred} (gm^{-3}-reactor h^{-1})	E (%)
		τ = 6.20 min, Q_L = 1.2 Lh^{-1}		
1.20	71.8	8.28	8.48	+2.42
2.30	64.0	14.15	15.69	+10.88
		τ = 4.50 min, Q_L = 1.9 Lh^{-1}		
0.65	76.4	6.62	6.16	-6.95
3.50	60.0	27.98	30.10	+7.58
		τ = 3.25 min, Q_L = 3.3 Lh^{-1}		
0.75	63.8	9.00	9.53	+5. 89
2.10	57.5	22.42	24.93	+11.19

[a]All symbols as defined in Table 6.4; Air and liquid in counter-current flow

is much better than the m-CB case. This is probably due to the fact that exit m-CB concentrations are much lower than those of o-DCB. At very low concentrations, as also discussed earlier, the model deviates from the experimental values more than usual and thus, this apparent better model performance with o-DCB.

Model-predicted o-DCB concentration profiles along the biofilter are shown in Figure 6.8. As can be seen, predictions and data for o-DCB concentrations in the air agree very nicely. Regarding oxygen, as was also the case with m-CB, the liquid phase

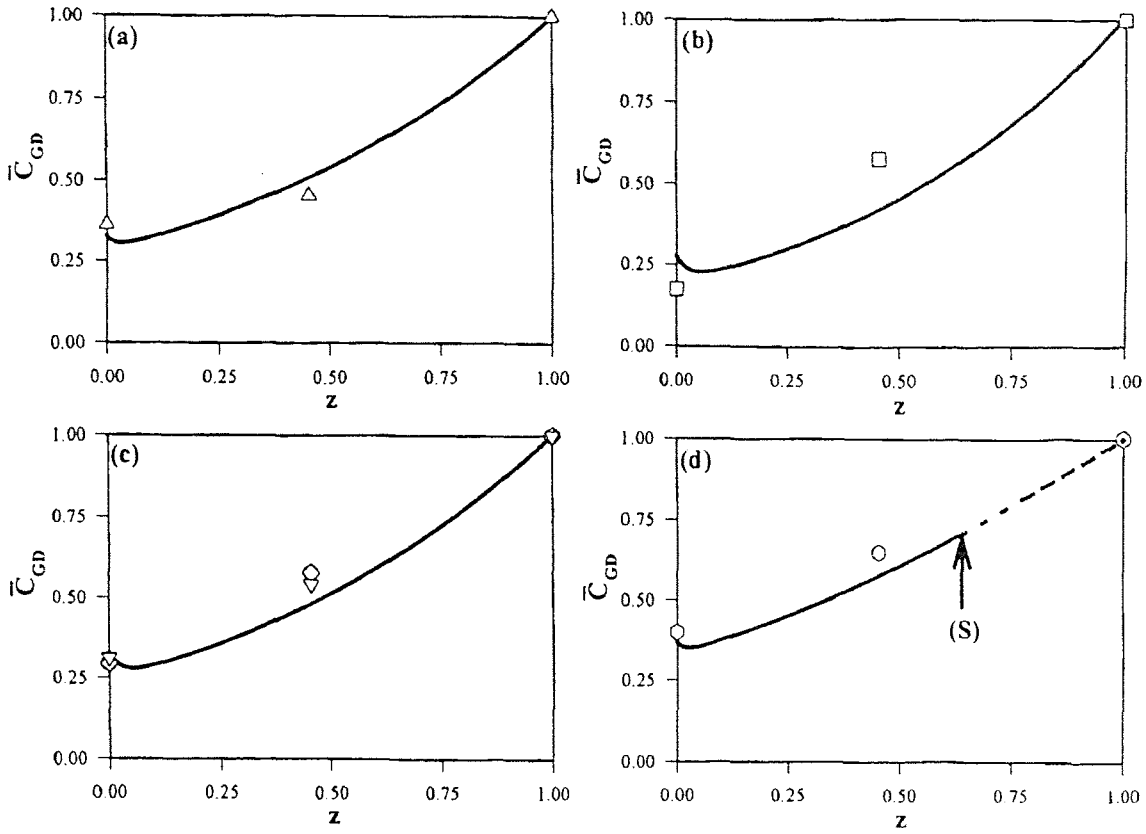

Figure 6.8 Model-predicted ortho-dichlorobenzene concentration profiles (curves) in the air along the biotrickling filter. Experimental concentration values are given by symbols. Values of C_{GDi} (gm^{-3}), Q_L (Lh^{-1}) and τ (min), respectively, are (a) 0.75, 3.3, and 3.25; (b) 1.17, 5.2, and 3.0; (c) 2.1, 5.2, and 3.0; (d) 3.50, 1.9, and 4.50. Dotted curves imply oxygen control ending at point (S). Counter-current flow of air and liquid.

concentration varies insignificantly and remains close to saturation when the inlet o-DCB concentration is low or varies considerably when the inlet o-DCB concentration is high. Figure 6.8(d) shows a case of high inlet o-DCB concentration. For this case, the model predicts that the oxygen presence in the liquid is between 60 and 75% of saturation throughout the biotrickling filter unit. Consequently, there is a segment of the unit close to the entrance of the polluted air (z = 1) where the process is oxygen-controlled. Point (S) in Figure 6.8(d) indicates the boundary between the oxygen- and o-DCB-controlled zones in the bed. This can be better understood by looking at the predicted concentration

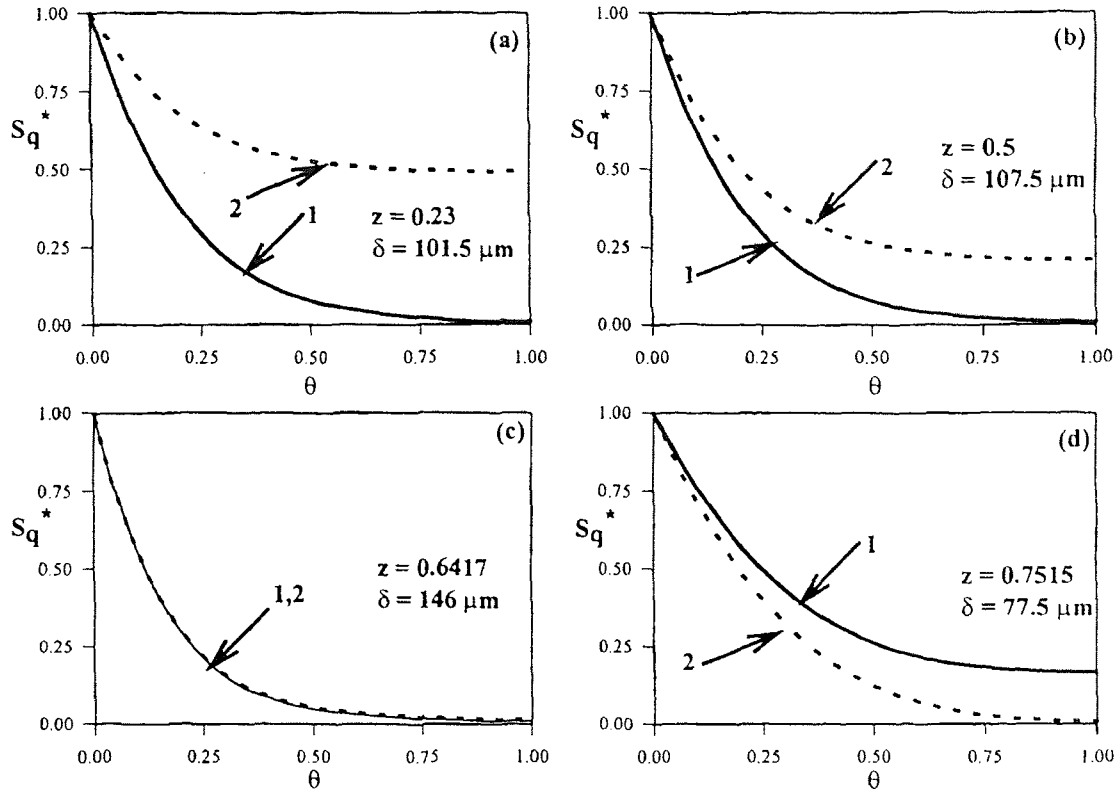

Figure 6.9 Model-predicted normalized concentration profiles in the active biofilm for ortho-dichlorobenzene (curves 1) and oxygen (curves 2) at four locations along the biotrickling filter column when C_{GDi} = 3.5 gm^{-3}, Q_L = 1.9 Lh^{-1}, and τ = 4.5 min. The effective biofilm thickness (δ) is predicted to vary significantly with z. Counter-current flow of liquid and air.

profiles in the biofilm shown in Figure 6.9. Observe that the relative position of the o-DCB (curve 1) and oxygen (curve 2) concentration profiles changes along the unit. The two profiles become identical (since values are normalized with those at the liquid/biofilm interface) at a particular location (Figure 6.9(c)) in the unit. This location is point (S) in Figure 6.8(d). Oxygen is depleted faster than o-DCB at values of z larger than 0.6417 and thus, about 35% of the unit is under oxygen control. At low inlet o-DCB concentration values the profiles in the biofilm resemble those of Figure 6.9(a) throughout the column.

All experiments reported in Table 6.11 were performed at a constant pH of about 6.8 which was found to be optimal for the o-DCB consortium when in suspension (see Figure 5.14). Some biotrickling filter experiments with o-DCB were performed at pH values lower than 6.8 and results are shown in Table 6.12. It is clear that, when all other conditions are identical, a pH lower than 6.8 leads to lower removal rates. However, this drop is far less than what is observed with suspended cultures where a pH of 5.1 or 4.8 reduces removal by more than 40% compared to the value obtained at pH of 6.8. The results shown in Table 6.12 seem to suggest that cells in the biofilm are protected from unfavorable pH conditions probably due to mass transfer effects. Similar is the behavior of m-CB removal at low pH values of the liquid in a biotrickling filter as discussed in Section 6.4 of this thesis.

Table 6.12. The effect of pH on the removal of ortho-dichlorobenzene (o-DCB) in a biotrickling filter.[a]

C_{GDi} (gm^{-3})	X (%)	R_{exp} (gm^{-3}-reactor h^{-1})	pH
	$Q_L = 1.2\ Lh^{-1}, \tau = 6.20$ min		
0.85	76.5	6.30	6.8±0.2
0.85	64.3	5.29	5.1±0.2
1.35	70.6	9.23	6.8±0.2
1.35	57.5	7.51	4.8±0.2
	$Q_L = 1.9\ Lh^{-1}, \tau = 4.50$ min		
0.50	77.6	5.07	6.8±0.2
0.50	70.6	4.61	5.5±0.2
1.50	62.9	12.66	6.8±0.2
1.50	53.5	10.77	5.5±0.2

[a]All symbols as defined in Table 6.4; Counter-current flow of liquid and air

As has been also the case of the study with mono-chlorobenzene (see Section 6.4), experiments with o-DCB vapor have also shown that operation of the unit under co-current flow of air and liquid is more efficient than operation under counter-current conditions. Results from experiments under co-current flow of liquid and o-DCB laden air are shown schematically in Figures 6.10 and 6.11 and in tabular form in Table 6.13. From the diagrams of Figures 6.10 and 6.11 one can see that, as was also true in all cases discussed earlier in this chapter, the model predicts nicely the gas phase concentration data with a tendency to overpredict the concentration value at the exit of the gas phase (z = 1). This overprediction is more pronounced as the inlet o-DCB concentration decreases.

For comparison purposes, Table 6.13 shows experimental data from pairs of

Table 6.13. Removal of ortho-dichlorobenzene vapor in a biotrickling filter under co- and counter-current flow of air and liquid[a].

Operation Mode	X (%)	R_{exp} (gm^{-3}-reactor h^{-1})	R_{pred} (gm^{-3}-reactor h^{-1})	E (%)
	C_{GDi} = 0.25±0.1 gm^{-3}, τ = 3.00 min, Q_L = 5.2 Lh^{-1}			
+[b]	80.6	4.03	3.62	-10.17
-[c]	71.1	3.55	3.12	-12.11
	C_{GDi} = 0.55±0.1 gm^{-3}, τ = 3.00 min, Q_L = 5.2 Lh^{-1}			
+	84.4	9.28	8.87	-4.42
-	79.6	8.92	8.11	-9.09
	C_{GDi} = 1.15±0.1 gm^{-3}, τ = 3.00 min, Q_L = 5.2 Lh^{-1}			
+	83.1	19.11	17.16	-10.20
-	78.9	18.15	16.51	-9.04
	C_{GDi} = 1.65±0.1 gm^{-3}, τ = 3.00 min, Q_L = 5.2 Lh^{-1}			
+	78.6	25.62	23.82	-7.03
-	73.3	23.90	22.34	-6.98
	C_{GDi} = 2.10±0.1 gm^{-3}, τ = 3.00 min, Q_L = 5.2 Lh^{-1}			
+	72.4	30.41	29.80	-2.00
-	70.7	29.69	28.43	-4.24

[a]All symbols as defined in Table 6.4; [b]co-current flow; [c]counter-current flow

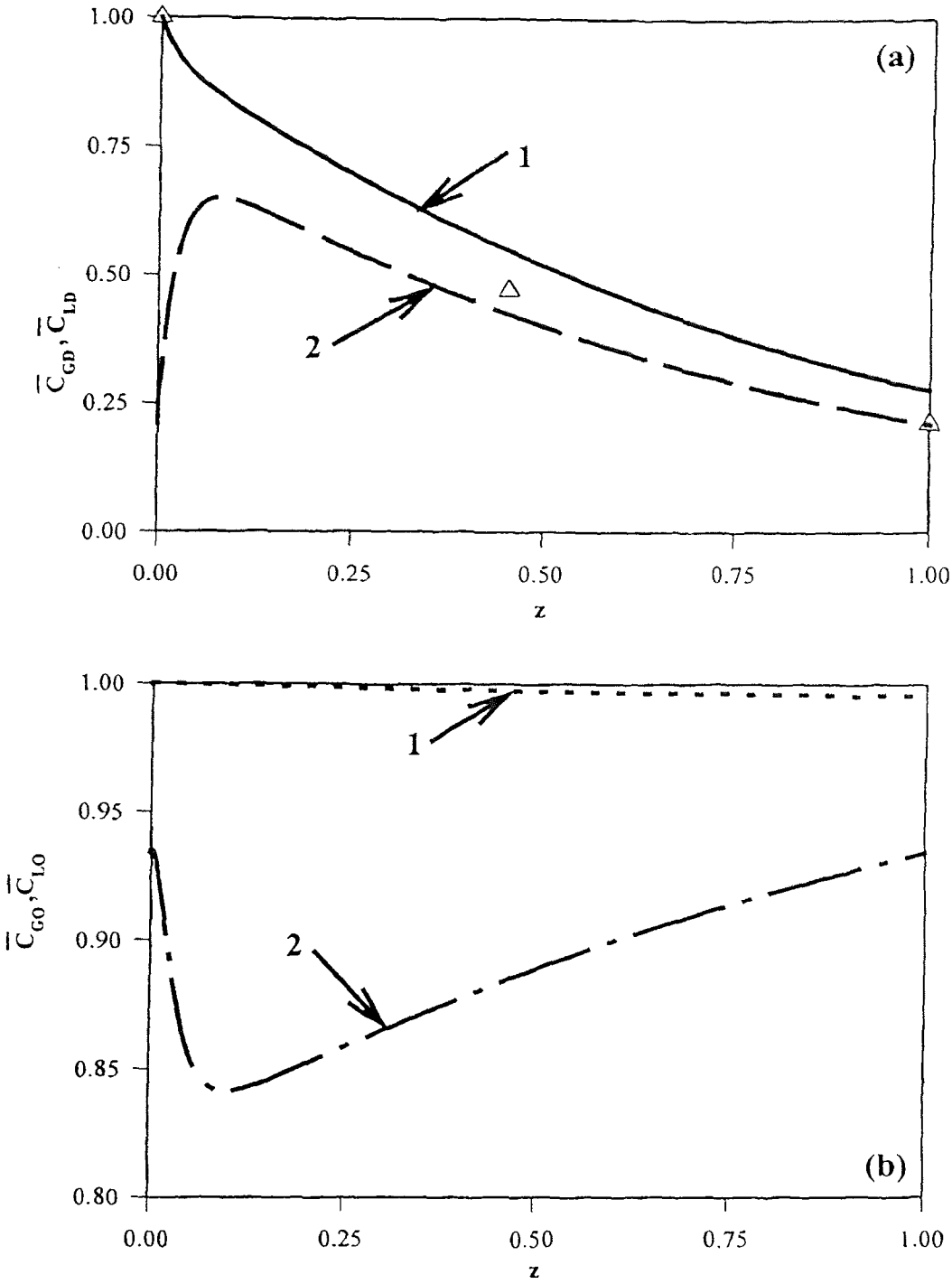

Figure 6.10 Model-predicted dimensionless concentration profiles of (a) o-DCB and (b) oxygen along the biotrickling filter. Curves 1 and 2 are for the gas and liquid phase, respectively. Symbols represent data from the gas phase (air). Experimental conditions: co-current flow of air and liquid; $C_{GDi} = 1.65\ gm^{-3}$; $Q_L = 5.2\ Lh^{-1}$; $\tau = 3.00$ min.

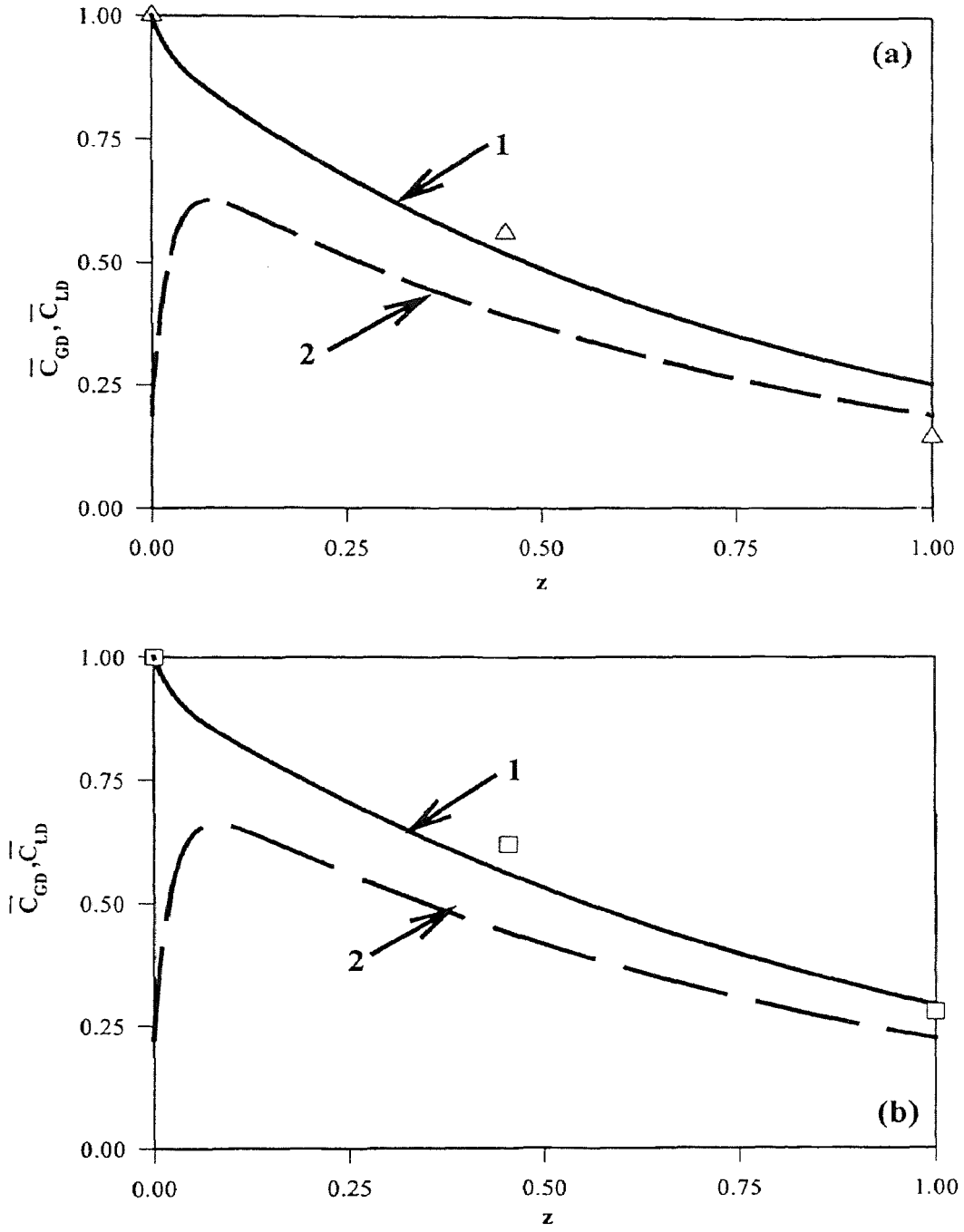

Figure 6.11 Model-predicted dimensionless o-DCB concentration profiles (curves 1: air, curves 2: liquid) along the biotrickling filter. Symbols represent data from the gas phase (air). Experimental conditions: (a) co-current flow of air and liquid; C_{GDi} = 0.56 gm^{-3}; Q_L = 5.2 Lh^{-1}; τ = 3.00 min; (b) co-current flow of air and liquid; C_{GDi} = 2.10 gm^{-3}; Q_L = 5.2 Lh^{-1}; τ = 3.00 min.

experiments in which the only difference is the relative direction of air and liquid flow. As can be seen from the table, when C_{GDi}, Q_L and τ are kept constant co-current flow leads to better results. In fact, the results suggest that in terms of percent o-DCB conversion co-current flow is increasingly better than counter-current flow as the inlet concentration decreases.

6.6 Parameter Sensitivity Analysis

As can be seen from the equations presented in Section 6.1, the model developed during the study reported here contains a large number of parameters. In order to determine which parameters affect most the model predictions and consequently the model itself, a sensitivity study was undertaken and its results are presented here.

Two sets of numerical studies were performed one using as base values those of o-DCB (Tables 6.11 and 6.13) and one using as base values those of m-CB (Tables 6.1 and 6.2).

When the o-DCB parameters were used as basis, a particular experiment was used as reference point. This experiment was performed under co-current flow of the liquid and gas phase, and with $C_{GDi} = 0.56\ gm^{-3}$, $\tau = 3.0$ min, $Q_L = 5.2\ Lh^{-1}$. The experimental value for the removal rate was 9.28 gm^{-3}-packing h^{-1}.

The results are given in Figures 6.12 through 6.14. On the x-axis of these graphs the relative value of the parameter under investigation is plotted. The relative value of a parameter is defined as the ratio of an assumed new value for the parameter divided by the base value of that parameter (reported in Tables 6.11 and 6.3). On the y-axis of the

graphs, the relative value of the removal rate is indicated. This is defined as the predicted removal rate under the assumed new value of a model parameter divided by the experimentally observed removal rate for the set of experimental conditions which was taken as basis (i.e., divided by 9.28 gm^{-3}-packing h^{-1}).

Figure 6.12 shows the results of sensitivity studies with the kinetic parameters

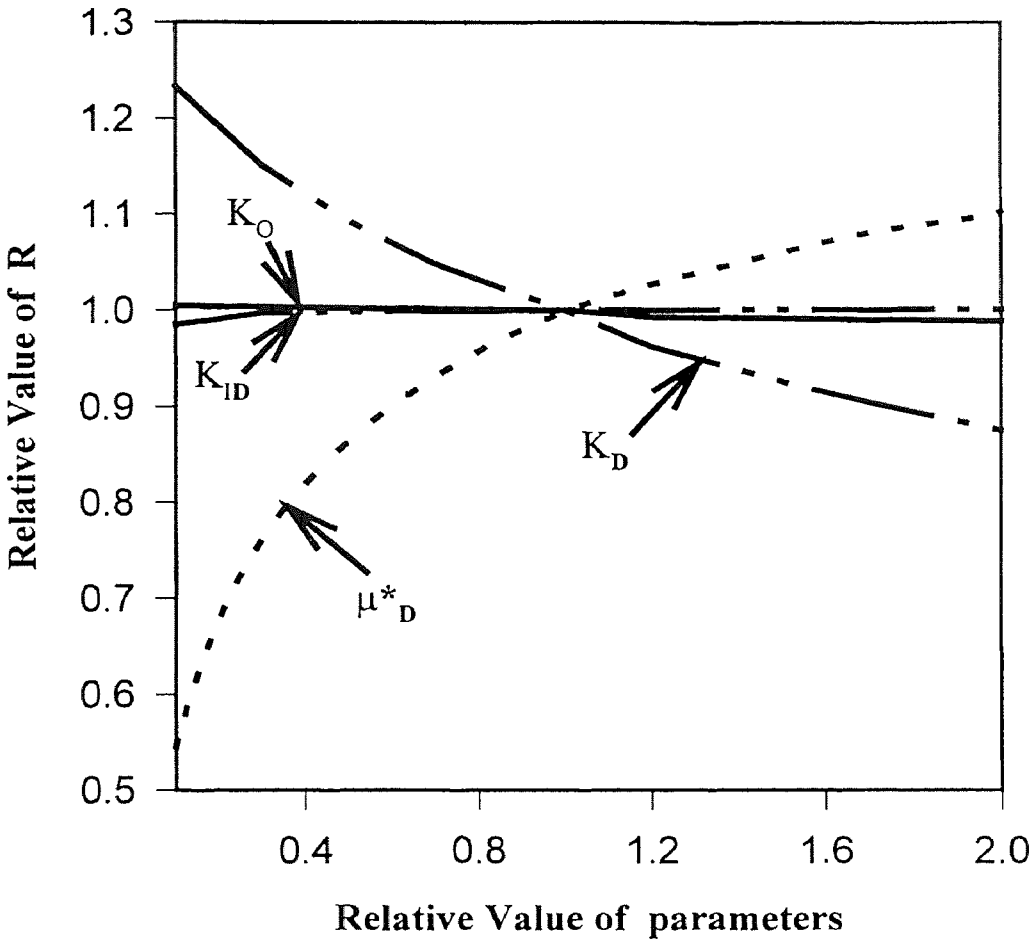

Figure 6.12 Sensitivity analysis of the effect of kinetic parameters on the removal rate of o-DCB. Experimental conditions: co-current flow of air and liquid; C_{GDi} = 0.56 gm^{-3}; Q_L = 5.2 Lh^{-1}; τ = 3.00 min. The (1,1) point corresponds to an actual removal rate of about 9.28 gm^{-3}-packing h^{-1}.

involved in kinetic expressions (6.17) and (6.18). As can be seen from the graph, two of the four kinetic parameters, μ^*_D and K_D, are important something which implies that a

zero- or first-order kinetic approximation cannot be made. It is also interesting to observe that the model is not sensitive to the value of K_O. This is particularly important as this parameter was not measured, but rather was estimated from published data as has been explained by Shareefdeen et al. (1993). Hence, when performing kinetic experiments for biofiltration purposes, one needs a relative accurate determination of μ^*_j and K_j while the importance of K_{lj} and K_O seems to be low.

From Figure 6.13 one can conclude the following: for relative biofilm density

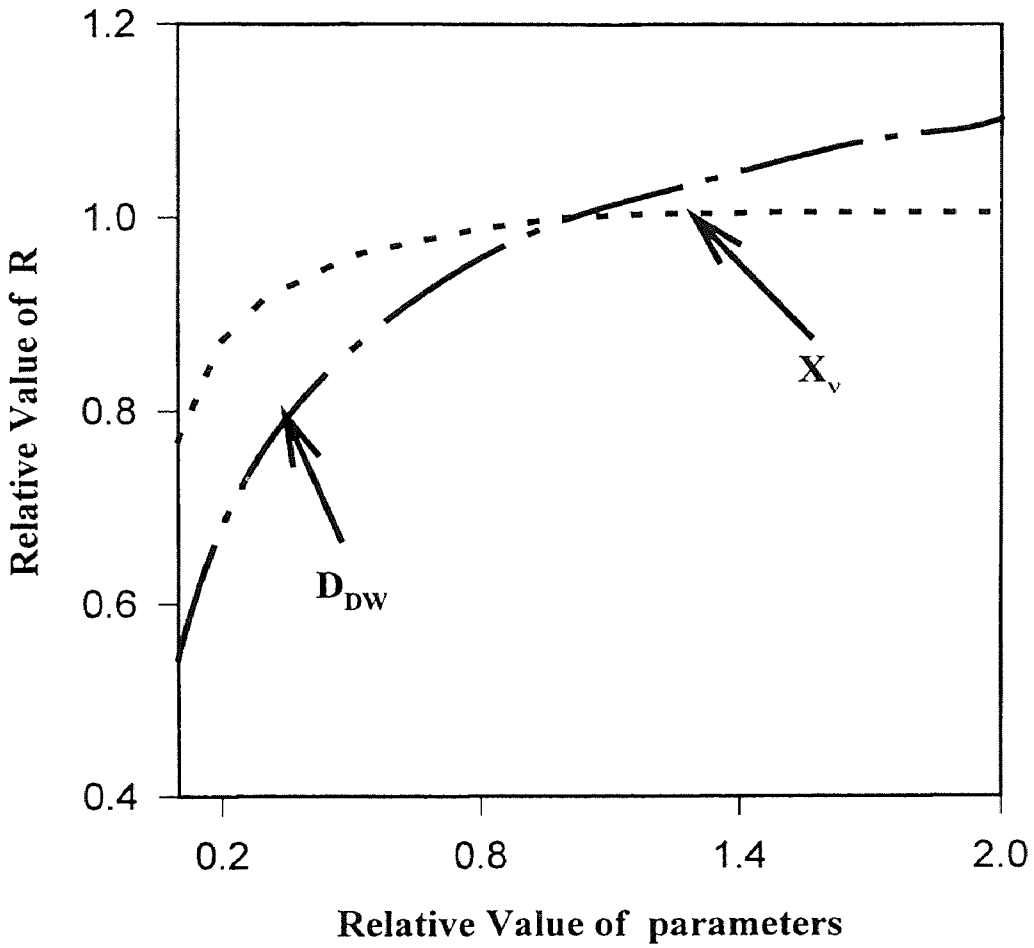

Figure 6.13 Sensitivity analysis of the effect of parameters X_v and D_{DW} on the removal rate of o-DCB. Experimental conditions: co-current flow of air and liquid; C_{GDi} = 0.56 gm^{-3}; Q_L = 5.2 Lh^{-1}; τ = 3.00 min. The (1,1) point corresponds to an actual removal rate of about 9.28 gm^{-3}-packing h^{-1}.

(X_v) values larger than 0.6, or actual values larger than 45 gm^{-3}, the predicted removal rate is insensitive to the actual X_v value. If the actual X_v value is between 7.5 and 45 gm^{-3} the error in the predicted value will be more than 20%. The value of pollutant diffusivity (D_{DW}) seems to be very important as shown in Figure 6.13. It appears that if the real D_{DW} value is larger than the one estimated (relative value larger than 1), the impact on the prediction of the removal rate is less than 10%. On the other hand, if the real value is less than the estimated one, the error in predicting removal rates can be very substantial.

Figure 6.14 shows the sensitivity of the removal rate to changes in the values of the distribution coefficient (m_D), the overall mass transfer coefficient (K_{LD}), and the yield coefficient (Y_D). Regarding the distribution coefficient, one can say that when the substance is very volatile (high m_D value), then it is present in very low concentrations inside the biolayer. Consequently, the kinetics are non-inhibitory, and the removal rates are high. The less volatile a substance is, the higher the probability of being under inhibitory kinetics throughout the column, and this leads to lower removal rates. These last observations are interesting in cases where one wants to predict the removal rates for a substance having kinetic constants similar to those of o-DCB, but being less or more volatile than o-DCB. Also, for o-DCB itself, one can estimate the removal rate when there are temperature changes, which result to changes in the values of m_D, assuming that these temperature variations do not have a serious impact on the kinetics. These observations and results are almost identical with those obtained in similar studies with conventional biofilters (Shareefdeen et al., 1993; Shareefdeen and Baltzis, 1994). As far

as mass transfer coefficients are concerned, it can be observed that the removal rate decreases drastically with K_{LD} but when the K_{LD} value is larger than the one estimated, the removal rate increases only slightly. Finally, regarding the yield coefficient (Y_D) it can be observed that when it is overestimated (relative value larger than 1) the removal rate is underestimated (R less than 1) although slightly only. Significant underestimation of Y_D can lead to relatively considerable overestimation in removal rate.

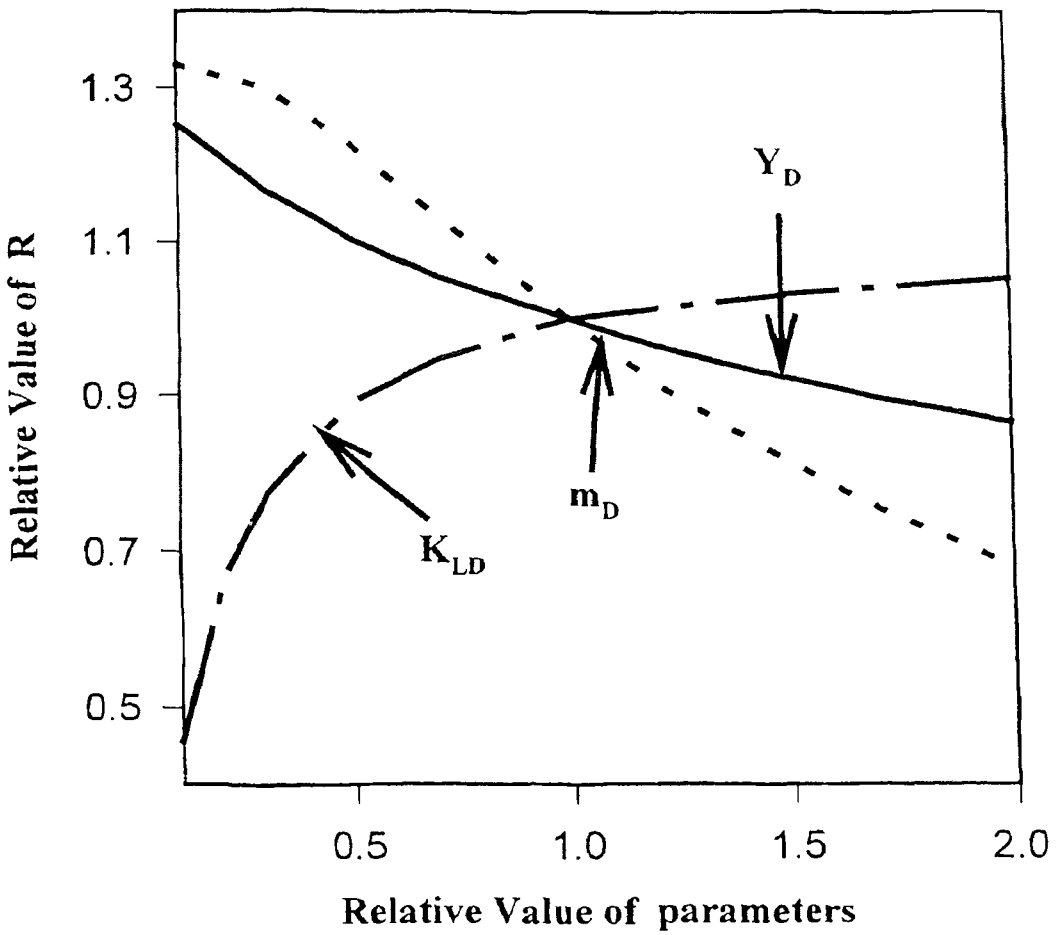

Figure 6.14 Sensitivity analysis of the effect of parameters m_D, K_{LD}, and Y_D on the removal rate of o-DCB. Experimental conditions: co-current flow of air and liquid; C_{GDi} = 0.56 gm^{-3}; Q_L = 5.2 Lh^{-1}; τ = 3.00 min. The (1,1) point corresponds to an actual removal rate of about 9.28 gm^{-3}-packing h^{-1}.

Conclusions almost identical to those reached from Figures 6.12 through 6.14 can be reached from Figures 6.15 and 6.16 which show results of sensitivity studies with the values of parameters for m-CB serving as basis (Tables 6.1 and 6.2). The experiment used as reference point was performed under co-current flow of air and liquid and with C_{GDi} = 1.80 gm^{-3}, τ = 3.65 min, Q_L = 4.8 Lh^{-1}. Under these conditions (see also Table 6.10) the experimental value for the removal rate is 27.83 gm^{-3}-packing h^{-1}. This value was used in determining the relative value of the removal rate (R).

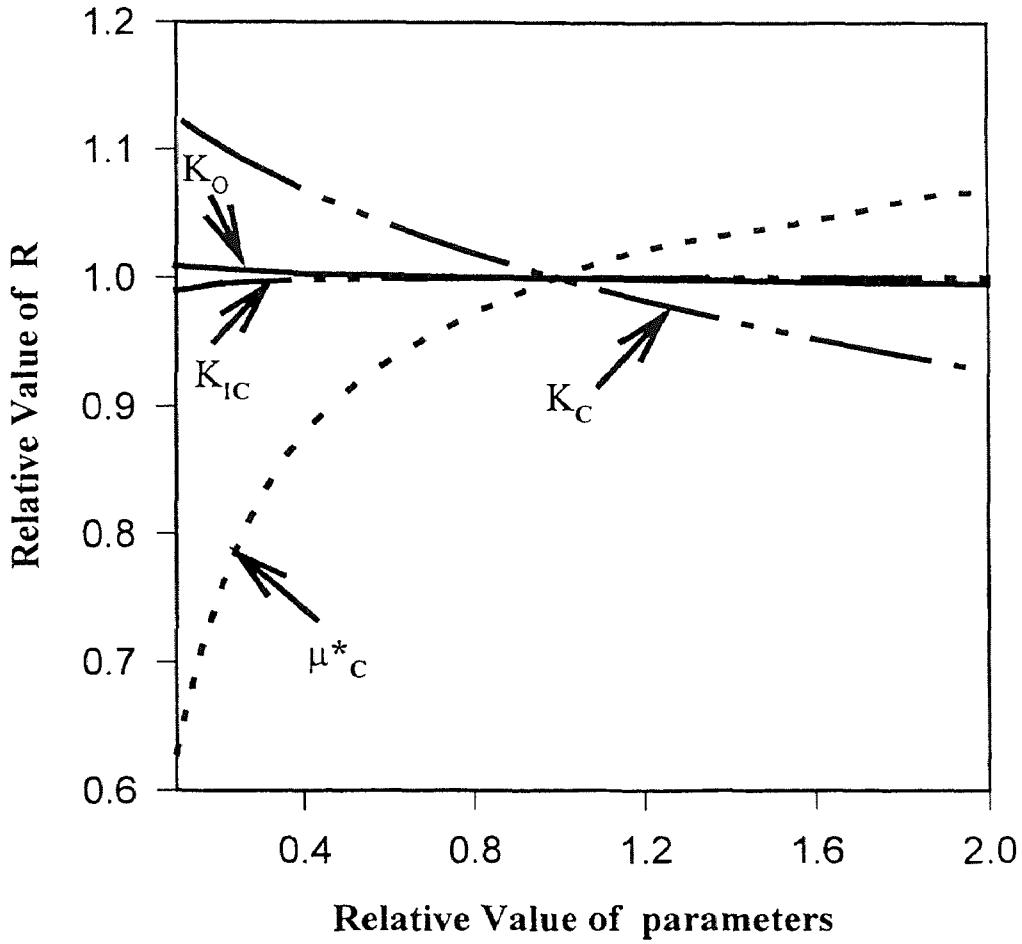

Figure 6.15 Sensitivity analysis of the effect of kinetic parameters on the removal rate of m-CB. Experimental conditions: co-current flow of air and liquid; C_{GCi} = 1.80 gm^{-3}; Q_L = 4.8 Lh^{-1}; τ = 3.65 min. The (1,1) point corresponds to an actual removal rate of about 27.83 gm^{-3}-packing h^{-1}.

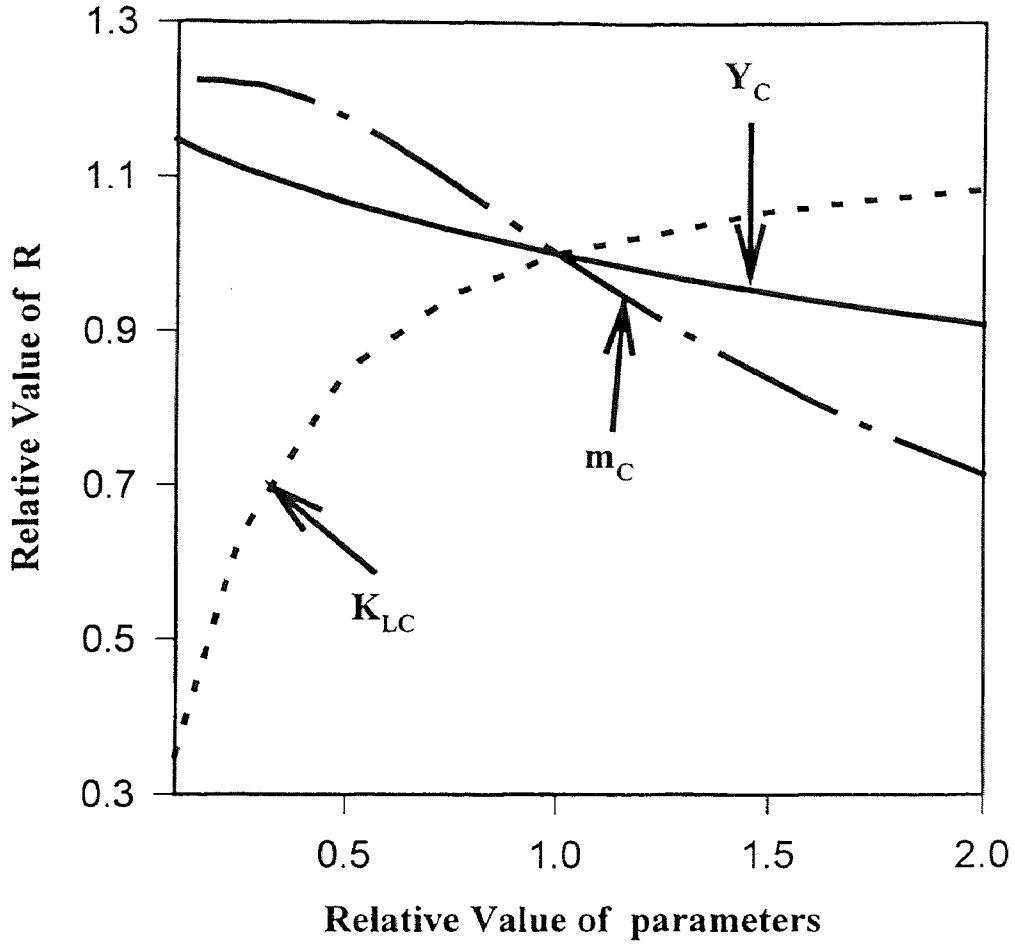

Figure 6.16 Sensitivity analysis of the effect of parameters m_C, K_{LC}, and Y_C on the removal rate of m-CB. Experimental conditions: co-current flow of air and liquid; C_{GCi} = 1.80 gm^{-3}; Q_L = 4.8 Lh^{-1}; τ = 3.85 min. The (1,1) point corresponds to an actual removal rate of about 27.83 gm^{-3}-packing h^{-1}.

A number of simulation runs were performed with the model in order to reveal the dependence of the removal rate on the oxygen concentration in the airstream. The results are presented in Figure 6.17. The relative value of C_{GOi} (gm^{-3}) varies from 0.1 to 2.0. A value larger than 1 implies that the airstream is enriched with oxygen. Calculations have been performed with o-DCB as model compound and for two inlet concentrations. At low inlet o-DCB concentrations (e.g., curve 1 in Figure 6.17), enriching the airstream

with oxygen does not lead to an improved removal rate. This is in agreement with the fact that at low inlet pollutant concentrations the process is not controlled by availability of oxygen in the biofilms. When the inlet o-DCB concentration is high (e.g., curve 2 in Figure 6.17), enriching the airstream with oxygen leads to improved removal rates. Doubling the oxygen content in the airstream leads to a removal rate which is almost 20% higher than its original (base) value. This is in agreement with the findings presented

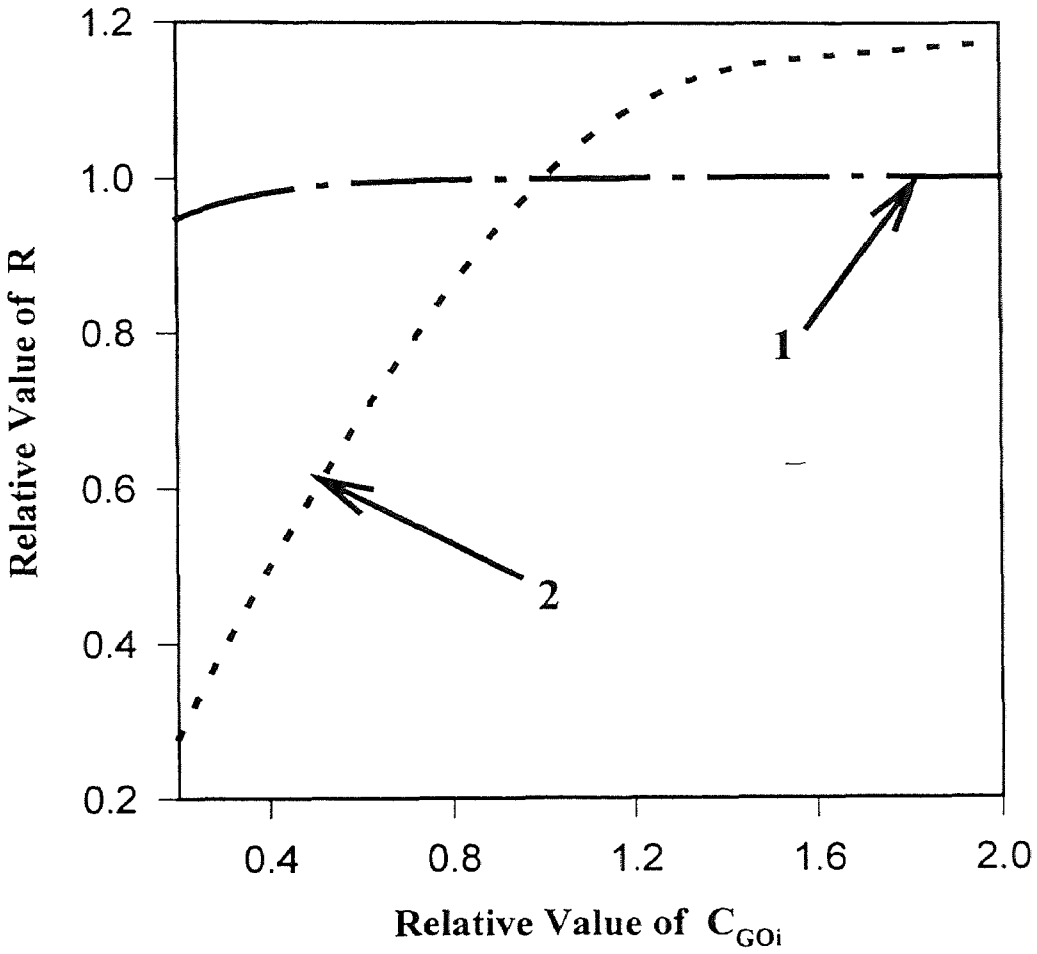

Figure 6.17 Effect of oxygen on the removal rate of o-DCB. Experimental conditions for curve 1: counter-current flow of air and liquid; $C_{GDi} = 0.65\ gm^{-3}$; $Q_L = 1.9\ Lh^{-1}$; $\tau = 4.50$ min and for curve 2: co-current flow of air and liquid; $C_{GDi} = 5.00\ gm^{-3}$; $Q_L = 1.9\ Lh^{-1}$; $\tau = 4.50$ min.

earlier; namely, that at high inlet o-DCB concentrations there is an oxygen-controlled zone along the reactor.

CHAPTER 7

STEADY-STATE REMOVAL OF VOC MIXTURES IN BIOTRICKLING FILTERS

In this chapter the work addressing the ultimate objective of this thesis is presented. As discussed in Chapter 3 the ultimate objective was to derive and experimentally validate a model describing removal of VOC mixtures in biotrickling filters. The general model presented in this chapter is a modification/extension of the model discussed in Chapter 6. The detailed work performed with airstreams carrying single VOCs (Chapter 6) served as basis for the general and more realistic case of mixtures. When addressing VOC mixtures removal, in addition to accounting for mass transfer and the role of oxygen, one has to take into consideration interactions among pollutants at the kinetic level. Such interactions are common among structurally similar compounds as was demonstrated in Chapter 5 for the case of mixtures involving m-CB and o-DCB. This mixture was used as the model system in experiments performed for validating the general model proposed here. As shown in subsequent sections, the model developed during the course of this study successfully describes data of m-CB/o-DCB mixtures removal and thus, the ultimate objective of this study was met.

7.1 General Theory

In deriving the model equations, the following assumptions have been made.

1. The biodegradation rate depends on the concentrations of the VOCs and oxygen, and

its functional form can be determined from suspended culture experiments.

2. When the surface of the solid packing is not completely covered with biofilm, the extent (surface) of the biofilm patch is much larger than its depth. Consequently, VOC and oxygen transfer into the biofilm through the side surfaces of the patch can be neglected, and diffusion/reaction in the biofilm can be described by using only the direction which is perpendicular to the main surface of the patch.
3. Reaction does not necessarily occur throughout the biolayer. If oxygen, or the VOCs get depleted before the biolayer/solid interface, there is an effective biolayer thickness (δ), in the sense of Williamson and McCarty (1976). In the biolayer, all compounds are transferred through passive diffusion.
4. Biodegradation of VOCs occurs only aerobically.
5. The thickness of the effective biolayer is very small relative to the main curvature of the solid particles and thus, planar geometry can be used.
6. The airstream passes through the trickling filter in plug flow.
7. VOCs and oxygen at the air/liquid interface are always in equilibrium distribution as dictated by Henry's law.
8. Diffusivities of VOCs and oxygen in the biofilm are equal to those in water multiplied by a correction factor determined via the correlation of Fan et al. (1987,1990).
9. At every cross-section of the filter bed there are neither velocity nor concentration gradients in the liquid phase. Constant VOC and oxygen concentrations in the liquid

imply no biodegradation in the liquid phase and negligible resistance to mass transfer from the bulk liquid to the liquid/biofilm interface.

10. The density of the biofilm (X_v) is constant throughout the biotrickling filter at all times.
11. The concentrations of VOC and oxygen in the biofilm at the liquid/biofilm interface are equal to those in the liquid phase.
12. Supplemental nutrients, such as nitrogen and phosphorous sources are not exerting rate limitation on the process.
13. No metabolites accumulate in the filter bed.
14. The void fraction of the filter bed is constant implying that the amount of biomass produced is sloughed off into the liquid and then discarded from the system during medium replenishment. Thus, a biomass balance is not needed for a complete system description.
15. The liquid medium is recirculated through the filter bed.

Under the assumptions above, removal of n VOCs in a biotrickling filter under steady state conditions can be described by the following mass balances.

I. Mass balances in the biofilm, at a position h along the column,

$$f(X_v)D_{jw}\frac{d^2S_j}{dx^2} = \frac{X_v}{Y_j}\mu_j(S_1,\ldots,S_j,\ldots,S_n,S_O); \qquad j = 1,\ldots,n \tag{7.1}$$

$$f(X_v)D_{ow}\frac{d^2S_O}{dx^2} = \sum_{j=1}^{n}\frac{X_v}{Y_{Oj}}\mu_j(S_1,\ldots,S_j,\ldots,S_n,S_O) \tag{7.2}$$

with corresponding boundary conditions

$$S_j = C_{Lj}, \quad j = 1,\ldots,n \quad \text{at} \quad x = 0 \tag{7.3}$$

$$\frac{dS_j}{dx} = 0, \quad j = 1,\ldots,n \quad \text{at} \quad x = \delta \tag{7.4}$$

$$S_O = C_{LO} \quad \text{at} \quad x = 0 \tag{7.5}$$

$$\frac{dS_O}{dx} = 0 \quad \text{at} \quad x = \delta \tag{7.6}$$

II. Mass balances in the liquid phase along the column,

$$u_L \frac{dC_{Lj}}{dh} = K_{Lj}\left(\frac{C_{Gj}}{m_j} - C_{Lj}\right) + f(X_v)D_{jW}A_S\left[\frac{dS_j}{dx}\right]_{x=0}; \quad j = 1,\ldots,n \tag{7.7}$$

$$u_L \frac{dC_{LO}}{dh} = K_{LO}\left(\frac{C_{GO}}{m_O} - C_{LO}\right) + f(X_v)D_{OW}A_S\left[\frac{dS_O}{dx}\right]_{x=0} \tag{7.8}$$

with corresponding boundary conditions

$$C_{Lj}(h = 0) = C_{Lj}(h = H), \quad j = 1,\ldots,n \tag{7.9}$$

$$C_{LO}(h = 0) = C_{LO}(h = H) \tag{7.10}$$

Conditions (7.9) and (7.10) reflect that the liquid is recirculated through the biotrickling filter bed as well as the assumption that no reaction occurs in the liquid phase.

III. Mass balances in the gas phase (airstream) along the biofilter column,

$$u_G \frac{dC_{Gj}}{dh} = \pm K_{Lj}\left(\frac{C_{Gj}}{m_j} - C_{Lj}\right); \quad j = 1,\ldots,n \tag{7.11}$$

$$u_G \frac{dC_{GO}}{dh} = \pm K_{LO}\left(\frac{C_{GO}}{m_O} - C_{LO}\right) \tag{7.12}$$

Equations (7.11) and (7.12) taken with the plus (+) sign describe counter-current flow of the airstream and the liquid stream, whereas when taken with the minus (-) sign they

describe co-current flow of the two phases. Depending on the mode of operation, the corresponding boundary conditions for equations (7.11) and (7.12) are as follows.

IIIa. Under counter-current flow conditions

$$C_{Gj} = C_{Gji}, \quad j = 1,\ldots,n \quad \text{at} \quad h = H \tag{7.13}$$

$$C_{GO} = C_{GOi} \quad \text{at} \quad h = H \tag{7.14}$$

IIIb. Under co-current flow conditions

$$C_{Gj} = C_{Gji}, \quad j = 1,\ldots,n \quad \text{at} \quad h = 0 \tag{7.15}$$

$$C_{GO} = C_{GOi} \quad \text{at} \quad h = 0 \tag{7.16}$$

Equations (7.1), (7.2), (7.7), (7.8), (7.11) and (7.12) constitute a system of 3(n+1) coupled differential equations which need to be solved subject to the 3(n+1) boundary conditions given by relations (7.3)-(7.6), (7.9), (7.10), (7.13) or (7.15), and (7.14) or (7.16).

Expressions $\mu_j\left(S_1,\ldots,S_j,\ldots,S_n,S_O\right)$ appearing in equations (7.1) and (7.2) reflect assumption 1. The dependence of the specific reaction rates on the availability of the carbon sources (VOCs) can be separated from the dependence on oxygen availability through the notion of interactive models (Bader, 1982). Hence, one can write:

$$\mu_j\left(S_1,\ldots,S_j,\ldots,S_n\right)f(S_O) = \mu_j\left(S_1,\ldots,S_j,\ldots,S_n,S_O\right) \tag{7.17}$$

Usually, biodegradation rates have a Monod-type dependence on oxygen and thus,

$$f(S_O) = \frac{S_O}{K_O + S_O} \tag{7.18}$$

The dependence of the specific biodegradation rate on the availability (i.e., the

concentrations) of VOCs, that is the functional form of $\mu_j(S_1,\ldots,S_j,\ldots,S_n)$, is determined by the number of VOCs present in the airstream and by whether these VOCs interact at the kinetic level or not. These kinetic expressions need to be known for the model equations to be solved.

7.2 Modeling and Pilot Scale Experimental Verification of Biofiltration of a mixture of Two VOCs Involved in a Competitive Kinetic Interaction in a Trickling Filter

In order to validate the general steady-state biofiltration model for VOC mixtures in a trickling biofilter, experiments were performed with airstreams laden with mono-chrorobenzene (m-CB)/ortho-dichlorobenzene (o-DCB) mixtures. As discussed in Chapter 5, biodegradation of m-CB and o-DCB mixtures involves cross-inhibitory effects. In fact, suspended culture kinetic experiments have shown that simultaneous biodegradation of m-CB and o-DCB follows kinetics involving a cross-inhibitory, competitive interaction. The work involved adaptation of the general model presented in Section 7.1 to the case of binary mixtures and experiments for model validation. The unit used in the experiments presented in Section 7.2.3 was in continuous operation for 8 months.

7.2.1 Model Development

Consider an airstream laden with m-CB and o-DCB that is treated in a trickling biofilter. This system can be described by the model discussed in Section 7.1 when n = 2. Thus

nine mass balances are needed. Three of the equations refer to the biofilm phase, three to the liquid phase, whereas the remaining three are for the gas phase (airstream).

I. Mass balances in the biofilm,

$$f(X_v)D_{CW}\frac{d^2S_C}{dx^2} = \frac{X_v}{Y_C}\mu_C(S_C,S_D,S_O) \tag{7.19}$$

$$f(X_v)D_{DW}\frac{d^2S_D}{dx^2} = \frac{X_v}{Y_D}\mu_D(S_C,S_D,S_O) \tag{7.20}$$

$$f(X_v)D_{OW}\frac{d^2S_O}{dx^2} = \frac{X_v}{Y_{OC}}\mu_C(S_C,S_D,S_O) + \frac{X_v}{Y_{OD}}\mu_D(S_C,S_D,S_O) \tag{7.21}$$

with corresponding boundary conditions

$$S_C = C_{LC};\quad S_D = C_{LD};\quad \text{and}\quad S_O = C_{LO}\quad \text{at}\quad x = 0 \tag{7.22}$$

$$\frac{dS_C}{dx} = \frac{dS_D}{dx} = \frac{dS_O}{dx} = 0\quad \text{at}\quad x = \delta \tag{7.23}$$

II. Mass balances in the liquid phase along the column,

$$u_L\frac{dC_{LC}}{dh} = K_{LC}\left(\frac{C_{GC}}{m_C} - C_{LC}\right) + f(X_v)D_{CW}A_S\left[\frac{dS_C}{dx}\right]_{x=0} \tag{7.24}$$

$$u_L\frac{dC_{LD}}{dh} = K_{LD}\left(\frac{C_{GD}}{m_D} - C_{LD}\right) + f(X_v)D_{DW}A_S\left[\frac{dS_D}{dx}\right]_{x=0} \tag{7.25}$$

$$u_L\frac{dC_{LO}}{dh} = K_{LO}\left(\frac{C_{GO}}{m_O} - C_{LO}\right) + f(X_v)D_{OW}A_S\left[\frac{dS_O}{dx}\right]_{x=0} \tag{7.26}$$

with corresponding boundary conditions

$$C_{LC}(h = 0) = C_{LC}(h = H) \tag{7.27}$$

$$C_{LD}(h = 0) = C_{LD}(h = H) \tag{7.28}$$

$$C_{LO}(h=0) = C_{LO}(h=H) \tag{7.29}$$

III. Mass balances in the gas phase (airstream),

$$u_G \frac{dC_{GC}}{dh} = \pm K_{LC}\left(\frac{C_{GC}}{m_C} - C_{LC}\right) \tag{7.30}$$

$$u_G \frac{dC_{GD}}{dh} = \pm K_{LD}\left(\frac{C_{GD}}{m_D} - C_{LD}\right) \tag{7.31}$$

$$u_G \frac{dC_{GO}}{dh} = \pm K_{LO}\left(\frac{C_{GO}}{m_O} - C_{LO}\right) \tag{7.32}$$

where the plus (+) sign refers to counter-current flow of the airstream and the liquid stream and the minus (-) sign refers to co-current flow of the two phases.

The corresponding boundary conditions for equations (7.30), (7.31) and (7.32) are

$$C_{GC} = C_{GCi};\quad C_{GD} = C_{GDi};\quad \text{and}\quad C_{GO} = C_{GOi}\quad \text{at}\quad h = H \tag{7.33}$$

under counter-current operation and

$$C_{GC} = C_{GCi};\quad C_{GD} = C_{GDi};\quad \text{and}\quad C_{GO} = C_{GOi}\quad \text{at}\quad h = 0 \tag{7.34}$$

under co-current operation.

Functions $\mu_C(S_C, S_D, S_O)$ and $\mu_D(S_C, S_D, S_O)$ appearing in equations (7.19)-(7.21) express the kinetics of biodegradation of the two VOCs and have the following forms which reflect assumption 1 of the general model and the kinetic cross-inhibition revealed in Chapter 5.

$$\mu_C(S_C, S_D, S_O) = \frac{\mu_C^* S_C S_O}{\left(K_C + S_C + \frac{S_C^2}{K_{IC}} + K_{CD} S_D\right)(K_O + S_O)} \tag{7.35}$$

$$\mu_D(S_C,S_D,S_O)=\frac{\mu_D^{\bullet}S_DS_O}{\left(K_D+S_D+\frac{S_D^2}{K_{ID}}+K_{DC}S_C\right)(K_O+S_O)} \tag{7.36}$$

With the exception of K_O, the values of the kinetic constants appearing in expressions (7.35)-(7.36) were obtained from suspended culture experiments as discussed in Chapter 5, and are listed in Table 7.1. Parameters K_{CD} and K_{DC} indicate and quantify cross-inhibition between m-CB and o-DCB.

By introducing the following dimensionless quantities,

$$\bar{S}_C=\frac{S_C}{K_C},\quad \bar{S}_D=\frac{S_D}{K_D},\quad \bar{S}_O=\frac{S_O}{K_O},\quad \bar{C}_{LC}=\frac{m_CC_{LC}}{C_{GCi}},$$

$$\bar{C}_{LD}=\frac{m_DC_{LD}}{C_{GDi}},\quad \bar{C}_{LO}=\frac{m_OC_{LO}}{C_{GOi}},\quad \bar{C}_{GC}=\frac{C_{GC}}{C_{GCi}},\quad \bar{C}_{GD}=\frac{C_{GD}}{C_{GDi}},$$

$$\bar{C}_{GO}=\frac{C_{GO}}{C_{GOi}},\quad \alpha_C=\frac{C_{GCi}}{m_CK_C},\quad \alpha_D=\frac{C_{GDi}}{m_DK_D},\quad \alpha_O=\frac{C_{GOi}}{m_OK_O},$$

$$\theta=\frac{x}{\delta},\quad z=\frac{h}{H},\quad \gamma_1=\frac{K_C}{K_{IC}},\quad \gamma_2=\frac{K_D}{K_{ID}},$$

$$\lambda_1=\frac{D_{CW}Y_CK_C}{D_{OW}Y_{OC}K_O},\quad \lambda_2=\frac{D_{DW}Y_DK_D}{D_{OW}Y_{OD}K_O},\quad \phi_1^2=\frac{X_v\delta^2\mu_C^{\bullet}}{f(X_v)Y_CD_{CW}K_C},$$

$$\phi_2^2=\frac{X_v\delta^2\mu_D^{\bullet}}{f(X_v)Y_DD_{DW}K_D},\quad \sigma_1=\frac{K_{CD}K_D}{K_C},\quad \sigma_2=\frac{K_{DC}K_C}{K_D},\quad \psi_C=\frac{K_{LC}H}{u_L},$$

$$\beta_1=\frac{K_{LD}}{K_{LC}},\quad \beta_2=\frac{K_{LO}}{K_{LC}},\quad \rho_C=\frac{K_{LC}H}{u_Gm_C},\quad \eta_C=\frac{f(X_v)D_{CW}A_SK_Cm_CH}{u_L\delta C_{GCi}},$$

$$\omega_1=\frac{C_{GCi}D_{DW}K_Dm_D}{C_{GDi}D_{CW}K_Cm_C},\quad \omega_2=\frac{C_{GOi}D_{OW}K_Om_O}{C_{GOi}D_{CW}K_Cm_C},\quad \varepsilon_1=\frac{m_CK_{LD}}{m_DK_{LC}},\quad \varepsilon_2=\frac{m_CK_{LO}}{m_OK_{LC}}$$

equations (7.19)-(7.34), when expressions (7.35) and (7.36) are also used, can be written

in dimensionless form as follows,

$$\frac{d^2\bar{S}_C}{d\theta^2} = \phi_1^2 \frac{\bar{S}_C \bar{S}_O}{\left(1+\bar{S}_C+\gamma_1\bar{S}_C^2+\sigma_1\bar{S}_D\right)\left(1+\bar{S}_O\right)} \tag{7.37}$$

$$\frac{d^2\bar{S}_D}{d\theta^2} = \phi_2^2 \frac{\bar{S}_D \bar{S}_O}{\left(1+\bar{S}_D+\gamma_2\bar{S}_D^2+\sigma_2\bar{S}_C\right)\left(1+\bar{S}_O\right)} \tag{7.38}$$

$$\frac{d^2\bar{S}_O}{d\theta^2} = \lambda_1\phi_1^2 \frac{\bar{S}_C \bar{S}_O}{\left(1+\bar{S}_C+\gamma_1\bar{S}_C^2+\sigma_1\bar{S}_D\right)\left(1+\bar{S}_O\right)} + \lambda_2\phi_2^2 \frac{\bar{S}_D \bar{S}_O}{\left(1+\bar{S}_D+\gamma_2\bar{S}_D^2+\sigma_2\bar{S}_C\right)\left(1+\bar{S}_O\right)} \tag{7.39}$$

$$\bar{S}_C = \alpha_C \bar{C}_{LC}; \quad \bar{S}_D = \alpha_D \bar{C}_{LD}; \quad \text{and} \quad \bar{S}_O = \alpha_O \bar{C}_{LO} \quad \text{at} \quad \theta = 0 \tag{7.40}$$

$$\frac{d\bar{S}_C}{d\theta} = \frac{d\bar{S}_D}{d\theta} = \frac{d\bar{S}_O}{d\theta} = 0 \quad \text{at} \quad \theta = 1 \tag{7.41}$$

$$\frac{d\bar{C}_{LC}}{dz} = \psi_C\left(\bar{C}_{GC} - \bar{C}_{LC}\right) + \eta_C\left[\frac{d\bar{S}_C}{d\theta}\right]_{\theta=0} \tag{7.42}$$

$$\frac{d\bar{C}_{LD}}{dz} = \psi_C\beta_1\left(\bar{C}_{GD} - \bar{C}_{LD}\right) + \eta_C\omega_1\left[\frac{d\bar{S}_D}{d\theta}\right]_{\theta=0} \tag{7.43}$$

$$\frac{d\bar{C}_{LO}}{dz} = \psi_C\beta_2\left(\bar{C}_{GO} - \bar{C}_{LO}\right) + \eta_C\omega_2\left[\frac{d\bar{S}_O}{d\theta}\right]_{\theta=0} \tag{7.44}$$

$$\bar{C}_{LC}(z=0) = \bar{C}_{LC}(z=1) \tag{7.45}$$

$$\bar{C}_{LD}(z=0) = \bar{C}_{LD}(z=1) \tag{7.46}$$

$$\bar{C}_{LO}(z=0) = \bar{C}_{LO}(z=1) \tag{7.47}$$

$$\frac{d\bar{C}_{GC}}{dz} = \pm\rho_C\left(\bar{C}_{GC} - \bar{C}_{LC}\right) \tag{7.48}$$

$$\frac{d\bar{C}_{GD}}{dz} = \pm\rho_C\varepsilon_1\left(\bar{C}_{GD} - \bar{C}_{LD}\right) \tag{7.49}$$

$$\frac{d\bar{C}_{GO}}{dz} = \pm\rho_C\varepsilon_2\left(\bar{C}_{GO} - \bar{C}_{LO}\right) \tag{7.50}$$

$$\bar{C}_{GC} = \bar{C}_{GD} = \bar{C}_{GO} = 1 \quad \text{at} \quad z = 1 \quad \text{(for counter-current flow)} \tag{7.51}$$

$$\bar{C}_{GC} = \bar{C}_{GD} = \bar{C}_{GO} = 1 \quad \text{at} \quad z = 0 \quad \text{(for co-current flow)} \tag{7.52}$$

Equations (7.37) through (7.39) along with boundary conditions (7.40)and (7.41) yield

$$\bar{S}_O = \lambda_1\left(\bar{S}_C - \alpha_C\bar{C}_{LC}\right) + \lambda_2\left(\bar{S}_D - \alpha_D\bar{C}_{LD}\right) + \alpha_O\bar{C}_{LO} \tag{7.53}$$

or

$$\bar{S}_C = \frac{1}{\lambda_1}\left(\bar{S}_O - \alpha_O\bar{C}_{LO}\right) - \frac{\lambda_2}{\lambda_1}\left(\bar{S}_D - \alpha_D\bar{C}_{LD}\right) + \alpha_C\bar{C}_{LC} \tag{7.54}$$

Because of relations (7.53) and (7.54), instead of solving the original set of equations (7.37)-(7.52) one can equivalently solve either one of the following sets of equations. Set 1: Equations (7.37), (7.38), (7.42)-(7.52) and from (7.40) and (7.41) only the conditions concerning $\bar{S}_C$ and $\bar{S}_D$. In this case, relation (7.53) needs to be substituted for $\bar{S}_O$ in equations (7.37) and (7.38). Set 2: Equations (7.38), (7.39), (7.42)-(7.52) and from (7.40) and (7.41) only the conditions concerning $\bar{S}_D$ and $\bar{S}_O$. In this case, relation (7.54) needs to be substituted for $\bar{S}_C$ in equations (7.38) and (7.39). Each one of the aforementioned sets of equations constitutes a non-linear and coupled boundary value problem in two directions, θ and z. Solving this problem requires a trial and error approach because of boundary conditions (7.45)-(7.47). Another case, Set 3 which is exactly symmetric to Set 2 can be considered. In Set 3 equation (7.54) needs to be solved

for $\bar{S}_D$ and then equation (7.38) with its corresponding boundary conditions can be eliminated.

7.2.2 Numerical Methodology

A computer code was developed for solving the model equations and is given as Appendix B of this dissertation. The logic/structure of this code is presented schematically in Figure 7.1.

7.2.3 Results and Discussion

Experiments were performed with airstreams carrying mono-chlorobenzene (m-CB) and ortho-dichlorobenzene (o-DCB) mixtures. The schematic of the experimental unit as well as the experimental methodology, have been discussed in Chapter 4 of this thesis. Experimental data on the removal of vapors of m-CB/o-DCB mixtures for various inlet m-CB and o-DCB concentrations, air residence times in the biotrickling filter-bed, and recirculation flow rates of the medium were collected. The experimental results were compared to the theoretical predictions obtained by solving the model equations. The values of the model parameters used in solving the equations are reported in Tables 7.1 and 7.2. Parameter values were either measured as discussed in Chapters 5 and 6, or estimated as explained in Chapter 6. In the case of mixtures no fitting approach was used for estimating the biolayer wetted surface area. Since the dimensions of the column and the size of packing material used for mixtures removal were the same as those used in the experiments with o-DCB alone (see Chapter 6), it was decided to use the fitting

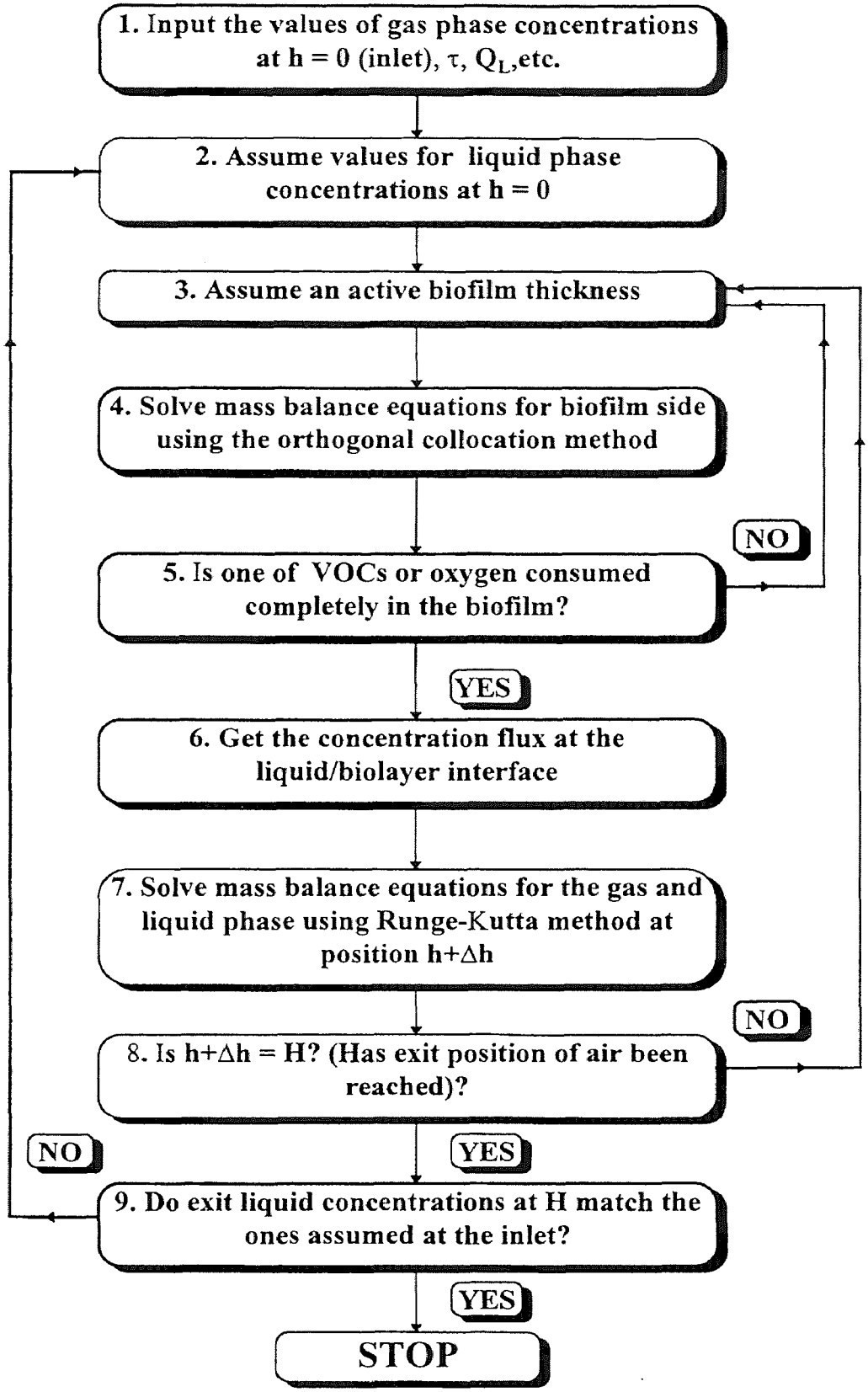

Figure 7.1 Structure of numerical methodology for solving the model equations under co-current operation

Table 7.1. Model parameter values for biofiltration of m-CB and o-DCB mixtures

Parameter	Numerical Value		Reference
	m-CB	**o-DCB**	
A_T (m^{-1})	623.36		Eckert (1961, 1975)
D_{jW} (m^2s^{-1})	0.81×10^{-9}	0.78×10^{-9}	Perry and Green (1984)
D_{jG} (m^2s^{-1})	0.78×10^{-5}	0.69×10^{-5}	Fuller et al. (1966)
d_{Pj} (m)	0.0127		Eckert (1961, 1975)
K_j (gm^{-3})	5.140	13.389	Present Study
K_{lj} (gm^{-3})	21.883	19.657	Present Study
K_{jq} (gm^{-3})	1.3	0.75	Present Study
m_j (-)	0.167	0.119	Yurteri et al. (1987)
V_{Pj} (m^3)	1.43×10^{-3}		Present study
Y_j (gg^{-1})	0.551	0.397	Present Study
Y_{Oj} (gg^{-1})	0.516	0.363	Present Study
μ_j^* (h^{-1})	0.154	0.146	Present Study
ξ_j	2.36		Present study
ξ_{1j}	2.55		Present study
ξ_{2j}	2.55		Present study
ξ_{2O}	7.12		Present study

Table 7.2. Model parameter values for biofiltration of m-CB and o-DCB mixtures

Parameter	Numerical Value	Reference
C_{GOi} (gm^{-3})	275	Shareefdeen et al. (1993)
D_{OW} (m^2s^{-1})	2.39×10^{-9}	Perry and Green (1984)
D_{OG} (m^2s^{-1})	2.03×10^{-5}	Perry and Green (1984)
$f(X_v)$ (-)	0.253	Fan et al. (1987, 1990)
g (ms^{-2})	9.81	Perry and Green (1984)
K_O (gm^{-3})	0.26	Shareefdeen et al. (1993)
m_O (-)	34.4	Shareefdeen et al. (1993)
S (m^2)	1.82×10^{-2}	Present study
X_v (kgm^{-3})	75	Present study
μ_G ($kgm^{-1}s^{-1}$)	0.018×10^{-3}	Perry and Green (1984)
μ_L ($kgm^{-1}s^{-1}$)	0.982×10^{-3}	Perry and Green (1984)
ρ_G (kgm^{-3})	1.193	Perry and Green (1984)
ρ_L (kgm^{-3})	997.85	Perry and Green (1984)
σ_L (Nm^{-1})	72×10^{-3}	Heggen (1983)
σ_P (Nm^{-1})	61×10^{-3}	Bolles and Fair (1982)
ξ_{10} (-)	0	Present study

coefficients from the o-DCB case. These coefficients ($\xi_j, \xi_{1j}, \xi_{2j}, \xi_{2O}$), reported in Table 7.1, were used in determining the wetted area and the overall mass transfer coefficients for the three compounds (m-CB, o-DCB, oxygen).

Results from experiments with m-CB/o-DCB mixture vapors under counter-current flow of air and liquid, constant liquid recirculation rate (6 Lh^{-1}) and various residence times are shown in Table 7.3. The residence times (τ) reported in the table are

Table 7.3. Experimental data and model predictions for biofiltration of mono-chlorobenzene/ortho-dichlorobenzene mixtures at Q_L = 6.0 Lh^{-1} and pH = 6.8±0.2 as a function of air residence time (τ).[a] Counter-current flow of liquid and air streams.

j	C_{Gji} (gm^{-3})	$C_{Gje,1}$ (gm^{-3})	$C_{Gje,2}$ (gm^{-3})	E_1 (%)	X (%)	R_{exp} (gm^{-3}-reactor h^{-1})	R_{pred}	E_2 (%)
				τ = 5.85 min				
C	0.97	0.15	0.07	-53.33	91.8	8.41	9.23	+9.75
D	0.30	0.05	0.05	+2.00	83.3	2.56	2.55	-0.39
C	0.76	0.07	0.11	+57.14	90.8	7.08	6.67	-5.79
D	0.10	0.02	0.02	+5.26	80.0	0.83	0.82	-1.21
				τ = 4.50 min				
C	0.45	0.06	0.09	+50.00	86.7	5.20	4.80	-7.69
D	0.05	0.01	0.01	-23.08	78.0	0.53	0.56	+5.66
C	1.60	0.21	0.31	+47.61	85.9	18.53	17.20	-7.18
D	0.17	0.04	0.03	-25.00	76.5	1.73	1.87	+8.09
				τ = 3.80 min				
C	2.04	0.37	0.44	+18.92	81.2	22.27	21.33	-4.22
D	0.68	0.21	0.14	-33.33	69.1	6.27	7.20	+14.83
				τ = 3. 20 min				
C	0.17	0.045	0.046	+22.22	73.5	2.34	2.32	-0.85
D	0.27	0.099	0.073	-26.26	63.3	3.21	3.69	+14.95
C	2.58	0.80	0.88	+10.00	69.0	33.38	31.88	-4.49
D	0.70	0.25	0.19	-24.00	64.3	8.44	9.56	+13.27
C	3.06	1.06	0.95	-10.38	65.4	37.50	39.56	+5.49
D	0.76	0.29	0.22	-24.14	61.8	8.81	10.13	+14.98

[a]C:mono-chlorobenzene, D:ortho-dichlorobenzene, all symbols as defined in Table 6.4

based on empty column. The real residence times for the airstreams in the biotrickling filter can be easily calculated via multiplying the reported values by 0.65 (i.e. the void fraction of the bed). In Table 7.3 the model-predicted exit VOC concentrations and removal rates are also reported. For the case of m-CB/o-DCB mixtures the predicted values agree well with the experimentally obtained exit concentrations. In all cases exit concentrations are predicted within less than 0.1 gm^{-3} and the (in some cases) large percentage differences are misleading because they are based on very low concentration values. Given the complexity of the process, the agreement between experimental and model-predicted values for the removal rate is very good especially for m-CB, as can be seen from the last column of Table 7.3.

In Figure 7.2 dimensionless model-predicted concentration profiles for m-CB, o-DCB and oxygen (curves 1 for air, curves 2 for liquid) are shown for one of the experiments performed. The agreement between experimental and model-predicted values is good not only at the exit of the biotrickling filter but at its middle point as well. This can also be seen from the diagrams of Figure 7.3 where model-predicted concentration profiles (curves) are compared to experimental data points for two more cases. Regarding oxygen, it has been found that when the total inlet VOC concentration (sum of m-CB and o-DCB) is low, the liquid phase concentration varies insignificantly and remains close to the saturation value as shown in Figure 7.2c (curve 2). Considerable variation is predicted when the total inlet VOC concentration is high. These results are exactly analogous to those obtained with single VOCs (discussed in Chapter 6).

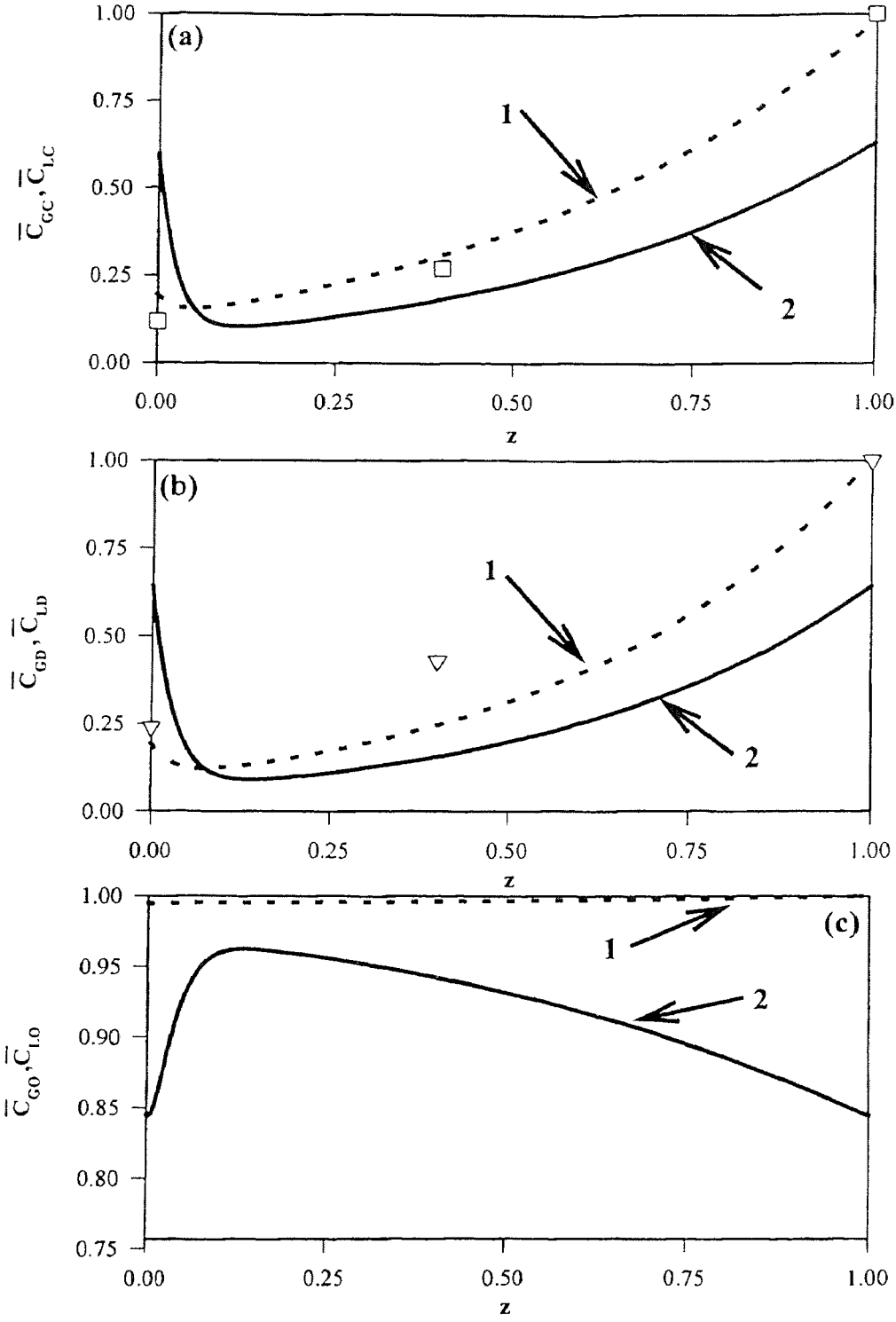

Figure 7.2 Model-predicted dimensionless concentration profiles of (a) m-CB, (b) o-DCB, and (c) oxygen along the biotrickling filter. Curves 1 and 2 are for the gas and liquid phase, respectively. Symbols represent data from the gas phase (air). Experimental conditions: counter-current flow of air and liquid; C_{GCi} = 1.60 gm^{-3}; C_{GDi} = 0.17 gm^{-3}; Q_L = 6.0 Lh^{-1}; τ = 4.50 min.

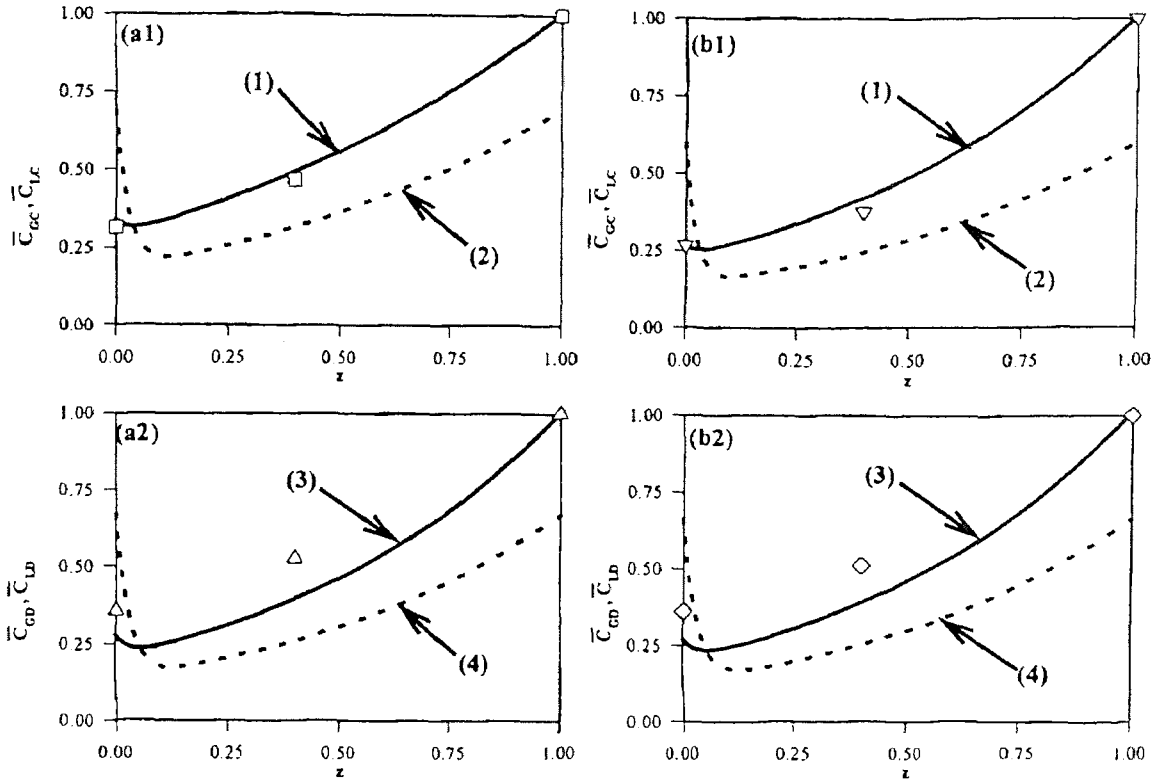

Figure 7.3 Model-predicted dimensionless concentration profiles of m-CB (curves 1: air, curves 2: liquid) and o-DCB (curves 3: air, curves 4: liquid) along the biotrickling filter when the values of C_{GCi} (gm^{-3}), C_{GDi} (gm^{-3}), Q_L (Lh^{-1}) and τ (min), respectively, are (a1, a2) 3.06, 0.76, 6.0, and 3.2; (b1, b2) 0.17, 0.27, 6.0, and 3.2. Symbols represent data from the gas phase (air). Counter-current flow of air and liquid.

The minimal importance of oxygen at low inlet m-CB/o-DCB mixture concentrations can also be seen from Figure 7.4 where computed VOC and oxygen concentration profiles in the biofilm have been plotted. Concentrations and position in the biofilm have been normalized with the values of corresponding concentrations at the biofilm/liquid interface and the effective biofilm thickness (δ), respectively. Observe that the relative position of VOCs (curves 1 and 2) and oxygen (curve 3) concentration profiles remain unchanged along the unit. VOCs are predicted to be depleted in the biolayer much before oxygen and thus, the process is not limited by oxygen. In the

particular example shown in Figure 7.4, m-CB and o-DCB are depleted at almost exactly the same location in the biolayer. Higher m-CB and/or o-DCB concentrations in the air would result in a reversal of the order in which oxygen and VOCs are depleted in the biolayer. It is also interesting to observe that, at least for the example of Figure 7.4, the value of δ does not vary along the column.

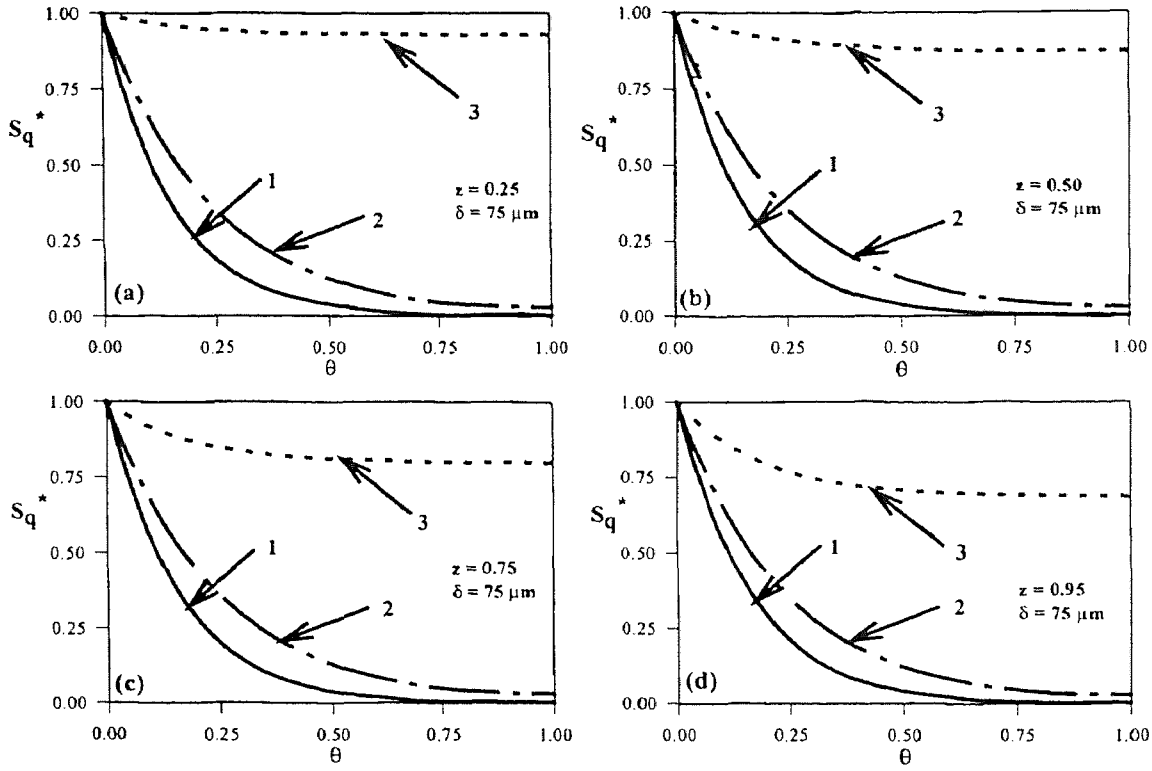

Figure 7.4 Model-predicted normalized concentration profiles in the active biofilm for m-CB (curves 1), o-DCB (curves 2) and oxygen (curves 3) at four locations along the biotrickling filter column operating under conditions same as those of Figure 7.2.

Another way to show that at low total inlet VOC concentrations oxygen does not limit the process is to perform model sensitivity studies assuming airstreams enriched with oxygen. Such a study was undertaken and its results are shown in Figure 7.5. In this

figure, a value larger than one on the x-axis implies that the airstream contains oxygen at levels higher than the atmospheric air. The diagram indicates that at low inlet mixture concentrations, enriching the airstream with oxygen does not lead to an improved removal rate; i.e., R (defined in Chapter 6) is equal to 1. The opposite occurs at high inlet mixture concentrations. However, high concentrations may be unrealistic especially in case of emission of chlorinated aromatic compounds.

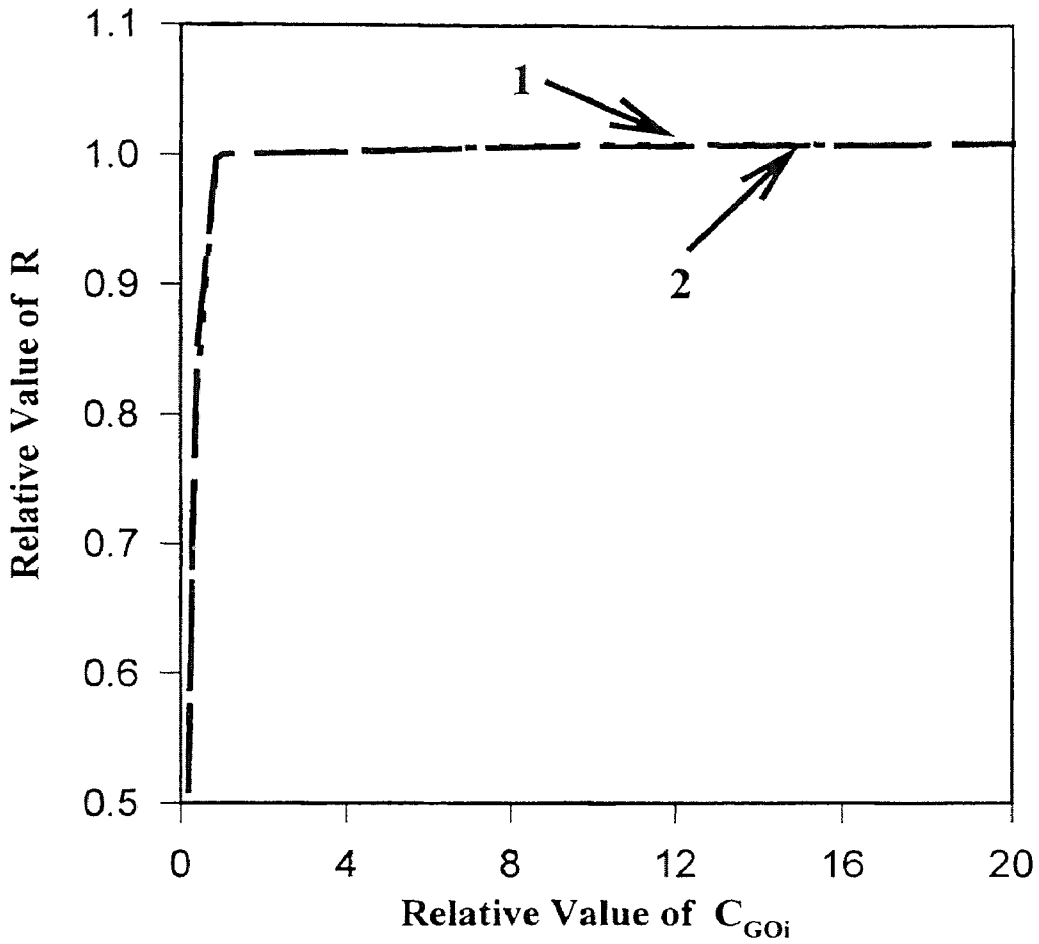

Figure 7.5 Model sensitivity studies on the effect of oxygen on the removal rate. Curves 1 and 2 are for m-CB and o-DCB, respectively, and indicate the effect of the inlet air oxygen concentration C_{GOi}. Conditions are those of Figure 7.3(a1,a2), and the (1,1) points represent removal of 39.56 and 10.13 g-m^{-3}-packing h^{-1} for m-CB and o-DCB, respectively.

Related to oxygen and its impact on the process is kinetic constant K_O. Results from model sensitivity studies, shown in Figure 7.6, imply that although oxygen does not exert rate limitation on the process at low inlet VOC concentrations it does have an impact on the process. In fact it is predicted that if the value of K_O is twenty times higher than the one valid for the culture used in the experiments, the removal rate may be 11% less than what was obtained during the experiment used as a basis for the

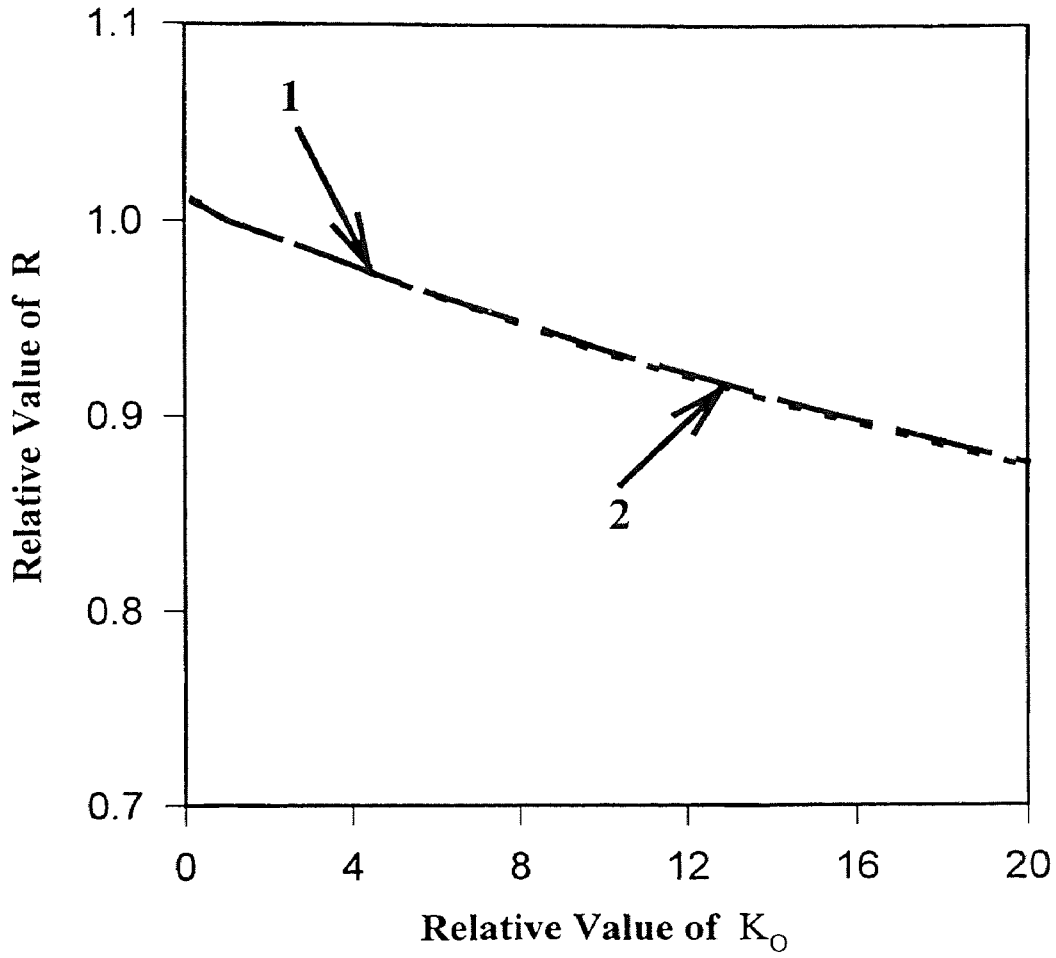

Figure 7.6 Model sensitivity studies on the effect of oxygen on the removal rate. Curves 1 and 2 are for m-CB and o-DCB, respectively, and indicate the effect of the kinetic constant K_O. Conditions are those of Figure 7.3(a1,a2), and the (1,1) points represent removal of 39.56 and 10.13 g-m^{-3}-packing h^{-1} for m-CB and o-DCB, respectively.

calculations used in preparing Figure 7.6. This suggests that microbial culture selection should not only be based on its ability to remove VOCs, but also on the affinity of the culture for oxygen.

Regarding the kinetic cross-inhibition between m-CB and o-DCB model sensitivity studies with constants K_{CD} and K_{DC} have shown (Figure 7.7) that it is not important. Increasing or decreasing these constants by an order of magnitude does not

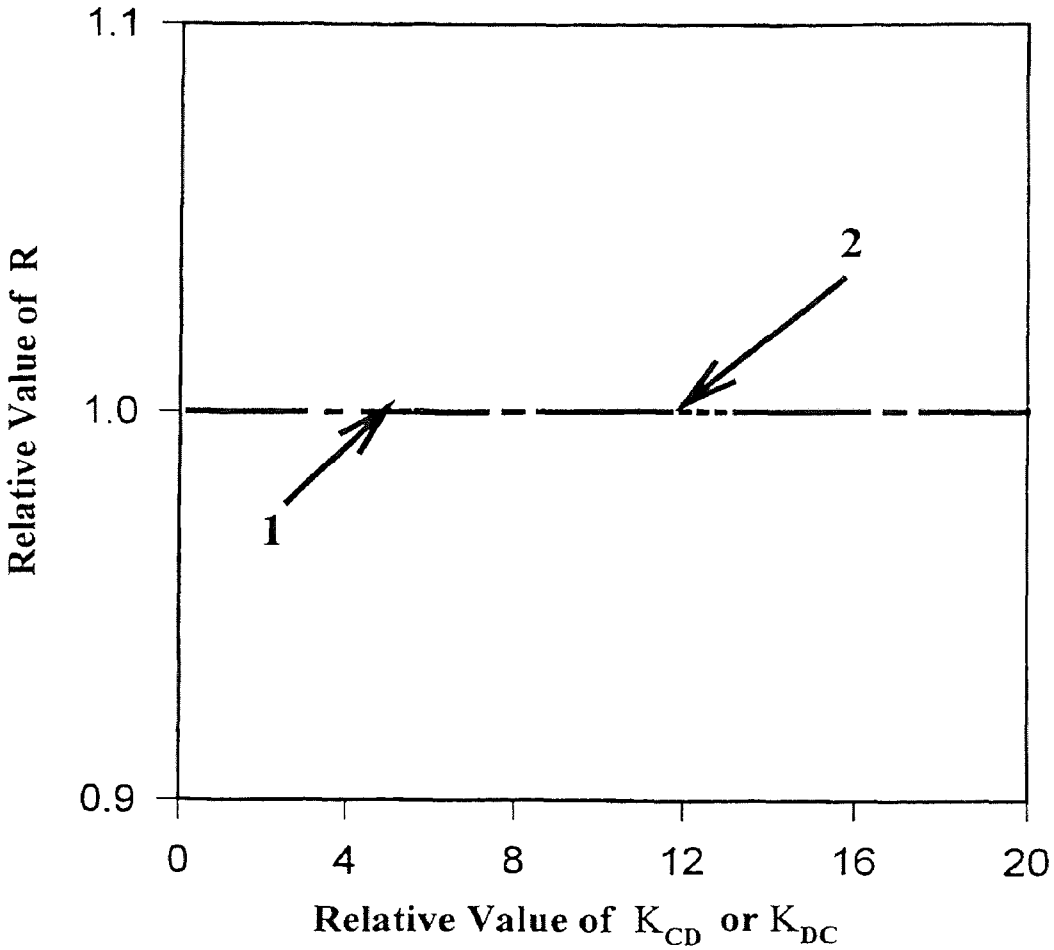

Figure 7.7 Model sensitivity studies on the effect of the kinetic interactions constant K_{CD} (curve 1) and K_{DC} (curve 2), on the removal of m-CB and o-DCB vapors. Conditions are those of Figure 7.3(a1,a2), and the (1,1) points represent removal of 39.56 and 10.13 g-m^{-3}-packing h^{-1} for m-CB and o-DCB, respectively.

alter the value of predicted removal rate as shown in Figure 7.7. One could then conclude that kinetic interactions can be neglected for the m-CB/o-DCB mixture when a biotrickling filter is sized/modeled. Similar studies with removal of benzene/toluene mixtures in conventional biofilters (Shareefdeen, 1994) have reached the opposite conclusion. The importance or unimportance of kinetic interactions may be characteristic of the particular VOC mixture. On the other hand, calculations have shown that if the study of Shareefdeen (1994) had assumed a surface area as high as the one for the biotrickling filter considered in the present study, the conclusion would had been that kinetic interactions in removal of benzene/toluene vapors is unimportant. Although possibly risky, due to lack of enough data, one could postulate that kinetic interactions are more important for conventional than for trickling biofilters.

In order to compare/predict the performance of trickling and conventional biofilters, calculations were performed with the model of Shareefdeen (1994) for the removal of mixtures under the conditions of the experiments reported in Table 7.3. In these calculations, no liquid phase was assumed, the m-CB and o-DCB kinetic constants from the present study were used, and the specific biofilm surface area was assumed to be the one reported by Shareefdeen (25 m^{-1}). The value of X_V was 75 Kgm^{-3}. The results and comparisons with values from Table 7.3 are shown in Table 7.4. As can be seen from the table, the prediction is that biotrickling filters can reach removal rates more than two orders of magnitude higher than those obtained with conventional biofilters. This difference is mainly due to higher biofilm areas formed in biotrickling filters due to

favorable growth conditions obtained via the supply of non-carbon containing nutrients for the biomass.

Table 7.4. Comparison of model predictions for biofiltration of m-CB/o-DCB mixtures in conventional and biotrickling filters at pH = 6.8±0.2 as a function of air residence time (τ)[a].

j	C_{Gji} (gm^{-3})	R_{pred}^{CB} (gm^{-3}-reactor h^{-1})	R_{pred}^{BTF} (gm^{-3}-reactor h^{-1})	G (%)
		τ = 5.85 min		
C	0.97	4.19	9.23	+120.29
D	0.30	1.41	2.55	+80.85
C	0.76	3.53	6.67	+88.95
D	0.10	0.49	0.82	+67.35
		τ = 4.50 min		
C	0.45	2.36	4.80	+103.39
D	0.05	0.27	0.56	+107.41
C	1.60	6.91	17.20	+148.91
D	0.17	0.82	1.87	+128.05
		τ = 3.20 min		
C	0.17	0.82	2.32 –	+182.92
D	0.27	1.31	3.69	+181.67
C	2.58	9.25	31.88	+244.65
D	0.70	3.13	9.56	+205.43
C	3.06	10.67	39.56	+270.76
D	0.76	3.28	10.13	+208. 84

[a]C: m-CB; D: o-DCB; C_{Gji}: inlet VOC concentration; R_{pred}^{CB}: predicted removal rate in a conventional biofilter; R_{pred}^{BTF}: predicted removal rate in a trickling biofilter; G: percent gain in VOC removal with a BTF

CHAPTER 8

CONCLUSIONS AND RECOMMENDATIONS

The main conclusion from this study is that, despite its complexity, biofiltration of VOC vapors in biotrickling filters can be successfully modeled with equations which accurately reflect kinetics of biodegradation and mass transfer effects.

Experimentally, this study has shown that biotrickling filters used in removal of chlorinated aromatic VOCs can be successfully operated over long periods of time. Biomass generation created no problems as excess amounts of it were removed during liquid replenishment with fresh medium. Daily changes of the medium allowed for maintenance of steady state conditions regarding effects from the availability of additional (non-carbon sources) nutrients for the biomass.

High removal rates and percent m-CB conversion were obtained under all conditions tested. Conversion of m-CB was never below 70% and at low concentrations exceeded 90%. A maximum removal rate of about 60 gm^{-3}-reactor h^{-1} was observed. It was also found that removal of o-DCB is more difficult when compared to m-CB because of much slower kinetics of o-DCB biodegradation. For this reason, a maximum removal rate of about 30 gm^{-3}-reactor h^{-1} was obtained. Conversion of pollutants was found to increase as the values of their inlet concentration and air flow rate decrease. In all cases, the flow rate of the liquid as well as its total amount were low, suggesting that biotrickling filters do not necessarily require large amounts of liquid (which is an

additional operating expense) in order to operate efficiently. However, for a given set of operating conditions, removal rates were found to increase with the flow of the liquid. This suggests that, for performing a given duty, one has to either use a larger unit with a low or moderate flow of liquid or use a smaller reactor with a large liquid flow rate. One can then conclude that in designing a biotrickling filter, capital cost (associated with size) and operating cost (associated with medium use) run in opposite directions and an interesting problem of optimal design has to be considered.

For single VOCs treated in biotrickling filters, the results obtained in the present study under co-current flow of liquid and air were superior to those obtained under counter-current conditions. Increased efficiencies under co-current flow operation can be attributed to higher driving forces for the transfer of VOC from the polluted air to the liquid. This transfer is a necessary step before the pollutant meets the biofilms where biodegradation occurs. It should be mentioned, however, that the differences from co- and counter-current operation are less pronounced at low inlet VOC concentrations.

Biotrickling filters appear to lead to biofilm-liquid interfacial areas much higher than the biofilm-air interfacial area achieved in classical biofiltrers. This is definitely a big plus, although one should keep in mind that in biotrickling filters there is an additional mass-transfer resistance (from the gas to the liquid). The actual surface area of the liquid-biofilm interface has never been measured. The indication from calculations performed during the course of this study is that coverage of particles with biofilm is in the range of 25-47% of the total particle area. This seems to be in accord with reports from other studies (Diks and Ottengraff, 1992).

The removal of pollutant(s) drops as the age of the liquid trickling through the bed increases. This is due to depletion of some essential nutrients for the organisms. It was found that rates remain relatively constant when the liquid (nutrients) is completely replenished daily.

Regarding modeling, the process was successfully described with a mathematical model which considers the stepwise pollutant and oxygen transfer from the air to the liquid and then to the reaction environment of the biofilms. Solution of the model equations yielded VOC(s) and oxygen concentration profiles in all three phases (airstream, liquid, biofilm). Despite the complexity of the model all its parameters were either measured or estimated and predictions agreed very nicely with all data that were collected. Although it was not measured, the concentration of oxygen in the liquid phase was found to be well below saturation when the inlet pollutant concentration is relatively high. As a result, the availability of oxygen in the biofilms can become the controlling factor for the process. In such cases, the biotrickling filter is predicted to consist of two zones. The zone close to the inlet of the polluted air is oxygen-limited whereas the zone close to the exhaust is VOC-limited.

The pH of the liquid was found to affect the removal of VOCs but not to the extent found with suspended cultures of the same microbial consortia. This suggests that the pH of the liquid is not a true indicator of the pH in the reaction environment of the biofilm. It appears that mass transfer limitations for the chloride ions shield the inner layers of the biofilms from unfavorable pH values. The implications can be economically

significant as periodic adjustment of pH may suffice and an expensive unit for tight pH-control may not be needed. This is a point needing further investigation.

Treatment of airstreams contaminated with mixtures of two chlorinated VOCs in biotrickling filters under steady-state conditions of operation was also described with a general mathematical model. The model accounts for potential kinetic interactions among the pollutants and effects of oxygen availability on biodegradation. Good agreement between model predictions and experimental data was found in almost all cases.

Detailed experiments with suspended cultures have generated a number of results during this study. First, it was found that m-CB and o-DCB get utilized by consortia following Andrews' inhibitory kinetics. When in mixture, the two compounds are involved in a kinetic cross-inhibitory interaction of the competitive type. Second, sensitivity studies with the BTF models have shown that in all cases two kinetic constants are important. Thus, first- or zero-order kinetic approximations are not justified. Additionally, kinetic interactions are not important at low concentrations such as those expected in emissions and as a result, they can be neglected when modeling removal of m-CB/o-DCB mixtures in BTFs. Another important conclusion is that the microbial consortia are stable and do not change composition over time in BTFs. It was in fact found that when biomass is taken from BTFs operating for 8 months and used in suspended culture kinetic studies, the kinetic constants obtained are essentially identical with those obtained when the original consortium is used. One can then conclude that BTFs are robust systems and are not subject to biomass contamination, at least when hard to biodegrade compounds (such as m-CB and o-DCB) are used. Finally, the kinetic

studies have revealed the first quantitative description of the effects of pH on m-CB and o-DCB biodegradation.

The present study has dealt with an engineering analysis of BTFs operating under steady state conditions. Future studies should address transient operation which is expected to be more common when emissions are treated in BTFs. Modeling of transient operation is not expected, however, to alter conceptually the proposed model. In the case of conventional biofilters, transient operation introduces a whole new process; namely, the physical adsorption of VOCs on the packing material. Such a process cannot happen in biotrickling filters due to the different nature of packing material used.

Future studies with BTFs should consider cases involving removal of relatively hydrophilic compounds, mixtures of hydrophobic/hydrophilic compounds and mixtures of structurally dissimilar compounds. Such dissimilarities may raise issues of biomass diversification and structuring in BTFs. Biomass inhomogeneity in BTFs is expected to lead to interesting experimental and modeling problems.

The present study has contributed significantly toward understanding biotrickling filters from the engineering analysis view point. Further studies can increase the potential for industrial applications of biotrickling filters based on rational engineering approaches rather than trial and error methodologies.

APPENDIX A

COMPUTER CODE FOR SOLVING THE STEADY-STATE MODEL DESCRIBING REMOVAL OF A SINGLE VOC IN A BIOTRICKLING FILTER

```
c*****************************************************
c This computer code numerically solves the steady state model presented
c  in Chapter 6 (Set 1). This model describes removal of a  single VOC in
c  a biotrickling filter. The code is based on the orthogonal collocation
c  method and the 4th-Runge-Kutta method. It uses an iteration procedure for
c  obtaining VOC and oxygen concentration profiles in the biofilm and in the
c  gas and liquid phase along the column. The computer code consists of
c  a main program CODE.FOR and a subroutine SUB.FOR (not included).
c  CASE 1: CO-CURRENT FLOW OF GAS AND LIQUID
c*****************************************************
      IMPLICIT REAL*8 (A-H,O-Z)
      PARAMETER (N = 10)
      PARAMETER (NG = 600)
      REAL HEIGHT(NG+1),GAS1(NG+1),GAS2(NG+1)
      REAL BQ1(NG+1),BQ2(NG+1)
      REAL SAV1,SAV2,TAV1,TAV2,DE1,DE2,LAST1,LAST2
      REAL  ERRORC,ERRORO,CL01,CL02
      REAL*8 A(0:N+1,0:N+1),B(0:N+1,0:N+1),V1(N+2),V2(N+2)
      REAL*8 XOLD(N),XINTP(N+2),Y(N+2)
      REAL*8 XDAT(N+1),YC(N+1),YO(N+1)
      REAL*8 ROOT(N+2),DIF1(N+2),DIF2(N+2),DIF3(N+2)
c
      EXTERNAL  FUN1,GUN1
      EXTERNAL  FUN2,GUN2
c
      COMMON /DEL/ DEL
      COMMON /SUR/ SUR
      COMMON /INDEX/ INDX
c
      COMMON /PRMA/ A
      COMMON /PRMB/  B
c
      COMMON /PRM1/ PHI
      COMMON /PRM2/ CG1
      COMMON /PRM3/ CG2
      COMMON /PRM4/ CL1
      COMMON /PRM5/ CL2
      COMMON /PRM6/ CL01
      COMMON /PRM7/ CL02
```

```
      COMMON /PRM8/ AL
      COMMON /PRM9/ W
      COMMON /PRM10/ G
      COMMON /PRM11/ R
      COMMON /PRM12/ E1
      COMMON /PRM13/ PSI
      COMMON /PRM14/BT
      COMMON /PRM15/AN
      COMMON /PRM16/AC
      COMMON /PRM17/AO
c
      COMMON /LIQUIDC/DERI1
      COMMON /LIQUIDO/DERI2
      COMMON /CG0/ACG01,ACG02
c
      OPEN(6,FILE='BTFCOLW.OUT',STATUS='NEW')
c
c  APPLY ORTHOGONAL COLLOCATION METHOD
c
      ALPHA=0.0
      BETA=0.0
c
      N0=1
      N1=1
      NT=N+N0+N1
c
c  CALCULATE THE COLLOCATION POINT
c
      CALL JCOBI (NT,N,N0,N1,ALPHA,BETA,DIF1,DIF2,DIF3,ROOT)
c
c  CALCULATE THE DISCRETIXATION MATRICES A & B
c
      DO 50 I=1,NT
      CALL DFOPR(NT,N,N0,N1,I,1,DIF1,DIF2,DIF3,ROOT,V1)
      CALL DFOPR(NT,N,N0,N1,I,2,DIF1,DIF2,DIF3,ROOT,V2)
      DO  60 J=1,NT
      A(I-1,J-1)=V1(J)
60    B(I-1,J-1)=V2(J)
50    CONTINUE
c
      INDX = 100
      WRITE (6,67) N
67    FORMAT( ' SOLUTION OF THE MODEL USING ORTHOGONAL
     & COLLOCATION ',/,' WITH[', I3,'] COL. POINTS',/)
c
```

```
      SUR = 133.3
c
      DE1=0.05
      DE2=0.05
      SAV1 = 0.0
      SAV2 = 0.0
      TAV1 =0.0
      TAV2 = 0.0
      CL01=0.2222
      CL02 =0.9133
c
c  INITIALIZE ITERAT TO ZERO
c
      ITERAT=0
  700 ITERAT=ITERAT+1
      WRITE (6,990) ITERAT
  990 FORMAT (////, 'ITERATION NUMBER:', I10)
 5000 WRITE (6,5005) CL01,CL02
 5005 FORMAT (3X,F14.6,3X,F14.6,3X)
c
      CG1 = 1.0
      CG2 = 1.0
      CL1 = CL01
      CL2 = CL02
c
      DELZ = 1./FLOAT(NG)
      Z = 0.0
      HEIGHT(1) = Z
      GAS1(1) = CG1
      GAS2(1) = CG2
      BQ1(1) = CL1
      BQ2(1) = CL2
      DO 100 IGAS = 2,NG+1
      WRITE (6,1000)  Z
 1000 FORMAT (3X,'HEIGHT = '5X, F14.7)
      DEL=130
    6 CALL PRM (PHI,AL,W,G,R,E1,PSI,BT,AN,AC,AO)
      IF (IGAS.EQ.NG) THEN
      INDX=1000
      ELSE
      INDEX=200
      ENDIF
c
c  INITIAL GUESS FOR Y
c
```

```
      DO 10 I=1,N
      XOLD(I)=0.1
   10 CONTINUE
c
      ITMAX = 100
      IPRINT = -1
      EPS1  = 1.E-9
      EPS2  = 1.E-9
c
c  *** IPRINT=1 ALL ITERATIONS ARE PRINTED***
      CALL NEWTON(ITMAX,N, IPRINT,EPS1,EPS2,XOLD)
c
c  INTERPOLAIION AT DESIRED VALUES
c
      CALL INTERP (XOLD,NT,ROOT, DIF1,XDAT,YC)
c
      SCF = YC(N+1)
      SOF = AL*(SCF-AC*CL1)+AO*CL2
      UPLM1 = AC*CL1*0.01
      UPLM2 = AO*CL2*0.01
      DEL = DEL*1E6
c
      IF (SOF.GT.0.0.AND.SOF.LE.UPLM2) THEN
      GO TO 5
      ELSEIF ((SCF.GT.0.0.AND.SCF.LE.UPLM1).OR.
      &(SOF.GT.0.0.AND.SOF.LE.UPLM2)) THEN
      GO TO5
      ELSEIF(DEL.LT.300) THEN
      DEL = DEL+5.0
      GO TO 6
      ELSEIF(DEL.GE.300) THEN
      DEL = 300
      GO TO 6
ELSE
ENDIF
c
   5  INDX = 3000
      CALL INTERP (XOLD,NT,ROOT,DIF1,XDAT,YC)
      CALL DERI (XOLD,DERI1,DERI2)
c
c  CALCULATE GAS PHASE AND LIQUID PHASE CONCENTRATION
c
      CALL RK4S(FUN1,GUN1,Z,CG1,CL1,DELZ)
 1001 WRITE (6,111) CG1,CL1
  111 FORMAT (3X,F14.6,3X,F14.6,3X)
```

```
      CALL RK4S (FUN2,GUN2,Z,CG2,CL2,DELZ)
1002  WRITE (6,112) CG2,CL2
112   FORMATt (3X,F14.6,3X,F14.6,3X)
      Z = Z-DELZ
      HEIGHT(IGAS) = Z
      GAS1(IGAS) = CG1
      GAS2(IGAS) = CG2
      BQ1(IGAS) = CL1
      BQ2(IGAS) = CL2
100   CONTINUE
600   CALL ERROR1 (CL1,ERRORC,CL01)
      CALL ERROR2 (CL2,ERRORO,CL02)
c
      IF (SAV1.GT.0.0.AND.TAV1.GT.0.0) THEN
      IF (SAV2.GT.0.0.AND.TAV2.GT.0.0) THEN
      IF (CL01.EQ.LAST1.AND.CL02.EQ.LAST2) THEN
      GO TO  400
      ELSE
      ENDIF
      ENDIF
      ENDIF
      IF (ERRORC.EQ.0.0.AND.ERRORO.EQ.0.0) THEN
      GO TO  400
      ELSE
      ENDIF
c
      LAST1=CL01
      LAST2=CL02
c
      IF (ERRORC.GT.0.0.AND.ERRORO.GT.0.0) THEN
      SAV1=CL01
      TAV1=CL02
      IF (SAV2.EQ.0.0.AND.TAV2.EQ.0.0) THEN
      CL01=CL01-DE1
      CL02=CL02-DE2
      ELSEIF (SAV2.EQ.0.0) THEN
      CL01=CL01-DE1
      CL02=(TAV1+TAV2)/2
      ELSEIF (TAV2.EQ.0.0) THEN
      CL01=(SAV1+SAV2)/2
      CL02=CL02-DE2
      ELSE
      CL01=(SAV1+SAV2)/2
      CL02=(TAV1+TAV2)/2
      ENDIF
```

```
      ENDIF
c
      IF (ERRORC.LT.0.0.AND.ERRORO.LT.0.0) THEN
      SAV2=CL01
      TAV2=CL02
      IF (SAV1.EQ.0.0.AND.TAV1.EQ.0.0) THEN
      CL01=CL01+DE1
      CL02=CL02+DE2
      ELSEIF (SAV1.EQ.0.0) THEN
      CL01=CL01+DE1
      CL02=(TAV1+TAV2)/2
      ELSEIF (TAV1.EQ.0.0) THEN
      CL01=(SAV1+SAV2)/2
      CL02=CL02+DE2
      ELSE
      CL01=(SAV1+SAV2)/2
      CL02=(TAV1+TAV2)/2
      ENDIF
      ENDIF
c
      IF (ERRORC.LT.0.0.AND.ERRORO.GT.0.0) THEN
      SAV2=CL01
      TAV1=CL02
      IF (SAV1.EQ.0.0.AND.TAV2.EQ.0.0) THEN
      CL01=CL01+DE1
      CL02 = CL02-DE2
      ELSEIF (SAV1.EQ0.0) THEN
      CL01= CL01+DE1
      CL02 = (TAV1+TAV2)/2
      ELSEIF (TAV2.EQ.0.0) THEN
      CL01 = (SAV1+SAV2)/2
      CL02 = CL02-DE2
      ELSE
      CL01 = (SAV1+SAV2)/2
      CL02 = (TAV1+TAV2)/2
      ENDIF
      ENDIF
c
      IF (ERRORC.GT.0.0.AND.ERRORO.LT.0.0) THEN
      SAV1 = CL01
      TAV2 = CL02
      IF (SAV2.EQ.0.0.AND.TAV1.EQ.0.0) THEN
      CL01 = CL01-DE1
      CL02 = CL02+DE2
      ELSEIF (SAV2.EQ.0.0) THEN
```

```
          CL01 = CL01-DE1
          CL02 = (TAV1+TAV2)/2
          ELSEIF (TAV1.EQ.0.0) THEN
          CL01= (SAV1+SAV2)/2
          CL02 = CL02+DE2
          ELSE
          CL01 = (SAV1+SAV2)/2
          CL02 = (TAV1+TAV21)/2
          ENDIF
          ENDIF
c
          GO TO 700
    400   WRITE(6,123)
          WRITE(6,22)
    22    FORMAT(//,5X,' GAS AND LIQUID PHASE CONCENTRATION
          &PROFILES',//)
          WRITE(6,13)
    13    FORMAT ('  ',12X, 'HEIGHT',10X,'CG(C)',10X,'CL(C) '/)
          WRITE(6,15)
    15    FORMAT ('  ',12X, 'HEIGHT',10X,'CG(O)',10X,'CL(O) '/)
          DO 44 IGAS = 1,NG+1
          WRI TE(6,33) HEIGHT(IGAS)
    44    CONTINUE
          DO 45 IGAS = 1,NG+1
          WRI TE(6,34) GAS1(IGAS)
    45    CONTINUE
          DO 46 IGAS = 1,NG+1
          WRITE (6,33) GAS2(IGAS)
    46    CONTINUE
          DO 47 IGAS = 1,NG+1
          WRITE (6,33) BQ1(IGAS)
    47    CONTINUE
          DO 48 IGAS =1,NG+1
          WRITE (6,34) BQ2(IGAS)
    48    CONTINUE
    33    FORMAT(3X,F14.6)
    34    FORMAT(3X,F14.6)
    123   FORMAT(' ____________________________________________________________',/)
          STOP
          END
c*************************************************************
c   INTERPOLATING THE RESULTS THAT YOU GET FROM
c   NEWTON RAPHSON SUBROUTINE
c*************************************************************
          SUBROUTINE INTERP (XOLD,NT,ROOT,DIF1,XDAT,YC)
```

```
      IMPLICIT REAL*8 (A-H,O-Z)
      PARAMETER(M = 10)
      REAL*8 XOLD(N),XINTP(N+2),Y1(N+2)
      REAL*8 XDAT(N+1), YC(N+1),YO(N+1)
      REAL*8 ROOT(N+2),DIF1(N+2),DIF2(N+2),DIF3(N+2)
      COMMON /PRM8/ AL
      COMMON /PRM16 / AC
      COMMON PRM17 /AO
      COMMON /PRM4/ CL1
      COMMON /PRM5/ CL2
      COMMON /INDEX/ INDX
c
      IF (INDX.EQ.3000) THEN
      WRITE(6,123)
      WRITE(6,12)
 12 FORMAT ('  ',10X, 'CONCENTRATION PROFILES IN THE BIOFILM ', /)
      WRITE(6,13)
   13 FORMAT (5X,' X ',18X,'S(C)',18X,'S(O)'//)
      ELSE
      ENDIF
c
      Y1(1) = AC*CL1
c
      DO 15 I =1,N
   15 Y1(I+1) = XOLD(I)
      Y1(NT) = Y1(NT-1)
c
      DO 20 I = 1,N+1
      DIST = FLOAT(I-1)/N
      CALL INTRP(NT,NT,DIST,ROOT, DIF1,XINTP)
      SC = 0.0
      DO 30 J = 1,NT
      SC = SC+XINTP(J)*Y1(J)
      30 CONTINUE
      IF (INDX.EQ.3000) THEN
      SO = (AL)*(SC-AC*CL1)+AO*CL2
      WRITE(6,40) DIST,SC,SO
      ELSE
      ENDIF
c  PLOT
      XDAT(I) = DIST
      YC(I) = SC
c
   20 CONTINUE
   40 FORMAT(5X,F7.2,5X,E14.6,5X,E14.6)
```

```
  123  FORMAT(' ____________________________________________________',/)
       RETURN
       END
c*************************************************************
c  CONSTRUCT THE JACOBIAN MATRIX AND ON THE LAST
c  COLUMN VECTOR -f
c*************************************************************
c  SUBROUTINE CALCN FOR EVALUTING THE AUGMENTED
c  JACOBIAN MATRIX
c  JAC*DEL=-F  SOLVING DEL
       SUBROUTINE CALCN(DXOLD,DF,N)
       IMPLICIT REAL*8 (A-H,O-Z)
       PARAMETER(M = 10)
       REAL*8 XOLD(M),DXOLD(M),DF(M,M+1),SUM1(M)
       REAl*8 A(0:M+1,0:M+1),B(0:M+1,0:M+1)
       COMMON /PRMA/ A
       COMMON /PRMB/ B
       COMMON /PRM1/ PHI
       COMMON /PRM4/ CL1
       COMMON /PRM5/ CL2
       COMMON /PRM8/ AL
       COMMON /PRM10/ G
       COMMON /PRM16/ AC
       COMMON /PRM17/ AO
       ORS = AO*CL2-AL*AC*CL1
c
       DO 1 I = 1,N
       XOLD(I) = DXOLD(I)
       DO 1 J =1,N+1
    1  DF(I,J) = 0.0
c
       DO 3 I = 1,N
    3  SUM1 (I) = 0.0
c
       DO 10 I = 1,N
       DO 20 J = 1,N
       IF (I.EQ.J) THEN
       P1=AL*XOLD(I)
       P2=P1+ORS
       P3=1.+P2
       P4=1.+XOLD(I)+G*XOLD(I)**2
       P5=1.-G*XOLD(I)**2
       DF(I,J) = B(I,J)-B(I,N+1)/A(N+1,N+1)*A(N+1,J)
       &-PHI*(P2*P3*P5+P1*P4)/((P4**2)*(P3**2))
       ELSE
```

```
      DF(I,J) = B(I,J)-B(I,N+1)/A(N+1,N+1)*A(N+1,J)
      ENDIF
      SUM1(I) = SUM1(I)+(B(I,J)-B(I,N+1)/A(N+1,N+1)*A(N+1,J))*XOLD(J)
   20 CONTINUE
      DF(I,N+1)=-(SUM1(I)+B(I,0)*AC*CL1-B(I,N+1)*
     &A(N+1,0)*AC*CL1/A(N+1,N+1)-
     &PHI*P2*XOLD(I)/(P3*P4))
   10 CONTINUE
      RETURN
      END
c*************************************************************
c  NEWTON RAPHSON TO SOLVE THE ALGEBRIC EQUATIONS
c*************************************************************
      SUBROUTINE NEWTON(ITMAX,N, IPRINT,EPS1,EPS2,XOLD)
      IMPLICIT REAL*8 (A-H,O-Z)
      PARAMETER (M=10)
      DIMENSION XOLD(M),XINC(M),A(M,M+1)
c  NEWTON RAPHSON ITERATION
c  WRITE(6,200) ITMAX, IPRINT,N,EPS1,EPS2,N,(XOLD(I), I = 1,N)
      WRITE (6,123)
      DO 9 ITER = 1, ITMAX
c  CALL ON CALCN TO SET UP THE A MATRIX
      CALL CALCN(XOLD,A,M)
c  CALL SIMUL TO COMPUTE JACOBIAN AND CORRECTION IN XINC
      NN = N+1
      INDIC = 1
      DETER = SIMUL (N,A,XINC,EPS1, INDIC,NN)
      IF (DETER.NE.0) GOTO 3
      WRITE(6,201)
      RETURN
c  CHECK FOR CONVERGENCE AND UPDATE XOLD VALUE
    3 ITCON = 1
      DO 5 I=1,N
      IF (DABS(XINC(I)).GT.EPS2) ITCON = 0
    5 XOLD(I) = XOLD(I)+XINC(I)
      IF (IPRINT.EQ.1) WRITE(6,202) ITER,DETER,N,(XOLD(I), I = 1,N)
      IF (ITCON.EQ.0) GOTO 9
c  WRITE(6,203) ITER,N,(XOLD(I),I=1,N)
      WRITE(6,2203) ITER
      RETURN
    9 CONTINUE
      WRITE(6,204)
      RETURN
c  FORMATS FOR INPUT AND OUTPUT STATEMENTS
  200 FORMAT(' ITMAX = ', I8,/' IPRINT = ', I8/' N     = ', I8/
```

```
     &    ' EPS1  = ',1PE14.1/' EPS2  = ',1PE14.1/10X,'XOLD(L)...XOLD(',
     &    I2,')'//(1H ,1P4E16.6))
     201  FORMAT(38H0MATRIX IS ILL-CONDITIONED OR SINGULAR)
     202  FORMAT(' ITER =', I8/  10H DETER = ,E18.5/
          $  26H        XOLD(L)...XOLD(,I2,1H) / (1H ,1P4E16.6) )
     203  FORMAT(' SUCCESSFUL CONVERGENCE'/'  ITER =',i3/10x,
          $'XOLD(L)...XOLD(', I2,')'//  (1H ,1P4E16.6) )
     2203 FORMAT(' SUCCESSFUL CONVERGENCE'/'  ITER =', I3/)
     204  FORMAT(' NO CONVERGENCE' )
     123  FORMAT(' ____________________________________________________________',/)
          END

c*************************************************************
          SUBROUTINE SVARI(SUR,DEL,B0,DFF1,DFF2,AKAP1,AKAP2,
          &AMM1, AMM2,AY1,AY2,AKSS1,AMU1,AKII1,AKOO1, ACG01,
          &ACG02,AUG,AUL,VV)
          IMPLICIT REAL*8 (A-H,O-Z)
          WRITE(6,123)
          WRITE(6,1)
     1    FORMAT ('  ',//, ' VARIABLES IN THE MODEL',//)
          WRITE(6,2)
     2    FORMAT (3X,'1 - VOC,/,3X,'2 - OXYGEN',/)
          WRITE(6,19) AUG
     19   FORMAT ('  ', 'GAS FLOW RATE (m3/hr)       = ', E14.3)
          WRITE(6,20) AUL
     20   FORMAT ('  ', 'LIQUID FLOW RATE(m3/hr)       = ', E14.3)
          WRITE(6,3) VV*1E6
     3    FORMAT ('  ', 'VOLUME OF THE COLUMN(cm3)   = ', F14.3)
          WRITE(6,4) SUR
     4    FORMAT ('  ', 'BIOLAYER SUR.AREA( m2/m3)   = ', F14.3)
          WRITE(6,44) B0
     44   FORMAT ('  ', 'BIOMASS CONC. (g/m3)        = ', E14.3)
          WRITE(6,5) DEL*1E3
     5    FORMAT ('  ', 'FILM THICKNESS (μm)         = ', F14.3)
          WRITE(6,18) ACG01
          WRITE(6,21) ACG02
     18   FORMAT ('  ', 'INLET CONC. (g/m3 OF VOC)(1) = ', F14.3)
     21   FORMAT ('  ', 'INLET CONC. (g/m3 OF AIR)(2) = ', F14.3)
          WRITE(6,31) AY1
     31   FORMAT ('  ', 'YIELD COEFFICIENT (1)       = ', F14.3)
          WRITE(6,32) AY2
     32   FORMAT ('  ', 'YIELD COEFFICIENT (2)       = ', F14.3)
          WRITE(6,51) DFF1*1E9/3600
          WRITE(6,54) DFF2*1E9/3600
```

```
   51   FORMAT (' ', 'DIFF. COEFF.(1)*1E9 (m2/s)  = ', F14.3)
   54   FORMAT (' ', 'DIFF. COEFF.(2)*1E9 (m2/s)  = ', F14.3)
        WRITE(6,56) AMM1
   56   FORMAT (' ', 'DIST. COEFF.      (1)    = ', E14.3)
        WRITE(6,57) AMM2
   57   FORMAT (' ', 'DIST. COEFF.      (2)    = ', E14.3)
        WRITE(6,48) AKAP1
   48   FORMAT (' ', 'MASS TRANSFER  COEFF   (1)    = ', E14.3)
        WRITE(6,49) AKAP2
   49   FORMAT (' ','MASS  TRANSFER COEFF    (2)    = ', E14.3)
        WRITE(6,123)
        WRITE(6,*) '        ANDREWS AND OTHER PARAMETERS'
        WRITE(6,6) AKSS1,AMU1, AKII1,AKOO1
    6   FORMAT (' ',/,' KS1 (g/m3) = ',E14.3,3X,'MU1 (1/hr) = ',F14.3,/,
   &         ' KSI1 (g/m3) = ',E14.3,3X,'KO1 (g/m3)= 'E14.3,/)
  123   FORMAT(' _____',/)
        RETURN
        END
c*************************************************************
c  SUBROUTINE FOR EVALUATING THE DERIVATIVES
c  NECESSARY FOR GAS AND LIQUID PHASE PROFILES
c*************************************************************
        SUBROUTINE DERI (XOLD, DERI1,DERI2)
        IMPLICIT REAL*8 (A-H,O-Z)
        PARAMETER (N=10)
        REAL*8 A(0:N+1,0:N+1),B(0:N+1,0:N+1)
        REAL*8 XOLD(N)
        COMMON /PRM16/ AC
        COMMON /PRM17/AO
        COMMON /PRM8/ AL
        COMMON /PRMA/ A
        COMMON /PRMB/ B
        COMMON /PRM4/ CL1
        COMMON /PRM5/CL2
        SUM1 = 0.0
        DO 10 J = 1,N
        SUM1 = SUM1+(A(0,J)-A(0,N+1)*A(N+1,J)/A(N+1,N+1))*XOLD(J)
   10   CONTINUE
        DERI1 = SUM1+(A(0,0)-A(0,N+1)*A(N+1,0)/A(N+1,N+1))*AC*CL1
        DERI2 = AL*DERI1
        WRITE(*,*) DERI1, DERI2
        RETURN
        END
c*************************************************************
c  FOR GAS AND LIQUID PHASE USING THE FOURTH ORDER
```

```
c   RUNGE KUTTA METHOD
c*************************************************************
      SUBROUTINE RK4S(F,G,Z,CG,CL,H)
      IMPLICIT REAL*8 (A-H,O-Z)
      H2 = 0.5*H
      START = Z
      B1 = H*F(Z,CG,CL)
      B2 = H*G(Z,CG,CL)
      B3 = H*F(Z+H2,CG+H2*B1,CL+H2*B2)
      B4 = H*G(Z+H2,CG+H2*B1,CL+H2*B2)
      B5 = H*F(Z+H2,CG+H2*B3,CL+H2*B4)
      B6 = H*G(Z+H2,CG+H2*B3,CL+H2*B4)
      B7 = H*F(Z+H,CG+H*B5,CL+H*B6)
      B8 = H*G(Z+H,CG+H*B5,CL+H*B6)
      CG = CG+(B1+2.*B3+2.*B5+B7)/6.
      CL = CL+(B2+2.*B4+2.*B6+B8)/6.
      Z = Z+H
      WRITE (*,*) CG,CL
      RETURN
      END
c*************************************************************
c    PURPOSE : GIVE THE FUNCTION FOR RK METHOD, IN THE
c   GAS PHASE BALANCE ; VOC (BLOCK A)
c*************************************************************
      FUNCTION FUN1(Z,CG,CL)
      IMPLICIT REAL*8 (A-H,O-Z)
      COMMON / PRM11/ R
      COMMON / PRM2/ CG1
      COMMON / PRM4/ CL1
      FUN1 = R*(CL1-CG1)
      RETURN
      END
c*************************************************************
c   PURPOSE : GIVE THE FUNCTION FOR RK METHOD, IN THE
c   LIQUID PHASE BALANCE ; VOC
c*************************************************************
      FUNCTION GUN1(Z,CG,CL)
      IMPLICIT REAL*8 (A-H,O-Z)
      COMMON / PRM13/ PSI
      COMMON /PRM15/AN
      COMMON / LIQUIDC/DERI1
      COMMON / PRM2/ CG1
      COMMON / PRM4/ CL1
      GUN1 =-PSI*(CL1-CG1)+AN*DERI1
```

```
      RETURN
      END
c*************************************************************
c  PURPOSE : GIVE THE FUNCTION FOR RK METHOD, IN THE
c  GAS PHASE BALANCE ; OXYGEN (BLOCK B)
c*************************************************************
      FUNCTION FUN2(Z,CG,CL)
      IMPLICIT REAL*8 (A-H,O-Z)
      COMMON / PRM11/R
      COMMON /PRM12/E1
      COMMON / PRM3/ CG2
      COMMON / PRM5/ CL2
      FUN2 = R*E1*(CL2-CG2)
      RETURN
      END
c*************************************************************
c  PURPOSE : GIVE THE FUNCTION FOR RK METHOD, IN THE
c  LIQUID PHASE BALANCE ; OXYGEN
c*************************************************************
      FUNCTION GUN2(Z,CG,CL)
      IMPLICIT REAL*8 (A-H,O-Z)
      COMMON / PRM13/ PSI
      COMMON / PRM14/ BT
      COMMON / PRM15/ AN
      COMMON / PRM9/ W
      COMMON / PRM3/ CG2
      COMMON / PRM5/ CL2
      COMMON / LIQUIDO/ DERI2
      GUN2 =-PSI*BT*(CL2-CG2)+AN*W*DERI2
      RETURN
      END
c*************************************************************
      SUBROUTINE ERROR1 (CL1,ERRORC,CL01)
      IMPLICIT REAL*8 (A-H,O-Z)
      COMMON / PRM4/ CL1
      COMMON / PRM6/ CL01
      ERRORC = CL1-CL01
      RETURN
      END
c*************************************************************
      SUBROUTINE ERROR2 (CL2,ERRORO,CL02)
      IMPLICIT REAL*8 (A-H,O-Z)
      COMMON /PRM5/ CL2
      COMMON /PRM7/ CL02
```

```
      ERRORO = CL2-CL02
      RETURN
      END
c*************************************************************
      SUBROUTINE PRM (PHI,AL,W,G,R,E1,PSI,BT,AN,AC,AO)
      IMPLICIT REAL*8 (A-H,O-Z)
      COMMON /DEL/ DEL
      COMMON /SUR/ SUR
      COMMON /INDEX/ INDX
      COMMON /CG0 /ACG01,ACG02
c
c  1-VOC
c  2-OXYGEN
      DEL = DEL*1E-6
      WRITE(6,80) DEL*1E6
c
      B0 = 75E3
      XV = B0/1000
      FD = 1-0.43*XV**0.92/(11.19+0.27*XV**0.99)
c
c  DIFFUSION COEFFICIENTS
      DFF1  = 0.691E-9 *3600.*FD
      DFF2  = 2.3807E-9 *3600.*FD
c
c  OVERALL MASS TRANSFER COEFFICIENTS
      AKAP1 = 12.258
      AKAP2 = 28.841
c
c  DISTRIBUTION COEFFICIENTS
      AMM1 = 0.119
      AMM2 = 34.4
c
c  YIELD COEFFICIENTS
      AY1 = 0.397
      AY2 = 0.363
c
c  KINETIC PARAMETERS
      AKSS1= 13.389
      AMU1  = 0.146
      AKII1 = 19.657
      AKOO1 = 0.26
c
c  INLET GAS CONCENTRATIONS
      ACG01 = 0.9
      ACG02 = 275
```

```
c
c  GAS FLOW RATE
       AUG = 0.2438
c
c  LIQUID FLOW RATE
       AUL = 0.0052
c
c  VOLUME OF  THE COLUMN
       VV = 0.0126
c
       IF (INDX.EQ.100) THEN
       CALL SVARI(SUR,DEL,B0,DFF1,DFF2,AKAP1,AKAP2,AMM1,
       &AMM2,AY1,AY2,AKSS1,AMU1,AKII1,AKOO1,ACG01,ACG02,
       &AUG,AUL,VV)
       ELSE
       ENDIF
c
       PHI = (AMU1*(DEL**2)*B0)/(DFF1*AY1*AKSS1)
       AL = (DFF1*AY1*AKSS1)/(AY2*AKOO1*DFF2)
       W = (AKOO1*DFF2*ACG01*AMM2)/(AKSS1*DFF1*ACG02*AMM1)
       G =AKSS1/AKII1
       R = (AKAP1*VV)/(AUG*AMM1)
       E1= (AMM1*AKAP2)/(AMM2*AKAP1)
       PSI =(AKAP1*VV)/AUL
       BT = AKAP2/AKAP1
       AN =(DFF1*SUR*AKSS1*VV*AMM1)/(DEL*AUL*ACG01)
       AC = ACG01/(AKSS1*AMM1)
       AO = ACG02/(AKOO1*AMM2)
c
       IF (INDX.EQ.1000) THEN
       WRITE(6,123)
       WRITE(6,71)
   71  FORMAT (' ','    PARAMETERS USED :', /)
       WRITE(6,72) PHI, G
       WRITE(6,73) E1,AN
       WRITE (6,74) AC,AO
   72  FORMAT (3X,'PHI^2  =  ',E14.6,
   &     3X,'GAMA   =  ',E14.6)
   73  FORMAT (3X,'EPS1   =  ',F14.6,
   &     3X,'N   =  ',E14.6)
       WRITE(6,75) AL
       WRITE(6,76) W
   75  FORMAT (3X,'LAMDA  =  ',E14.6)
   76  FORMAT ( 3X,'OMEGA  =  ',E14.6)
       WRITE(6,77) R,PSI,BT
```

```
   77   FORMAT (3X,'RO   =  ',E14.6,
   &       3X,'PSI    =  ',E14.6,
   &     /,3X,'BETA   =  ',F14.3,/)
   74   FORMAT (3X,'STATHC  =  ',E14.6,
   &       3X'STATHO   =  ',E14.6)
   80   FORMAT (3X,'DEL.(μm)=    ',F14.3,/)
   123  FORMAT(' ____________________________________________________',/)
        ELSE
        ENDIF
        RETURN
        END
c*******END OF MAIN PROGRAM**************************
c
c  CASE 2: COUNTER-CURRENT FLOW OF GAS AND LIQUID
c  IN  BLOCK A, LINE 6 SHOULD BE:
c   FUN1 = -R*(CL1-CG1)
c  IN  BLOCK B, LINE 6 SHOULD BE:
c   FUN2 = -R*E1*(CL2-CG2)
```

APPENDIX B

COMPUTER CODE FOR SOLVING THE STEADY-STATE MODEL DESCRIBING REMOVAL OF A MIXTURE OF TWO VOCS IN A BIOTRICKLING FILTER

```
c*************************************************
c  This computer code numerically solves the steady state model presented
c  in Chapter 7. This model describes removal of a mixture of two VOCs in
c  a biotrickling filter. The code is based on the orthogonal collocation
c  method and the 4th-Runge-Kutta method. It uses an iteration procedure for
c  obtaining VOC and oxygen concentration profiles in the biofilm and in the
c  gas and liquid phase along the column. The computer code consists of
c  program CODEMX.FOR and a subroutine SUBMX.FOR (not included).
c  CASE 1: CO-CURRENT FLOW OF GAS AND LIQUID
c*************************************************
      IMPLICIT REAL*8 (A-H,O-Z)
      PARAMETER (N = 10)
      PARAMETER (NG = 600)
      REAL HEIGHT(NG+1),GAS1(NG+1),GAS2(NG+1),GAS3(NG+1)
      REAL BQ1(NG+1),BQ2(NG+1),BQ3(NG+1)
      REAL SAV1,SAV2,TAV1,TAV2,GAV1,GAV2
      REAL DE1,DE2,DE3,LAST1,LAST2,LAST3
      REAL  ERRORC,ERRORD,ERRORO,CL01,CL02,CL03
      REAL*8 A(0:N+1,0:N+1),B(0:N+1,0:N+1),V1(N+2),V2(N+2)
      REAL*8 XOLD(N),XINTP(N+2),Y(N+2)
      REAL*8 XDAT(N+1),YC(N+1),YD(N+1),YO(N+1)
      REAL*8 ROOT(N+2),DIF1(N+2),DIF2(N+2),DIF3(N+2)
c
      EXTERNAL  FUN1,GUN1
      EXTERNAL  FUN2,GUN2
      EXTERNAL  FUN3,GUN3
c
      COMMON /DEL/ DEL
      COMMON /SUR/ SUR
      COMMON /INDEX/ INDX
c
      COMMON /PRMA/ A
      COMMON /PRMB/  B
c
      COMMON /PRM1/ PHI1,PHI2
      COMMON /PRM2/ CG1
      COMMON /PRM3/ CG2
      COMMON /PRM4/ CL1
      COMMON /PRM5/ CL2
```

```
      COMMON /PRM6/ CL01
      COMMON /PRM7/ CL02
      COMMON /PRM8/ AL1,AL2
      COMMON /PRM9/ W1,W2
      COMMON /PRM10/ G1,G2
      COMMON /PRM11/ R
      COMMON /PRM12/ E1,E2
      COMMON /PRM13/ PSI
      COMMON /PRM14/BT1,BT2
      COMMON /PRM15/AN
      COMMON /PRM16/AC
      COMMON /PRM17/AO
      COMMON /PRM18/AD
      COMMON /PRM19/CG3
      COMMON /PRM20/CL3
      COMMON /PRM21/CL03
c
      COMMON /LIQUIDC/DERI1
      COMMON /LIQUIDD/DERI2
      COMMON /LIQUIDO/DERI3
      COMMON /CG0/ACG01,ACG02,ACG03
c
      OPEN(6,FILE='BTFCOLWMX.OUT',STATUS='NEW')
c
c  APPLY ORTHOGONAL COLLOCATION METHOD
c
      ALPHA=0.0
      BETA=0.0
c
      N0=1
      N1=1
      NT=N+N0+N1
c
c  CALCULATE THE COLLOCATION POINT
c
      CALL JCOBI (NT,N,N0,N1,ALPHA,BETA,DIF1,DIF2,DIF3,ROOT)
c
c  CALCULATE THE DISCRETIXATION MATRICES A & B
c
      DO 50 I=1,NT
      CALL DFOPR(NT,N,N0,N1,I,1,DIF1,DIF2,DIF3,ROOT,V1)
      CALL DFOPR(NT,N,N0,N1,I,2,DIF1,DIF2,DIF3,ROOT,V2)
      DO  60 J=1,NT
      A(I-1,J-1)=V1(J)
60    B(I-1,J-1)=V2(J)
```

```
   50   CONTINUE
c
        INDX = 100
        WRITE (6,67) N
   67   FORMAT( ' SOLUTION OF THE MODEL USING ORTHOGONAL
       &  COLLOCATION ',/,' WITH[', I3,'] COL. POINTS',/)
c
        SUR = 133.3
c
        DE1 = 0.05
        DE2 = 0.05
        DE3 = 0.05
        SAV1 = 0.0
        SAV2 = 0.0
        SAV3 = 0.0
        TAV1 =0.0
        TAV2 = 0.0
        TAV3 = 0.0
        CL01=0.2222
        CL02 =0.9133
        CL03 = 0.119
c  INITIALIZE ITERAT TO ZERO
c
        ITERAT=0
  700   ITERAT=ITERAT+1
        WRITE (6,990) ITERAT
  990   FORMAT (////, 'ITERATION NUMBER:', I10)
  5000  WRITE (6,5005) CL01,CL02,CL03
  5005  FORMAT (3X,F14.6,3X,F14.6,3X,F14.6,3X)
c
        CG1 = 1.0
        CG2 = 1.0
        CG3 = 1.0
        CL1 = CL01
        CL2 = CL02
        CL3 = CL03
c
        DELZ = 1./FLOAT(NG)
        Z = 0.0
        HEIGHT(1) = Z
        GAS1(1) = CG1
        GAS2(1) = CG2
        GAS3(1) = CG3
        BQ1(1) = CL1
        BQ2(1) = CL2
```

```
      BQ3(1) = CL3
      DO 100 IGAS=2,NG+1
      WRITE (6,1000)  Z
 1000 FORMAT (3X,'HEIGHT = '5X, F14.7)
      DEL=90
    6 CALL PRM (PHI1,PHI2,AL1,AL2,W1,W2,G1,G2,R,E1,E2,
      &PSI,BT1,BT2,AN,AC,AD,AO,S1,S2)
      IF (IGAS.EQ.NG) THEN
      INDX=1000
      ELSE
      INDEX=200
      ENDIF
c
c  INITIAL GUESS FOR Y
c
      DO 10 I=1, 2*N
      XOLD(I)=0.1
   10 CONTINUE
c
      ITMAX = 100
      IPRINT =  -1
      EPS1 = 1.E-9
      EPS2  =  1.E-9
c
c  *** IPRINT=1 ALL ITERATIONS ARE PRINTED***
      CALL NEWTON(ITMAX,2*N,IPRINT,EPS1,EPS2,XOLD)
c
c  INTERPOLAIION AT DESIRED VALUES
c
      CALL INTERP (XOLD,NT,ROOT, DIF1,XDAT,YC,YD)
c
      SCF = YC(N+1)
      SDF = YD(N+1)
      SOF =(AL1)*(SCF-AC*CL1)+(AL2)*(SDF-AD*CL2)+AO*CL3
      UPLM1 = AC*CL1*0.01
      UPLM2 = AD*CL2*0.01
      UPLM3 = AO*CL3*0.01
      DEL = DEL*1E6
c
      IF (SOF.GT.0.0.AND.SOF.LE.UPLM3) THEN
      GO TO 5
      ELSEIF ((SCF.GT.0.0.AND.SCF.LE.UPLM1).OR.
      &(SDF.GT.0.0.AND.SDF.LE.UPLM2).OR.
      &(SOF.GT.0.0.AND.SOF.LE.UPLM3)) THEN
      GO TO5
```

```
          ELSEIF(DEL.LT.300) THEN
          DEL = DEL+2.0
          GO TO 6
          ELSEIF(DEL.GE.300) THEN
          DEL = 300
          GO TO 6
ELSE
ENDIF
c
    5     INDX = 3000
          CALL INTERP (XOLD,NT,ROOT,DIF1,XDAT,YC,YD)
          CALL DERI (XOLD,DERI1,DERI2,DERI3)
c
c   CALCULATE GAS PHASE AND LIQUID PHASE CONCENTRATION
c
          CALL RK4S(FUN1,GUN1,Z,CG1,CL1,DELZ)
  1001    WRITE (6,111) CG1,CL1
  111     FORMAT (3X,F14.6,3X,F14.6,3X)
          CALL RK4S (FUN2,GUN2,Z,CG2,CL2,DELZ)
  1002    WRITE (6,112) CG2,CL2
  112     FORMAT (3X,F14.6,3X,F14.6,3X)
          CALL RK4S(FUN3,GUN3,Z,CG3,CL3,DELZ)
  1003    WRITE (6,113) CG3,CL3
  113     FORMAT (3X,F14.6,3X,F14.6,3X)
          Z = Z-DELZ
          HEIGHT(IGAS) = Z
          GAS1(IGAS) = CG1
          GAS2(IGAS) = CG2
          GAS3(IGAS) = CG3
          BQ1(IGAS) = CL1
          BQ2(IGAS) = CL2
          BQ3(IGAS) = CL3
  100     CONTINUE
  600     CALL ERROR1 (CL1,ERRORC,CL01)
          CALL ERROR2 (CL2,ERRORD,CL02)
          CALL ERROR3 (CL3,ERRORO,CL03)
c
          IF ((SAV1.GT.0.0.AND.TAV1.GT.0.0).AND.GAV1.GT.0.0) THEN
          IF ((SAV2.GT.0.0.AND.TAV2.GT.0.0)).AND.GAV2.GT.0.0) THEN
          IF ((CL01.EQ.LAST1.AND.CL02.EQ.LAST2)).AND.CL03.EQ.LAST3)
          &THEN
          GO TO  400
          ELSE
          ENDIF
          ENDIF
```

```
      ENDIF
      IF ((ERRORC.EQ.0.0.AND.ERRORD.EQ.0.0)).AND.ERRORO.EQ.0.0)
      &THEN
      GO TO  400
      ELSE
      ENDIF
c
      LAST1 = CL01
      LAST2 = CL02
      LAST3 = CL03
c
      IF ((ERRORC.GT.0.0.AND.ERRORO.GT.0.0)).AND.ERRORO.GT.0.0)
      &THEN
      SAV1=CL01
      TAV1=CL02
      GAV1=CL03
      IF ((SAV2.EQ.0.0.AND.TAV2.EQ.0.0)).AND.GAV2.EQ.0.0) THEN
      CL01=CL01-DE1
      CL02=CL02-DE2
      CL03=CL03-DE3
      ELSEIF (SAV2.EQ.0.0) THEN
      CL01=CL01-DE1
      CL02=(TAV1+TAV2)/2
      CL03=(GAV1+GAV2)/2
      ELSEIF (TAV2.EQ.0.0) THEN
      CL01=(SAV1+SAV2)/2
      CL02=CL02-DE2
      CL03=(GAV1+GAV2)/2
      ELSEIF (GAV2.EQ.0.0) THEN
      CL01=(SAV1+SAV2)/2
      CL02=(TAV1+TAV2)/2
      CL03=CL03-DE3
      ELSE
      CL01=(SAV1+SAV2)/2
      CL02=(TAV1+TAV2)/2
      CL03=(GAV1+GAV2)/2
      ENDIF
      ENDIF
c
      IF ((ERRORC.LT.0.0.AND.ERRORD.LT.0.0).AND.ERRORO.LT.00)
      &THEN
      SAV2=CL01
      TAV2=CL02
      GAV2=CL03
      IF ((SAV1.EQ.0.0.AND.TAV1.EQ.0.0).AND.GAV1.EQ.00) THEN
```

```
CL01=CL01+DE1
CL02=CL02+DE2
CL03=CL03+DE3
ELSEIF (SAV1.EQ.0.0) THEN
CL01=CL01+DE1
CL02=(TAV1+TAV2)/2
CL03=(GAV1+GAV2)/2
ELSEIF (TAV1.EQ.0.0) THEN
CL01=(SAV1+SAV2)/2
CL02=CL02+DE2
CL03=(GAV1+GAV2)/2
ELSEIF (GAV1.EQ.0.0) THEN
CL01=(SAV1+SAV2)/2
CL02=(TAV1+TAV2)/2
CL03=CL03+DE3
ELSE
CL01=(SAV1+SAV2)/2
CL02=(TAV1+TAV2)/2
CL03=(GAV1+GAV2)/2
ENDIF
ENDIF
c
IF ((ERRORC.GT.0.0.AND.ERRORD.GT.0.0).AND.ERRORO.LT.00)
&THEN
SAV1=CL01
TAV1=CL02
GAV2=CL03
IF ((SAV2.EQ.0.0.AND.TAV2.EQ.0.0).AND.GAV1.EQ.00) THEN
CL01=CL01-DE1
CL02=CL02-DE2
CL03=CL03+DE3
ELSEIF (SAV2.EQ.0.0) THEN
CL01=CL01-DE1
CL02=(TAV1+TAV2)/2
CL03=(GAV1+GAV2)/2
ELSEIF (TAV2.EQ.0.0) THEN
CL01=(SAV1+SAV2)/2
CL02=CL02-DE2
CL03=(GAV1+GAV2)/2
ELSEIF (GAV1.EQ.0.0) THEN
CL01=(SAV1+SAV2)/2
CL02=(TAV1+TAV2)/2
CL03=CL03+DE3
ELSE
CL01=(SAV1+SAV2)/2
```

```
CL02=(TAV1+TAV2)/2
CL03=(GAV1+GAV2)/2
ENDIF
ENDIF
c
IF ((ERRORC.GT.0.0.AND.ERRORD.LT.0.0).AND.ERRORO.LT.00)
&THEN
SAV1=CL01
TAV2=CL02
GAV2=CL03
IF ((SAV2.EQ.0.0.AND.TAV1.EQ.0.0).AND.GAV1.EQ.00) THEN
CL01=CL01-DE1
CL02=CL02+DE2
CL03=CL03+DE3
ELSEIF (SAV2.EQ.0.0) THEN
CL01=CL01-DE1
CL02=(TAV1+TAV2)/2
CL03=(GAV1+GAV2)/2
ELSEIF (TAV1.EQ.0.0) THEN
CL01=(SAV1+SAV2)/2
CL02=CL02+DE2
CL03=(GAV1+GAV2)/2
ELSEIF (GAV1.EQ.0.0) THEN
CL01=(SAV1+SAV2)/2
CL02=(TAV1+TAV2)/2
CL03=CL03+DE3
ELSE
CL01=(SAV1+SAV2)/2
CL02=(TAV1+TAV2)/2
CL03=(GAV1+GAV2)/2
ENDIF
ENDIF
c
IF ((ERRORC.LT.0.0.AND.ERRORD.LT.0.0).AND.ERRORO.GT.00)
&THEN
SAV2=CL01
TAV2=CL02
GAV1=CL03
IF ((SAV1.EQ.0.0.AND.TAV1.EQ.0.0).AND.GAV2.EQ.00) THEN
CL01=CL01+DE1
CL02=CL02+DE2
CL03=CL03-DE3
ELSEIF (SAV1.EQ.0.0) THEN
CL01=CL01+DE1
CL02=(TAV1+TAV2)/2
```

```
      CL03=(GAV1+GAV2)/2
      ELSEIF (TAV1.EQ.0.0) THEN
      CL01=(SAV1+SAV2)/2
      CL02=CL02+DE2
      CL03=(GAV1+GAV2)/2
      ELSEIF (GAV2.EQ.0.0) THEN
      CL01=(SAV1+SAV2)/2
      CL02=(TAV1+TAV2)/2
      CL03=CL03-DE3
      ELSE
      CL01=(SAV1+SAV2)/2
      CL02=(TAV1+TAV2)/2
      CL03=(GAV1+GAV2)/2
      ENDIF
      ENDIF
C
      IF ((ERRORC.LT.0.0.AND.ERRORD.GT.0.0).AND.ERRORO.GT.00)
      &THEN
      SAV2=CL01
      TAV1=CL02
      GAV1=CL03
      IF ((SAV1.EQ.0.0.AND.TAV2.EQ.0.0).AND.GAV2.EQ.00) THEN
      CL01=CL01+DE1
      CL02=CL02-DE2
      CL03=CL03-DE3
      ELSEIF (SAV1.EQ.0.0) THEN
      CL01=CL01+DE1
      CL02=(TAV1+TAV2)/2
      CL03=(GAV1+GAV2)/2
      ELSEIF (TAV2.EQ.0.0) THEN
      CL01=(SAV1+SAV2)/2
      CL02=CL02-DE2
      CL03=(GAV1+GAV2)/2
      ELSEIF (GAV2.EQ.0.0) THEN
      CL01=(SAV1+SAV2)/2
      CL02=(TAV1+TAV2)/2
      CL03=CL03-DE3
      ELSE
      CL01=(SAV1+SAV2)/2
      CL02=(TAV1+TAV2)/2
      CL03=(GAV1+GAV2)/2
      ENDIF
      ENDIF
C
```

```
IF ((ERRORC.LT.0.0.AND.ERRORD.GT.0.0).AND.ERRORO.LT.00)
&THEN
SAV2=CL01
TAV1=CL02
GAV2=CL03
IF ((SAV1.EQ.0.0.AND.TAV2.EQ.0.0).AND.GAV1.EQ.00) THEN
CL01=CL01+DE1
CL02=CL02-DE2
CL03=CL03+DE3
ELSEIF (SAV1.EQ.0.0) THEN
CL01=CL01+DE1
CL02=(TAV1+TAV2)/2
CL03=(GAV1+GAV2)/2
ELSEIF (TAV2.EQ.0.0) THEN
CL01=(SAV1+SAV2)/2
CL02=CL02-DE2
CL03=(GAV1+GAV2)/2
ELSEIF (GAV1.EQ.0.0) THEN
CL01=(SAV1+SAV2)/2
CL02=(TAV1+TAV2)/2
CL03=CL03+DE3
ELSE
CL01=(SAV1+SAV2)/2
CL02=(TAV1+TAV2)/2
CL03=(GAV1+GAV2)/2
ENDIF
ENDIF
c
IF ((ERRORC.GT.0.0.AND.ERRORD.LT.0.0).AND.ERRORO.GT.00)
&THEN
SAV1=CL01
TAV2=CL02
GAV1=CL03
IF ((SAV2.EQ.0.0.AND.TAV1.EQ.0.0).AND.GAV2.EQ.00) THEN
CL01=CL01-DE1
CL02=CL02+DE2
CL03=CL03-DE3
ELSEIF (SAV2.EQ.0.0) THEN
CL01=CL01-DE1
CL02=(TAV1+TAV2)/2
CL03=(GAV1+GAV2)/2
ELSEIF (TAV1.EQ.0.0) THEN
CL01=(SAV1+SAV2)/2
CL02=CL02+DE2
CL03=(GAV1+GAV2)/2
```

```
      ELSEIF (GAV2.EQ.0.0) THEN
      CL01=(SAV1+SAV2)/2
      CL02=(TAV1+TAV2)/2
      CL03=CL03-DE3
      ELSE
      CL01=(SAV1+SAV2)/2
      CL02=(TAV1+TAV2)/2
      CL03=(GAV1+GAV2)/2
      ENDIF
      ENDIF
c
      GO TO 700
  400 WRITE(6,123)
      WRITE(6,22)
   22 FORMAT(//,5X,' GAS AND LIQUID PHASE CONCENTRATION
     &PROFILES',//)
      WRITE(6,13)
   13 FORMAT ('  ',12X, 'HEIGHT',10X,'CG(C)',10X,'CL(C) '/)
      WRITE(6,15)
   15 FORMAT ('  ',12X, 'HEIGHT',10X,'CG(D)',10X,'CL(D) '/)
      WRITE(6,16)
   16 FORMAT ('  ',12X, 'HEIGHT',10X,'CG(O)',10X,'CL(O) '/)
      DO 44 IGAS = 1,NG+1
      WRI TE(6,33) HEIGHT(IGAS)
   44 CONTINUE
      DO 45 IGAS = 1,NG+1
      WRI TE(6,34) GAS1(IGAS)
   45 CONTINUE
      DO 46 IGAS = 1,NG+1
      WRITE (6,33) GAS2(IGAS)
   46 CONTINUE
      DO 47 IGAS = 1,NG+1
      WRITE (6,33) GAS3(IGAS)
   47 CONTINUE
      DO 48 IGAS = 1,NG+1
      WRITE (6,33) BQ1(IGAS)
   48 CONTINUE
      DO 49 IGAS =1,NG+1
      WRITE (6,34) BQ2(IGAS)
   49 CONTINUE
      DO 51 IGAS =1,NG+1
      WRITE (6,34) BQ3(IGAS)
   51 CONTINUE
   33 FORMAT(3X,F14.6)
   34 FORMAT(3X,F14.6)
```

```
  123 FORMAT(' _____',/)
      STOP
      END
c*************************************************************
c  INTERPOLATING THE RESULTS THAT YOU GET FROM
c  NEWTON RAPHSON SUBROUTINE
c*************************************************************
      SUBROUTINE INTERP (XOLD,NT,ROOT,DIF1,XDAT,YC,YD)
      IMPLICIT REAL*8 (A-H,O-Z)
      PARAMETER(M = 10)
      REAL*8 XOLD(2*N),XINTP(N+2),Y1(N+2),Y2(N+2)
      REAL*8 XDAT(N+1),YC(N+1),YD(N+1),YO(N+1)
      REAL*8 ROOT(N+2),DIF1(N+2),DIF2(N+2),DIF3(N+2)
      COMMON /PRM8/ AL1,AL2
      COMMON /PRM16 / AC
      COMMON PRM17 /AO
      COMMON PRM18 /AD
      COMMON /PRM4/ CL1
      COMMON /PRM5/ CL2
      COMMON /PRM20/ CL3
      COMMON /INDEX/ INDX
c
      IF (INDX.EQ.3000) THEN
      WRITE(6,123)
      WRITE(6,12)
   12 FORMAT (' ',10X, 'CONCENTRATION PROFILES IN THE BIOFILM ', /)
      WRITE(6,13)
   13 FORMAT (5X,' X ',11X,'S(C)',14X,'S(D)',11X,'S(O)'//)
      ELSE
      ENDIF
c
      Y1(1) = AC*CL1
      Y2(1) = AD*CL2
c
      DO 15 I =1,N
   15 Y1(I+1) = XOLD(I)
      Y1(NT) = Y1(NT-1)
      DO 16 I = 1,N
   16 Y2(I+1) = XOLD(I+N)
      Y2(NT) = Y2(NT-1)
c
      DO 20 I = 1,N+1
      DIST = FLOAT(I-1)/N
      CALL INTRP(NT,NT,DIST,ROOT,DIF1,XINTP)
      SC = 0.0
```

```
      SD = 0.0
      DO 30 J = 1,NT
      SC = SC+XINTP(J)*Y1(J)
      SD = SD+XINTP(J)*Y2(J)
      30 CONTINUE
      IF (INDX.EQ.3000) THEN
      SO = (AL1)*(SC-AC*CL1)+AL2*(SD-AD*CL2)+AO*CL3
      WRITE(6,40) DIST,SC,SD,SO
      ELSE
      ENDIF
c  PLOT
      XDAT(I) = DIST
      YC(I) = SC
      YD(I) = SD
c
   20 CONTINUE
   40 FORMAT(5X,F7.2,5X,E14.6,5X,E14.6,5X,E14.6)
   123 FORMAT(' ____________________________________________________',/)
      RETURN
      END
c*************************************************************
c  CONSTRUCT THE JACOBIAN MATRIX AND ON THE LAST
c  COLUMN VECTOR -f
c*************************************************************
c  SUBROUTINE CALCN FOR EVALUTING THE AUGMENTED
c  JACOBIAN MATRIX
c  JAC*DEL=-F  SOLVING DEL
      SUBROUTINE CALCN(DXOLD,DF,N)
      IMPLICIT REAL*8 (A-H,O-Z)
      PARAMETER(M = 10)
      REAL*8 XOLD(2*M),DXOLD(2*M),DF(2*M,2*M+1)
      REAL*8 SUM1(2*M),SUM2(2*M)
      REAl*8 A(0:M+1,0:M+1),B(0:M+1,0:M+1)
      COMMON /PRMA/ A
      COMMON /PRMB/ B
      COMMON /PRM1/ PHI1,PHI2
      COMMON /PRM4/ CL1
      COMMON /PRM5/ CL2
      COMMON /PRM20/ CL3
      COMMON /PRM8/ AL1,AL2
      COMMON /PRM10/ G1,G2
      COMMON /PRM16/ AC
      COMMON /PRM17/ AO
      COMMON /PRM18/ AD
     *  ORS = AO*CL3-AL1*AC*CL1-AL2*AD*CL2
```

```
c
      DO 1 I = 1,2*N
      XOLD(I) = DXOLD(I)
      DO 1 J =1,(2*N+1)
1     DF(I,J) = 0.0
c
      DO 3 I = 1,2*N
      SUM1 (I) = 0.0
3     SUM2 (I) = 0.0
c
      DO 10 I = 1,N
      DO 20 J = 1,N
      IF (I.EQ.J) THEN
      P1 = 1+XOLD(I)+G1*(XOLD(I))**2+AS1*XOLD(I+N)
      P2 = 1+AL1*XOLD(I)+AL2*XOLD(I+N)+ORS
      P3 = 2*AL1*XOLD(I)+AL2*XOLD(I+N)+ORS
      P4 = P1*AL1+P2*(1+2*G1*XOLD(I))
      P5 = AL1*XOLD(I)+AL2*XOLD(I+N)+ORS
      DF(I,J) = B(I,J)-B(I,N+1)/A(N+1,N+1)*A(N+1,J)
     &-PHI1*(P1*P2*P3-XOLD(I)*P5*P4)/ ((P1**2)*(P2**2))
      ELSE
      DF(I,J) = B(I,J)-B(I,N+1)/A(N+1,N+1)*A(N+1,J)
      ENDIF
      SUM1(I) = SUM1(I)+(B(I,J)-B(I,N+1)/A(N+1,N+1)*A(N+1,J))*XOLD(J)
20    CONTINUE
      DF(I,(2*N+1)) =-(SUM1(I)+B(I,0)*AC*CL1-B(I,N+1)*
     &A(N+1,0)*AC*CL1/A(N+1,N+1)-
     &PHI1*P5*XOLD(I)/(P1*P2))
10    CONTINUE
c
      DO 12 I = N+1,2*N
      DO 22 J = N+1,2*N
      IF(I.EQ.J) THEN
      Q1 = 1+XOLD(I)+G2*(XOLD(I))**2+AS2*XOLD(I-N)
      Q2 = 1+AL1*XOLD(I-N)+AL2*XOLD(I)+ORS
      Q3 = AL1*XOLD(I-N)+2*AL2*XOLD(I)+ORS
      Q4 = Q1*AL2+Q2*(1+2*G2*XOLD(I))
      Q5 = AL1*XOLD(I-N)+AL2*XOLD(I)+ORS
      DF(I,J) = B(I-N,J-N)-B(I-N,N+1)/A(N+1,N+1)*A(N+1,J-N)
     &-PHI2*(Q1*Q2*Q3-XOLD(I)*Q5*Q4)/ ((Q1**2)*(Q2**2))
      ELSE
      DF(I,J) = B(I-N,J-N)-B(I-N,N+1)/A(N+1,N+1)*A(N+1,J-N)
      ENDIF
      SUM2(I) = SUM2(I)+(B(I-N,J-N)-B(I-N,N+1)/A(N+1,N+1)
     &*A(N+1,J-N))*XOLD(J)
```

```
      22 CONTINUE
      DF(I,(2*N+1))=-(SUM2(I)+B(I-N,0)*AD*CL2-B(I-N,N+1)*
     &A(N+1,0)*AD*CL2/A(N+1,N+1)-
     &PHI2*Q5*XOLD(I)/(Q1*Q2))
      12 CONTINUE
      RETURN
      END
c*********************************************************
c  NEWTON RAPHSON TO SOLVE THE ALGEBRIC EQUATIONS
c*********************************************************
      SUBROUTINE NEWTON(ITMAX,N, IPRINT,EPS1,EPS2,XOLD)
      IMPLICIT REAL*8 (A-H,O-Z)
      PARAMETER (M=10)
      DIMENSION XOLD(2*M),XINC(2*M),A(2*M,2*M+1)
c  NEWTON RAPHSON ITERATION
c  WRITE(6,200) ITMAX, IPRINT,2*N,EPS1,EPS2,2*N,(XOLD(I), I = 1,2*N)
      WRITE (6,123)
      DO 9 ITER = 1, ITMAX
c  CALL ON CALCN TO SET UP THE A MATRIX
      CALL CALCN(XOLD,A,M)
c  CALL SIMUL TO COMPUTE JACOBIAN AND CORRECTION IN XINC
      NN = N+1
      INDIC = 1
      DETER = SIMUL (N,A,XINC,EPS1, INDIC,NN)
      IF (DETER.NE.0) GOTO 3
      WRITE(6,201)
      RETURN
c  CHECK FOR CONVERGENCE AND UPDATE XOLD VALUE
   3  ITCON = 1
      DO 5 I=1,N
      IF (DABS(XINC(I)).GT.EPS2) ITCON = 0
   5  XOLD(I) = XOLD(I)+XINC(I)
      IF (IPRINT.EQ.1) WRITE(6,202) ITER,DETER,N,(XOLD(I), I = 1,N)
      IF (ITCON.EQ.0) GOTO 9
c  WRITE(6,203) ITER,N,(XOLD(I),I=1,N)
      WRITE(6,2203) ITER
      RETURN
   9  CONTINUE
      WRITE(6,204)
      RETURN
c  FORMATS FOR INPUT AND OUTPUT STATEMENTS
   200  FORMAT(' ITMAX = ', I8,/' IPRINT = ', I8/' N     = ', I8/
   &    ' EPS1  = ',1PE14.1/' EPS2  = ',1PE14.1/10X,'XOLD(L)...XOLD(',
   &    I2,')'//(1H ,1P4E16.6))
   201  FORMAT(38H0MATRIX IS ILL-CONDITIONED OR SINGULAR)
```

```
  202  FORMAT(' ITER =', I8/  10H DETER = ,E18.5/
       $  26H         XOLD(L)...XOLD(,I2,1H) / (1H ,1P4E16.6) )
  203  FORMAT(' SUCCESSFUL CONVERGENCE'/'  ITER =',i3/10x,
       $'XOLD(L)...XOLD(', I2,')'//  (1H ,1P4E16.6) )
 2203  FORMAT(' SUCCESSFUL CONVERGENCE'/'  ITER =', I3/)
  204  FORMAT(' NO CONVERGENCE' )
  123  FORMAT(' _____',/)
       END

c*************************************************************
       SUBROUTINE SVARI(SUR,DEL,B0,DFF1,DFF2,DFF3,AKAP1,
       &AKAP2,AKAP3,AMM1,AMM2,AMM3,AY1,AY2,AY13,AY23,
       &AKSS1,AMU1,AKII1,AKSS2,AMU2,AKII2,AKOO1,AKSS12,
       &AKSS21,ACG01,ACG02,ACG03,AUG,AUL,VV)
       IMPLICIT REAL*8 (A-H,O-Z)
       WRITE(6,123)
       WRITE(6,1)
  1    FORMAT (' ',//,' VARIABLES IN THE MODEL',//)
       WRITE(6,2)
  2    FORMAT (3X,'1 - VOC,/,3X,'2 -VOC,3X,'2 - OXYGEN',/)
       WRITE(6,19) AUG
  19   FORMAT (' ', 'GAS FLOW RATE (m3/hr)       = ', E14.3)
       WRITE(6,20) AUL
  20   FORMAT (' ', 'LIQUID FLOW RATE(m3/hr)      = ', E14.3)
       WRITE(6,3) VV*1E6
  3    FORMAT (' ', 'VOLUME OF THE COLUMN(cm3)    = ', F14.3)
       WRITE(6,4) SUR
  4    FORMAT (' ', 'BIOLAYER SUR.AREA( m2/m3)    = ', F14.3)
       WRITE(6,44) B0
  44   FORMAT (' ', 'BIOMASS CONC. (g/m3)         = ', E14.3)
       WRITE(6,5) DEL*1E3
  5    FORMAT (' ', 'FILM THICKNESS (μm)          = ', F14.3)
       WRITE(6,18) ACG01
       WRITE(6,21) ACG02
       WRITE(6,24) ACG03
  18   FORMAT (' ', 'INLET CONC. (g/m3 OF VOC 1)(1) = ', F14.3)
  21   FORMAT (' ', 'INLET CONC. (g/m3 OF VOC 2)(2) = ', F14.3)
  24   FORMAT (' ', 'INLET CONC. (g/m3 OF AIR)(3) = ', F14.3)
       WRITE(6,31) AY1
  31   FORMAT (' ', 'YIELD COEFFICIENT (1)        = ', F14.3)
       WRITE(6,32) AY2
  32   FORMAT (' ', 'YIELD COEFFICIENT (2)        = ', F14.3)
       WRITE(6,33) AY13
  33   FORMAT (' ', 'YIELD COEFFICIENT (13)       = ', F14.3)
```

```
      WRITE(6,34) AY23
 34   FORMAT (' ', 'YIELD COEFFICIENT (23)      = ', F14.3)
      WRITE(6,51) DFF1*1E9/3600
      WRITE(6,54) DFF2*1E9/3600
      WRITE(6,59) DFF3*1E9/3600
 51   FORMAT (' ', 'DIFF. COEFF.(1)*1E9 (m2/s)  = ', F14.3)
 54   FORMAT (' ', 'DIFF. COEFF.(2)*1E9 (m2/s)  = ', F14.3)
 59   FORMAT (' ', 'DIFF. COEFF.(3)*1E9 (m2/s)  = ', F14.3)
      WRITE(6,56) AMM1
 56   FORMAT (' ', 'DIST. COEFF.      (1)    = ', E14.3)
      WRITE(6,57) AMM2
 57   FORMAT (' ', 'DIST. COEFF.      (2)    = ', E14.3)
      WRITE(6,60) AMM3
 60   FORMAT (' ', 'DIST. COEFF.      (3)    = ', E14.3)
      WRITE(6,48) AKAP1
 48   FORMAT (' ', 'MASS TRANSFER  COEFF   (1)    = ', E14.3)
      WRITE(6,49) AKAP2
 49   FORMAT (' ','MASS  TRANSFER COEFF    (2)    = ', E14.3)
      WRITE(6,61) AKAP3
 61   FORMAT (' ','MASS  TRANSFER COEFF    (3)    = ', E14.3)
      WRITE(6,123)
      WRITE(6,*) '       ANDREWS AND OTHER PARAMETERS'
      WRITE(6,6) AKSS1,AMU1, AKII1,AKOO1
 6    FORMAT (' ',/,' KS1 (g/m3) = ',E14.3,3X,'MU1 (1/hr) = ',F14.3,/,
&          ' KSI1 (g/m3) = ',E14.3,3X,'KO1 (g/m3)= 'E14.3,/)
      WRITE(6,7) AKSS2,AMU2, AKII2,AKOO1
 7    FORMAT (' ',/,' KS2 (g/m3) = ',E14.3,3X,'MU2 (1/hr) = ',F14.3,/,
&          ' KSI2 (g/m3) = ',E14.3,3X,'KO1 (g/m3)= 'E14.3,/)
      WRITE(6,8) AKSS12,AKSS21
 8    FORMAT (' ',/,' KS12 (g/m3) = ',E14.3,3X, KS21 (g/m3) = ',E14.3,/)
 123  FORMAT(' _____',/)
      RETURN
      END
c*************************************************************
c  SUBROUTINE FOR EVALUATING THE DERIVATIVES
c  NECESSARY FOR GAS AND LIQUID PHASE PROFILES
c*************************************************************
      SUBROUTINE DERI (XOLD,DERI1,DERI2,DERI3)
      IMPLICIT REAL*8 (A-H,O-Z)
      PARAMETER (N=10)
      REAL*8 A(0:N+1,0:N+1),B(0:N+1,0:N+1)
      REAL*8 XOLD(2*N)
      COMMON /PRM16/ AC
      COMMON /PRM17/AO
      COMMON /PRM18/AD
```

```
      COMMON /PRM8/ AL1,AL2
      COMMON /PRMA/ A
      COMMON /PRMB/ B
      COMMON /PRM4/ CL1
      COMMON /PRM5/CL2
      COMMON /PRM20/CL3
c
      SUM1 = 0.0
      SUM2 = 0.0
      DO 10 J = 1,N
      SUM1 = SUM1+(A(0,J)-A(0,N+1)*A(N+1,J)/A(N+1,N+1))*XOLD(J)
      SUM2 = SUM2+(A(0,J)-A(0,N+1)*A(N+1,J)/A(N+1,N+1))*XOLD(J+N)
   10 CONTINUE
      DERI1 = SUM1+(A(0,0)-A(0,N+1)*A(N+1,0)/A(N+1,N+1))*AC*CL1
      DERI2 = SUM2+(A(0,0)-A(0,N+1)*A(N+1,0)/A(N+1,N+1))*AD*CL2
      DERI3 = (AL1)*DERI1+(AL2)*DERI2
      WRITE(*,*) DERI1,DERI2,DERI3
      RETURN
      END
c*************************************************************
c  FOR GAS AND LIQUID PHASE USING THE FOURTH ORDER
c  RUNGE KUTTA METHOD
c*************************************************************
      SUBROUTINE RK4S(F,G,Z,CG,CL,H)
      IMPLICIT REAL*8 (A-H,O-Z)
      H2 = 0.5*H
      START = Z
      B1 = H*F(Z,CG,CL)
      B2 = H*G(Z,CG,CL)
      B3 = H*F(Z+H2,CG+H2*B1,CL+H2*B2)
      B4 = H*G(Z+H2,CG+H2*B1,CL+H2*B2)
      B5 = H*F(Z+H2,CG+H2*B3,CL+H2*B4)
      B6 = H*G(Z+H2,CG+H2*B3,CL+H2*B4)
      B7 = H*F(Z+H,CG+H*B5,CL+H*B6)
      B8 = H*G(Z+H,CG+H*B5,CL+H*B6)
      CG = CG+(B1+2.*B3+2.*B5+B7)/6.
      CL = CL+(B2+2.*B4+2.*B6+B8)/6.
      Z = Z+H
      WRITE (*,*) CG,CL
      RETURN
      END
c*************************************************************
c   PURPOSE : GIVE THE FUNCTION FOR RK METHOD, IN THE
c  GAS PHASE BALANCE ; VOC 1 (BLOCK A)
```

```
c*************************************************************
      FUNCTION FUN1(Z,CG,CL)
      IMPLICIT REAL*8 (A-H,O-Z)
      COMMON / PRM11/ R
      COMMON / PRM2/ CG1
      COMMON / PRM4/ CL1
      FUN1 = R*(CL1-CG1)
      RETURN
      END
c*************************************************************
c  PURPOSE : GIVE THE FUNCTION FOR RK METHOD, IN THE
c  LIQUID PHASE BALANCE ; VOC 1
c*************************************************************
      FUNCTION GUN1(Z,CG,CL)
      IMPLICIT REAL*8 (A-H,O-Z)
      COMMON / PRM13/ PSI
      COMMON /PRM15/AN
      COMMON / LIQUIDC/DERI1
      COMMON / PRM2/ CG1
      COMMON / PRM4/ CL1
      GUN1 =-PSI*(CL1-CG1)+AN*DERI1
      RETURN
      END
c*************************************************************
c  PURPOSE : GIVE THE FUNCTION FOR RK METHOD, IN THE
c  GAS PHASE BALANCE ; VOC 2 (BLOCK B)
c*************************************************************
      FUNCTION FUN2(Z,CG,CL)
      IMPLICIT REAL*8 (A-H,O-Z)
      COMMON / PRM11/R
      COMMON /PRM12/E1,E2
      COMMON / PRM3/ CG2
      COMMON / PRM5/ CL2
      FUN2 = R*E1*(CL2-CG2)
      RETURN
      END
c*************************************************************
c  PURPOSE : GIVE THE FUNCTION FOR RK METHOD, IN THE
c  LIQUID PHASE BALANCE ; VOC 2
c*************************************************************
      FUNCTION GUN2(Z,CG,CL)
      IMPLICIT REAL*8 (A-H,O-Z)
      COMMON / PRM13/ PSI
      COMMON / PRM14/ BT1,BT2
```

```
      COMMON / PRM15/ AN
      COMMON / PRM9/ W1,W2
      COMMON / PRM3/ CG2
      COMMON / PRM5/ CL2
      COMMON / LIQUIDD/ DERI2
      GUN2 =-PSI*BT1*(CL2-CG2)+AN*W1*DERI2
      RETURN
      END
c*************************************************************
c  PURPOSE : GIVE THE FUNCTION FOR RK METHOD, IN THE
c  GAS PHASE BALANCE ; OXYGEN (BLOCK C)
c*************************************************************
      FUNCTION FUN3(Z,CG,CL)
      IMPLICIT REAL*8 (A-H,O-Z)
      COMMON / PRM11/R
      COMMON /PRM12/E1,E2
      COMMON / PRM19/ CG3
      COMMON / PRM20/ CL3
      FUN3 = R*E2*(CL3-CG3)
      RETURN
      END
c*************************************************************
c  PURPOSE : GIVE THE FUNCTION FOR RK METHOD, IN THE
c  LIQUID PHASE BALANCE ; OXYGEN
c*************************************************************
      FUNCTION GUN3(Z,CG,CL)
      IMPLICIT REAL*8 (A-H,O-Z)
      COMMON / PRM13/ PSI
      COMMON / PRM14/ BT1,BT2
      COMMON / PRM15/ AN
      COMMON / PRM9/ W1,W2
      COMMON / PRM19/ CG3
      COMMON / PRM20/ CL3
      COMMON / LIQUIDO/ DERI3
      GUN3 =-PSI*BT2*(CL3-CG3)+AN*W2*DERI3
      RETURN
      END
c*************************************************************
      SUBROUTINE ERROR1 (CL1,ERRORC,CL01)
      IMPLICIT REAL*8 (A-H,O-Z)
      COMMON /PRM4/ CL1
      COMMON /PRM6/ CL01
      ERRORC = CL1-CL01
      RETURN
```

```
      END
c*************************************************************
      SUBROUTINE ERROR2 (CL2,ERRORD,CL02)
      IMPLICIT REAL*8 (A-H,O-Z)
      COMMON /PRM5/ CL2
      COMMON / PRM7/ CL02
      ERRORD = CL2-CL02
      RETURN
c *************************************************************
      SUBROUTINE ERROR3 (CL3,ERRORO,CL03)
      IMPLICIT REAL*8 (A-H,O-Z)
      COMMON /PRM20/ CL3
      COMMON / PRM21/ CL03
      ERRORO = CL3-CL03
      RETURN
*************************************************************
      SUBROUTINE PRM (PHI1,PHI2,AL1,AL2,W1,W2,G1,G2,
     &R,E1,E2,PSI,BT1,BT2,AN,AC,AD,AO,AS1,AS2)
      IMPLICIT REAL*8 (A-H,O-Z)
      COMMON /DEL/ DEL
      COMMON /SUR/ SUR
      COMMON /INDEX/ INDX
      COMMON /CG0 /ACG01,ACG02,ACG03
c
c  1-VOC
c  2-VOC
c  3-OXYGEN
      DEL = DEL*1E-6
      WRITE(6,85) DEL*1E6
c
      B0 = 75E3
      XV = B0/1000
      FD = 1-0.43*XV**0.92/(11.19+0.27*XV**0.99)
c
c  DIFFUSION COEFFICIENTS
      DFF1  = 0.781E-9 *3600.*FD
      DFF2  = 0.691E-9 *3600.*FD
      DFF3  = 2.3807E-9 *3600.*FD
c
c  OVERALL MASS TRANSFER COEFFICIENTS
      AKAP1 = 11.18
      AKAP2 = 10.27
      AKAP3 = 31.57
c
c  DISTRIBUTION COEFFICIENTS
```

```
      AMM1 = 0.167
      AMM2 = 0.119
      AMM3 = 34.4
c
c  YIELD COEFFICIENTS
      AY1 = 0.551
      AY1 = 0.397
      AY13 = 0.516
      AY22 = 0.363
c
c  KINETIC PARAMETERS
      AKSS1= 5.14
      AMU1  = 0.154
      AKII1 = 21.883
      AKSS2= 13.389
      AMU2  = 0.146
      AKII2 = 19.657
      AKSS12= 1.3
      AKSS21= 0.75
      AKOO1 = 0.26
c
c  INLET GAS CONCENTRATIONS
      ACG01 = 0.17
      ACG02 = 0.27
      ACG03 = 275

c  GAS FLOW RATE
      AUG = 0.27
c
c  LIQUID FLOW RATE
      AUL = 0.006
c
c  VOLUME OF  THE COLUMN
      VV = 0.0143
c
      IF (INDX.EQ.100) THEN
      CALL SVARI(SUR,DEL,B0,DFF1,DFF2,DFF3,AKAP1,AKAP2,AKAP3,
     &AMM1,AMM2,AMM3,AY1,AY2,AY13,AY23,AKSS1,AMU1,
     &AKII1,AKSS2,AMU2,AKII2,AKOO1,AKSS12,AKSS21,ACG01,
     &ACG02,ACG03,AUG,AUL,VV)
      ELSE
      ENDIF
c
      PHI1 = (AMU1*(DEL**2)*B0)/(DFF1*AY1*AKSS1)
      PHI2 = (AMU2*(DEL**2)*B0)/(DFF2*AY2*AKSS2)
```

```
      AL1 = (DFF1*AY1*AKSS1)/(AY13*AKOO1*DFF3)
      AL2 = (DFF2*AY2*AKSS2)/(AY23*AKOO1*DFF3)
      W1 = (AKSS2*DFF2*ACG01*AMM2)/(AKSS1*DFF1*ACG02*AMM1)
      W2 = (AKOO1*DFF3*ACG01*AMM3)/(AKSS1*DFF1*ACG03*AMM1)
      G1 =AKSS1/AKII1
      G2 =AKSS2/AKII2
      AS1 = (AKSS12*AKSS2)/AKSS1
      AS2 = (AKSS21*AKSS1)/AKSS2
      R = (AKAP1*VV)/(AUG*AMM1)
      E1= (AMM1*AKAP2)/(AMM2*AKAP1)
      E2= (AMM1*AKAP3)/(AMM3*AKAP1)
      PSI =(AKAP1*VV)/AUL
      BT1 = AKAP2/AKAP1
      BT2 = AKAP3/AKAP1
      AN =(DFF1*SUR*AKSS1*VV*AMM1)/(DEL*AUL*ACG01)
      AC = ACG01/(AKSS1*AMM1)
      AD = ACG02/(AKSS2*AMM2)
      AO = ACG03/(AKOO1*AMM3)
C
      IF (INDX.EQ.1000) THEN
      WRITE(6,123)
      WRITE(6,71)
   71 FORMAT (' ','    PARAMETERS USED :', /)
      WRITE(6,72) PHI1,PHI2
      WRITE(6,73) AL1, AL2
      WRITE (6,74) W1,W2
   72 FORMAT (3X,'PHI1^2  =  ',E14.6,
     &       3X,'PHI2^2  =  ',E14.6)
   73 FORMAT (3X,'LAMDA1  =  ',E14.6,
     &       3X,'LAMDA2  =  ',E14.6)
   74 FORMAT (3X,'OMEGA1  =  ',E14.6,
     &       3X,'OMEGA2  =  ',E14.6)
      WRITE(6,75) G1,G2
      WRITE(6,76) E1,E2
      WRITE(6,77) R,AN
   75 FORMAT (3X,'GAMA1  =  ',E14.6,
     &       3X,'GAMA2  =  ',E14.6)
   76 FORMAT (3X,'EPS1  =  ',F14.6,
     &       3X,'EPSI2  =  ',F14.6)
   77 FORMAT (3X,'RO  =  ',E14.6,
     &       3X,'N  =  ',E14.6)
      WRITE(6,78) BT1,BT2
      WRITE(6,79) PSI,AC
      WRITE(6,80) AD,AO
   78 FORMAT (3X,'BETA1  =  ',F14.3,
```

```
     &       3X,'BETA2   =  ',F14.3)
  79 FORMAT (3X,'PSI    =  ',E14.6,
     &       3X,'STATHC  =  ',E14.6)
  80 FORMAT (3X,'STATHD  =  ',E14.6,
     &       3X,'STATHO  =  ',E14.6)
     WRITE(6,81) S1,S2
  81 FORMAT (3X,'SIGMA1  =  ',E14.6,
     &       3X,'SIGMA2  =  ',E14.6)
  85 FORMAT (3X,'DEL.(μm)=   ',F14.3,/)
  123 FORMAT(' ____________________________________________________',/)
     ELSE
     ENDIF
     RETURN
     END
c*******END OF MAIN PROGRAM**************************
c
c  CASE 2: COUNTER-CURRENT FLOW OF GAS AND LIQUID
c  IN  BLOCK A, LINE 6 SHOULD BE:
c  FUN1 = -R*(CL1-CG1)
c  IN  BLOCK B, LINE 6 SHOULD BE:
c  FUN2 = -R*E1*(CL2-CG2)
c  IN  BLOCK C, LINE 6 SHOULD BE:
c  FUN3 = -R*E2*(CL3-CG3)
```

REFERENCES

1. Alonso, C., Suidan, M.T., Sorial, G.A., Smith, F.L., Biswas P., Smith, P.J., Brenner, R.C., "Gas Treatment in Trickle-Bed Biofilters: Biomass, How Much is Enough?" *Biotechnol. Bioeng.* 54 (1997): 583-594.

2. Andrews, J.F., "A Mathematical Model for the Continuous Culture of Microorganisms Utilizing Inhibitory Substrates." *Biotechnol. Bioeng.* 10 (1968): 707-723.

3. Antoniou, P., Hamilton, J., Koopman, B., Jain, R., Holloway, B., Lyberatos, G., Svoronos, S.A., "Effect of Temperature and pH on the Effective Maximum Specific Growth Rate of Nitrifying Bacteria." *Water Res.* 24(1990): 97-101.

4. Apel, W.A., Dugan, P.R., and Wiebe, M.R., "Use of Methanotropic Bacteria in Gas Phase Bioreactors to Abate Methane in Coal Mine Atmospheres." *Fuel.* 70 (1990): 1001-1003.

5. Arcangeli, J.P. and E. Arvin, "Modeling of Toluene Biodegradation and Biofilm Growth in a Fixed Biofilm Reactor." *Wat. Sci. Tech.* 26 (1992): 617-626.

6. Bader, F.G., "Kinetics of Double-Substrate Limited Growth." pp. 1-32. In: *Microbial Population Dynamics.* M.J. Bazin (ed), CRC Press, Boca Raton, FL,1982.

7. Bailey, J.E., Ollis, D.F., *Biochemical Engineering Fundamentals*. McGraw-Hill Inc, New York, 1986.

8. Baltzis, B.C., "Biofiltration of VOC Vapors.", Chapter 5 pp. 119-150, in *Biological Treatment of Hazardous Wastes*, G.A. Lewandowski and L.J. DeFilippi (eds.), John Wiley & Sons Inc., New York (1998).

9. Baltzis, B.C. and D.S. de la Cruz, "Removal of Xylene Vapors in a Biotrickling Filter.", 89th Annual A&WMA Meeting, Paper no. 96-RP87C.01, Nashville, TN, 1996.

10. Baltzis, B.C., Wojdyla, S.M., Zarook, S.M., "Modeling Biofiltration of VOC Mixtures under Steady-State Conditions." *J. Environ. Eng.* 123 (1997): 599-605.

11. Bolles, L.W., Fair, J.R., "Improved Mass-Transfer Model Enhances Packed-Column Design." *Chemical Eng.*, July (1982): 109-116.

12. Deshusses, M.A., Hamer, G., Dunn, I.J., "Behavior of Biofilters for Waste Air Biotreatment. 1. Dynamic Model Development." *Environ. Sci. Technol.* 29 (1995a) 1048-1058.

13. Deshusses, M.A., Hamer, G., Dunn, I.J., "Behavior of Biofilters for Waste Ai Biotreatment. 2. Experimental Evaluation of a Dynamic Model." *Environ. Sci Technol.* 29 (1995b): 1059-1068.

14. Diks, R.M.M. and S.P.P. Ottengraf, "Verification Studies of a Simplified Model fo Removal of Dichloromethane from Waste Gases Using a Biological Trickling Filte (Part. I)." *Bioprocess Eng.* 6 (1991a) : 93-99.

15. Diks, R.M.M. and S.P.P. Ottengraf, "Verification Studies of a Simplified Model fo Removal of Dichloromethane from Waste Gases Using a Biological Trickling Filte (Part. II)." *Bioprocess Eng.* 6 (1991b): 131-140.

16. Dikshitulu S., Baltzis, B.C., Lewandowski, G.A., Pavlou, S., "Competition betwee Two Microbial Populations in a Sequencing Fed-Batch Reactor: Theory Experimental Verification, and Implications for Waste Treatment Applications." *Biotechnol. Bioeng.* 42 (1993): 643-656.

17. Djebbar Y. and R. M. Narbaitz, "Mass Transfer Correlations for Air Stripping Towers." *Environmental Progress.* 14 (1995): 137-145.

18. Eckert, J.S., "Design Techniques for Sizing Packed Tower." *Chemical Engineering Progress.* 57 (1961): 54-58.

19. Eckert, J.S., "How Tower Packings Behave." *Chemical Engineering Progress.* Apri (1975):70-76.

20. Fan, L.S., K Fujie, T.R. Long, and W.T. Tang, "Characteristics of a Draft-Tube Gas Liquid-Solid Fluidized-Bed Bioreactor with Immobilized Living Cells for Pheno Degradation." *Biotechnol. Bioeng.* 30 (1987): 498-504.

21. Fan, L.S., R. Leyva-Ramos, K.D. Wisecarver, and B.J. Zehner, "Diffusion of Pheno through a Biofilm Grown on Activated Carbon Particles in a Draft-Tube Three-Phas Fluidized-Bed Bioreactor." *Biotechnol. Bioeng.* 35 (1990): 279-286.

22. Finlayson, B.A., *Nonlinear Analysis in Chemical Engineering*, McGraw-Hill Inc New York (1980).

23. Fuller, N.E., P.D. Schettler, and J.G. Giddings, "A New Method for Prediction of Binary Gas-Phase Diffusion Coefficients." *Industrial and Engineering Chemistry.* 58 (1966): 19-27.

24. Hartmans, S. and Tramper, T., "Dichloromethane Removal from Waste Gases with a Trickle-Bed Bioreactor." *Bioprocess Eng.* 6 (1991): 83-92.

25. Heggen, R.J., "Thermal Dependent Physical Properties of Water." *J. of Hydraulic Engineering.* 109 (1983): 298-302.

26. Hodge, S.D., Devinny, J.S., "Modeling Removal of Air Contaminants by Biofiltration." *J. Environ. Eng.* 121 (1995): 21-32.

27. Kavanaugh, M.G. and R.R. Trussell, "Design of Aeration Towers to Strip Volatile Contaminants from Drinking Water." *Journal of American Water Work Association.* 80 (1980): 684-692.

28. Lamarche, P. and R. Droste, "Air Stripping Mass Transfer Correlations for Volatile organics." *Journal of American Water Work Association.* 89 (1989): 78-89.

29. Monod, J., *Recherches sur la croissance des cultures bacterienes. Hermann et Cie*, Paris, 1942.

30. Mukhopadhyay, N. and E.C. Moretti, "Current and Potential Future Industrial Practices for Reducing and Controlling Volatile Organic Compounds." AIChE Center for Waste Reduction Technologies, New York, NY (1993).

31. Ockeloen, H.F., T.J. Overcamp, and C.P.L. Grady, Jr. "A Biological Fixed-Film Simulation Model for the Removal of Volatile Organic Air Pollutants.", 85th Annual A&WMA Meeting, Paper no. 92-116.05, Kansas City, MO (1992).

32. Oh, Y.S., Bartha, R., "Design and Performance of a Trickling Air Biofilter for Chlorobenzene and o-Dichlrorobenzene Vapors." *Appl. Environ. Microbiol.* 60 (1994): 2717-2722.

33. Oh, Y.S., Shareefdeen, Z., Baltzis, B.C., Bartha, R., "Interactions between Benzene, Toluene and p-Xylene (BTX) during Their Biodegradation." *Biotechnol. Bioeng.* 44 (1994): 533-538.

34. Onda, K., H. Takeuchi, and Y. Okumoto, "Mass Transfer Coefficients between Gas and Liquid Phases in Packed Columns." *Journal of Chemical Engineering of Japan.* 1 (1968): 56-62.

35. Ottengraf, S.P.P., van den Oever, A.H.C., "Kinetics of Organic Compound Removal from Waste Gases with a Biological Filter." *Biotechnol. Bioeng.* 25 (1983): 3089-3102.

36. Pedersen, A.R., Arvin, E., "Removal of Toluene in Waste Gases Using a Biological Trickling Filter." *Biodegradation.* 6 (1995): 109-118.

37. Perry, R.H. and Green, D., *Perry's Chemical Engineer's Handbook*, Sixth Edition, McGraw-Hill Inc, New York (1984).

38. Shareefdeen, Z., "Engineering analysis of a packed-bed biofilter for removal of volatile organic compound (VOC) emissions." Ph.D. Dissertation, New Jersey Institute of Technology, Newark, NJ (1994).

39. Shareefdeen, Z., B.C. Baltzis, Y.S. Oh, and R. Bartha, "Biofiltration of Methanol Vapor." *Biotechnol. Bioeng.* 41 (1993): 512-524.

40. Shareefdeen, Z. and B.C. Baltzis, "Biofiltration of Toluene Vapor under Steady-State and Transient Conditions: Theory and Experimental Results." *Chem. Eng. Sci.* 49 (1994a): 4347-4360.

41. Shuler, M.L., Kargi, F., *Bioprocess engineering.* Prentice -Hall, Englewood Cliffs, NJ (1992).

42. Smith, P.J., Biswas, P., Suidan, M.T., Brenner, R.C., "Treatment of Volatile Organic Compounds in Waste Gases Using a Trickling Biofilter System: A Modeling Approach.", 86th Annual A&WMA Meeting, Paper no. 93-TP-52A.05, Denver, CO (1993).

43. Sorial, A.G., F.L. Smith, M.T. Suidam, P. Biswas, and R.G. Brenner, "Evaluation of Trickle Bed Biofilter Media for Toluene Removal." *Journal of the Air & Waste Management Association.* 45 (1995): 801-810.

44. Togna, A.P. and M. Singh, "Biological Vapor-Phase Treatment Using Biofilter and Biotrickling Filter Reactors: Practical Operating Regimes." *Environmental Progress.* 13 (1994): 94-97.

45. Tonga, A.P. and M. Singh, "A Comparative Study of Biofilter and Biotrickling Filter Performance for Isopentane Removal.", 87th Annual A&WMA Meeting, Paper no. 94.RP115B.04, Cincinnati, OH (1994).

46. Turek, F., Lange, R., "Mass Transfer in Trickle-Bed Reactors at Low Reynolds Numbers." *Chem. Eng. Sci.* 36 (1981): 569-579.

47. Utgikar, V., Y. Shan and R. Govind, "Biodegradation of Volatile Organic Compounds in Aerobic and Anaerobic Biofilters.", 17th Annual Hazardous Waste Research Symposium, Cincinnati, OH (1991).

48. Villandensen, J. and M.L. Michelsen, *Solution of Differential Equation Models by Polynomial Approximation*, Prentice Hall Inc, NJ (1978).

49. Wang, J.-H., Baltzis, B.C., Lewandowski, G.A., "Fundamental Denitrification Kinetic Studies with *P. Denitrificans*." *Biotechnol. Bioeng.* 47 (1995): 26-41.

50. Wang, K-W., Baltzis, B.C., Lewandowski, G.A., "Kinetics of Phenol Biodegradation in the Presence of Glucose." *Biotechnol. Bioeng.* 51 (1996): 87-94.

51. Williamson, K., McCarty, P.L., "A model of substrate utilization by bacteria films." *J. Water Pollut. Control Fed.* 48 (1976): 9-24.

52. Williamson, K., McCarty, P.L., "Verification studies of the biofilm model for bacterial substrate utilization." *J. Water Pollut. Control Fed.* 48 (1976): 281-296.

53. Yurteri, G., F.D. Ryan, J.J. Callow, and M. Gurol, "The Effects of Chemical Composition of Water on Henry's Law Constant." *Journal WPCF.* 59 (1987): 950-956.